WWW.OEAW.AC.AT

ÖAW ÖSTERREICHISCHE AKADEMIE DER WISSENSCHAFTEN

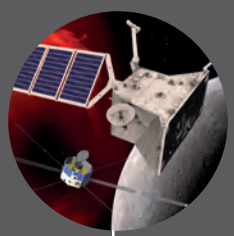

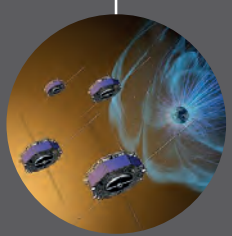

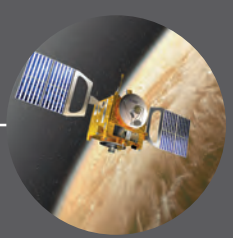

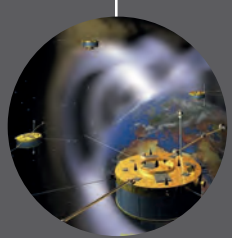

2030 ATHENA
COMET INTERCEPTOR, ARIEL
PLATO, HELIOSWARM
SMILE, SPACEWEATHER FOLLOW-ON
JUICE, FORESAIL-2, CSES-2
MACAO SCIENCE 1
CUTE
2020 TIANWEN-1, **SOLAR ORBITER**
CHEOPS
BEPICOLOMBO, CSES-1, INSIGHT, GEO-KOMPSAT-2A
MAGNETOSPHERIC MULTISCALE
VAN ALLEN PROBES
JUNO, YINGHUO
2010
GOCE
THEMIS
COROT, STEREO
VENUS EXPRESS
ROSETTA
MARS EXPRESS, DOUBLESTAR
2000 **CLUSTER**
EQUATOR-S
CASSINI/HUYGENS, MIR, DEEP SPACE 1
INTERBALL
AUSTROMIR
1990
PHOBOS
VEGA 1/2
SPACELAB 1
VENERA 13/14
1980

IWF INSTITUT FÜR WELTRAUMFORSCHUNG

ANNUAL REPORT 2021

WWW.OEAW.AC.AT/IWF

ÖAW ÖSTERREICHISCHE AKADEMIE DER WISSENSCHAFTEN

IWF INSTITUT FÜR WELTRAUMFORSCHUNG

COVER IMAGE

Timeline of the 42 space missions including more than 100 flight instruments to which IWF contributed significantly over the last five decades (© *JUICE* - Spacecraft: ESA/ATG medialab; Jupiter: NASA/ESA/J. Nichols (University of Leicester); Ganymede: NASA/JPL; Io: NASA/JPL/University of Arizona; Europa: NASA/JPL/DLR ESA/ATG medialab; © *BepiColombo:* ESA, © *Solar Orbiter*, *CHEOPS:* ESA/ATG medialab; © *MMS:* NASA/Goddard/Conceptual Image Lab; © *Venus Express:* ESA-D. Ducros; © *Rosetta* - Spacecraft: ESA/ATG medialab; Comet: ESA/Rosetta/NavCam; © *Cluster:* ESA; © *Cassini/Hugens:* ESA-D. Ducros; © *Spacelab-1:* NASA).

TABLE OF CONTENTS

THE DIRECTOR'S PAGE 2021

The year 2021 has seen many successes and challenges with the Corona-19 virus pandemic holding our societies in a tight grip. The Austrian Space Research Institute (Institut für Weltraumforschung, IWF) has nevertheless persevered in its research of the solar system and beyond. Some of the many, proud achievements will be presented in this Annual Report 2021.

In October 2021, I joined the Space Research Institute of the Austrian Academy of Sciences in Graz as new director in succession of Prof. Dr. Wolfgang Baumjohann, the director of the past 17 years. I thank all IWF members, the OeAW as well as my TU Graz and KFU colleagues for the warm welcome. My start as the new IWF director is a big step, bringing changes, some bigger than others. I am grateful for this opportunity which already turned into intense collaborative efforts at the OeAW and in the wider Graz science area. I am looking forward to what we jointly will achieve.

IWF looks at a proud record of 23 active space mission participations which is a tremendous manifestation of engineering and research skills as well as of scientific foresight. The majority of these missions is devoted to understanding the solar system, which still holds many secrets, for example the origin of water on Earth, the origin and evolution of Mercury or the formation of the icy moons orbiting Jupiter and Saturn.

Our solar system is just one of many planetary systems in our galaxy. However, as it is the most important one for humankind, we also bear great responsibility for it.

In true scientific spirit, which is that of adventurers who continuously push the boundaries of knowledge,

IWF Director Prof. Dr. Christiane Helling (© Chris Scott).

IWF investigates and explores the solar system and extrasolar planets; those worlds beyond the solar system. IWF will intensify its activities on exoplanet studies resulting in now eight research groups that synergize their expertise. Our joint research will be driven by three interdisciplinary challenges:

- The unexpected large diversity of exoplanets and exoplanetary systems.
- The degree of fine-tuning in the solar system that allowed Earth to become the habitable system we know today.
- The responsibility for humankind for planet Earth.

With the best of wishes,
Christiane Helling

The eight research groups of the Space Research Institute in Graz.

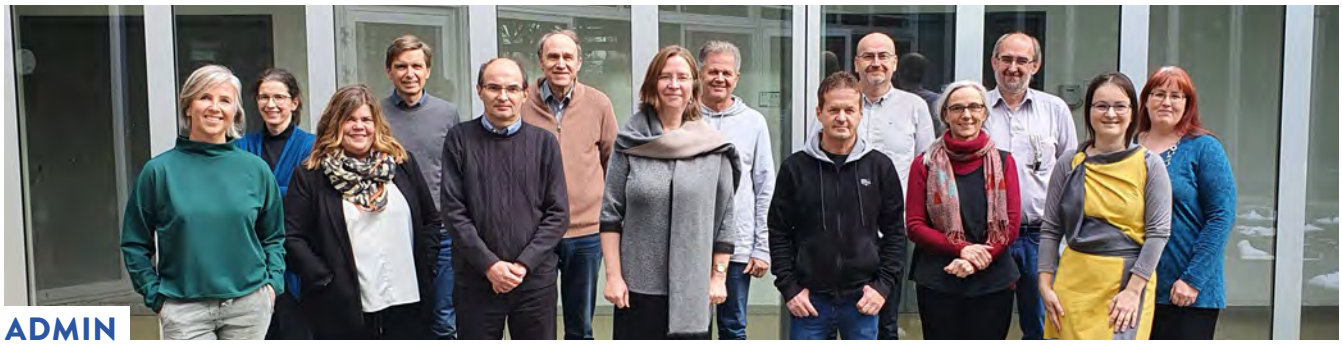

ADMIN

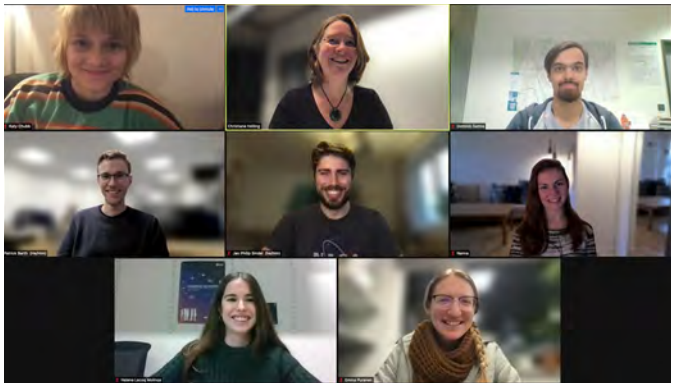

HELLING

FOSSATI

WOITKE

LAMMER

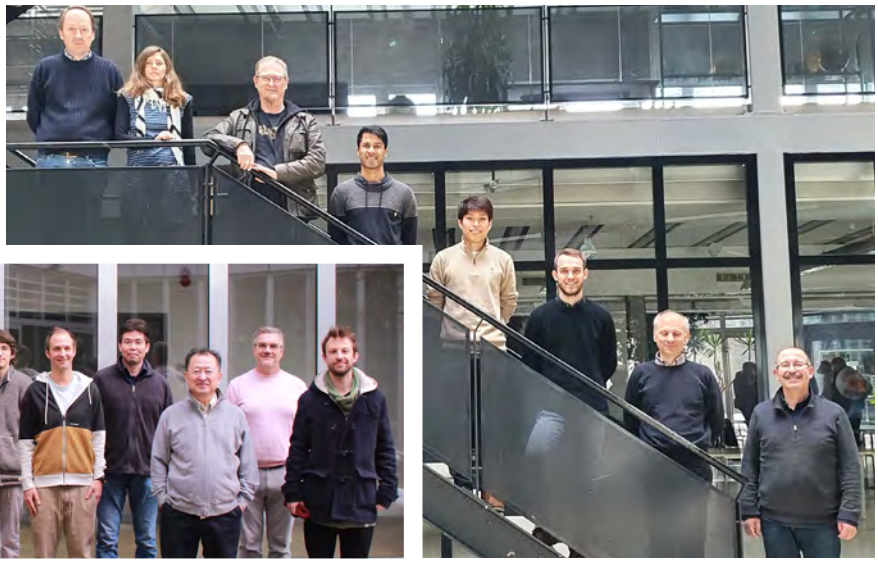

NAKAMURA

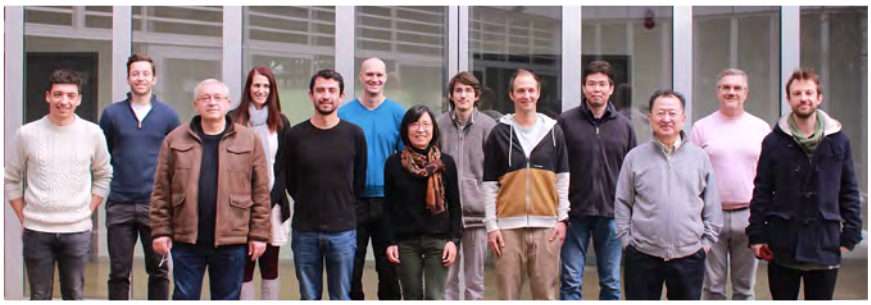

MAGNES & STELLER

KIRCHNER

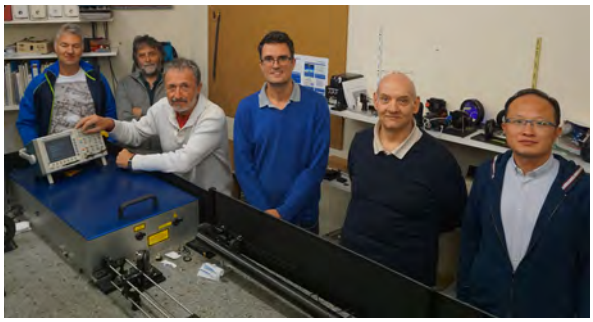

INTRODUCTION

The Space Research Institute in Graz focuses on the physics of our solar system and the diversity of exoplanets. With about 100 staff members from 20 nations it is one of the largest institutes of the Austrian Academy of Sciences (Österreichische Akademie der Wissenschaften, OeAW).

IWF develops and builds space-qualified instruments and analyzes and interprets the data returned by them. Its core engineering expertise is in building magnetometers and on-board computers, as well as in satellite laser ranging, which is performed at a station operated by IWF at the Lustbühel Observatory. In terms of science, the institute concentrates on the physics of solar and extrasolar planets, planet-forming disks, and space plasmas.

IWF cooperates closely with international space agencies and with numerous other national and international research institutions. Tight cooperations exist with the European Space Agency (ESA).

The institute is currently involved in 23 active and future international space missions; among these:

- The *Cluster* mission continues to provide unique data to better understand space plasma processes.
- The four *MMS* spacecraft perform multi-point measurements to study the dynamics of the Earth's magnetosphere.
- The first China Seismo-Electromagnetic Satellite *(CSES-1)* is studying the Earth's ionosphere. *CSES-2* will follow in early 2023.
- On its way to Mercury, *BepiColombo,* had its second gravity assist maneuver at Venus in August and passed by Mercury for the first time in October.
- *CHEOPS (CHaracterizing ExOPlanets Satellite)* continued nominal science operations, characterizing exoplanets around bright stars.
- ESA's *Solar Orbiter* flew by Venus in August and Earth in November to change its orbit around the Sun.
- The NASA CubeSat *CUTE (Colorado Ultraviolet Transit Experiment)* was launched in September to perform low-resolution transmission spectroscopy of transiting exoplanets at near-ultraviolet wavelengths.

CUTE was launched on 27 September 2021 from the Vandenberg US Airforce base in California aboard a United Launch Alliance (ULA) Atlas V rocket carrying also the *Landsat 9* mission (© ULA).

- ESA's *JUpiter ICy moons Explorer (JUICE*, launch: 2023) will investigate Jupiter and three of its largest moons, Ganymede, Callisto, and Europa.
- The *FORESAIL-2* (launch: 2023) CubeSat will characterize the variability of ultra-low frequency waves in the inner magnetosphere.
- *SMILE* (launch: 2024) is designed to study the interaction between the solar wind and Earth's magnetosphere.
- *PLATO (*launch: 2026) is a space-based observatory to search for planets orbiting alien stars.
- *Comet Interceptor* (launch: 2029) will characterize in detail, for the first time, a dynamically-new comet or interstellar object.

HIGHLIGHTS IN 2021

- On their journeys to the Sun and to Mercury, *Solar Orbiter* and *BepiColombo* flew by Venus in August and *BepiColombo* had its first encounter with its target planet Mercury in October. IWF contributed to 21 out of 58 articles on *Solar Orbiter* published in a special issue of the journal Astronomy & Astrophysics.
- Using observations by the Italian Telescopio Nazionale Galileo (TNG) on La Palma and innovative data analysis, six molecules were detected simultaneously in the atmosphere of an extrasolar planet for the first time. The results about the hot gas giant HD209458b were presented in Nature.
- So-called ion cyclotron waves around Mercury were reported for the first time and published in the Geophysical Research Letters.
- An interdisciplinary volume "Reading Terrestrial Planet Evolution in Isotopes and Element Measurements" was published, which discusses how future studies of exoplanet atmospheres could change the understanding of the solar system planets.
- The Graz-Lustbühel laser station pioneered the use of a megahertz laser to determine the distances to near-Earth satellites. The results were published in the journal Optics Letters.

THE YEAR 2021 IN NUMBERS

Members of the institute published 179 papers in refereed international journals, of which 43 were first author publications. During the same period, articles with authors from the institute were cited 8726 times in the international literature. In addition, 41 talks (8 invited) and 15 posters were presented (virtually) by IWF members at international conferences. Institute members were involved in the organization of seven international meetings, e.g. EGU General Assembly and EPSC.

IWF STRUCTURE AND FUNDING

In October, Christiane Helling followed Wolfgang Baumjohann as IWF Director. Werner Magnes serves as Deputy Director.

Christiane Helling simultaneously holds a university professorship in space science at the Graz University of Technology.

Wolfgang Baumjohann hands over the signature folder to Christiane Helling (© OeAW/IWF/Scherr).

IWF now hosts eight research groups:

- Exoplanet Weather and Climate (Lead: Christiane Helling)
- Exoplanet Characterization and Evolution (Lead: Luca Fossati)
- Planet-Forming Disks and Astrochemistry (Lead: Peter Woitke)
- Solar System Planetary Physics (Lead: Helmut Lammer)
- Space Plasma Physics (Lead: Rumi Nakamura)
- On-Board Computers (Lead: Manfred Steller)
- Space Magnetometers (Lead: Werner Magnes)
- Satellite Laser Ranging (Lead: Georg Kirchner)

IWF is mainly financed by the OeAW and to a lesser extent through competitive grants from the Austrian Research Promotion Agency (FFG), the Austrian Science Fund (FWF), the European Union, and ESA.

NEAR-EARTH SPACE

Near-Earth space is most suitable to study fundamental space plasma processes through advanced, in-situ measurements of charged particles together with electric and magnetic fields at high cadence. In particular, multi-point spacecraft missions further our understanding of complex plasma processes by differentiating spatial structure from temporal changes. IWF has been participating in a number of near-Earth space missions from the planning and proposal phase, to the development and building of new hardware, and finally the operation and calibration of the instruments. Data taken from these missions have been extensively analyzed at IWF with different methods and by theoretical modeling to compare with the observations.

New studies dealing with the interactions between solar wind and magnetosphere, the magnetosheath, and with different plasma instabilities were completed based on both the data analysis of the IWF-supported missions and theoretical studies. Among the different results one of the highlights of this year is the 3D fully kinetic particle-in-cell simulation of turbulent magnetic reconnection. The simulation showed how a turbulent, electron- to larger-scale island evolution causes an efficient cross-scale energy transfer from micro- to macro-scales, and leads to a strong electron energization within the growing magnetic islands. Such simulations provide hints for interpreting the in-situ observations of magnetic reconnection by the *Magnetospheric Multi-Scale (MMS)* mission. While magnetic reconnection operates in a small-region, its consequence can be observed in extended regions due to accelerated plasma jetting out from the reconnection region and rapid magnetic flux transport, which are detected far away from the reconnection site. *MMS* observations, with their high-temporal resolution capabilities, enabled the detection of the accelerated electrons and ions streaming from the reconnection site. The differences among species and energies of these outflowing particles, as well as among the four spacecraft, were used to determine the change in the reconnection rate and location of the acceleration site of the particles from remote observations.

This knowledge gained from near-Earth space observations contribute to understand the space plasma process applicable to other plasma environments within our solar system and beyond.

Aurora australis illuminating the Earth's upper atmosphere; photo taken from aboard the International Space Station (© NASA).

CLUSTER

ESA's *Cluster* mission is designed to study different plasma processes created by the interaction between the solar wind and the Earth's magnetosphere. This first four-spacecraft mission has been successfully operating for twenty years starting from its launch in August 2000 and is currently planned to be extended until 2024. IWF leads and/or participates in five instruments and has contributed to data archiving activities at the *Cluster Science Archives (CSA)* in addition to the science data analysis.

THEMIS/ARTEMIS

NASA's five-spacecraft mission *THEMIS (Time History of Events and Macroscale Interactions during Substorms)*, was launched in 2007. In 2010, the two outer spacecraft were sent to an orbit around the Moon and renamed *ARTEMIS (Acceleration, Reconnection, Turbulence and Electrodynamics MISsion)*. The inner three probes remained in their near-Earth orbit.

THEMIS studies dynamical processes, such as substorms, that cause aurora and different plasma processes in the magnetosphere and solar wind up to lunar distance. An extension of both missions has been approved until 2022. IWF is participating in processing and analyzing magnetometer data.

MMS

NASA's *Magnetospheric Multi-Scale (MMS)* mission, launched in 2015, explores the dynamics of the Earth's magnetosphere and the underlying energy transfer processes. Four identically equipped spacecraft carry out measurements in the Earth's magnetosphere with highest temporal and spatial measurements ever flown in space. *MMS* investigates the small-scale basic plasma processes, which transport, accelerate and energize plasmas in thin boundary and current layers. Extension of *MMS* has been approved until 2022.

IWF has taken the lead for the *Active Spacecraft POtential Control (ASPOC)* of the satellites and is participating in the *Electron Drift Instrument (EDI)* and the *Digital FluxGate magnetometer (DFG)*. In addition to the operation of these instruments and the scientific data analysis, IWF is contributing to inflight calibration activities and also deriving a new data product such as the density determined from the controlled spacecraft potential.

To enhance the usability of the *MMS* data, a dedicated study using *MMS*'s *Fast Plasma Investigation (FPI)* instrument data in the solar wind was performed. Although *MMS* is designed to investigate magnetic reconnection and other magnetosheath and magnetospheric boundary processes, *MMS's* orbit also carries the spacecraft into the pristine solar wind since 2017. In the solar wind the plasma is characterized by colder temperatures and beams in the velocity distribution function that are much narrower than in the magnetosheath, which challenge the use of plasma moment data. As the solar wind is not the main target for *MMS*, the plasma measurements from *FPI* are not optimized for that environment. To better understand the limitations of *MMS* data, a comparison was performed between the *MMS* plasma data and the *OMNI* plasma measurements. The *OMNI* measurements come from the *Wind* or the *ACE* spacecraft, which are designed for the solar wind and are a perfect reference measurement for comparison.

The results show that the ion density is underestimated by *MMS* (see figure), whereas the electron density and ion velocity are well estimated. On the other hand, the ion temperature is overestimated by up to four times the value from *OMNI*. The results presented suggest that the best practice for using *MMS* in the solar wind is that the electron density should be used as opposed to the ion density. The ion velocity can be used if spacecraft spin effects are removed. Finally, the ion temperature should not be used for the calculation of plasma parameters such as plasma beta (the ratio of thermal to magnetic pressure); *OMNI* data should be used instead of *MMS*.

Roberts et al., J. Geophys. Res., 125, e2021JA029784, 2021.

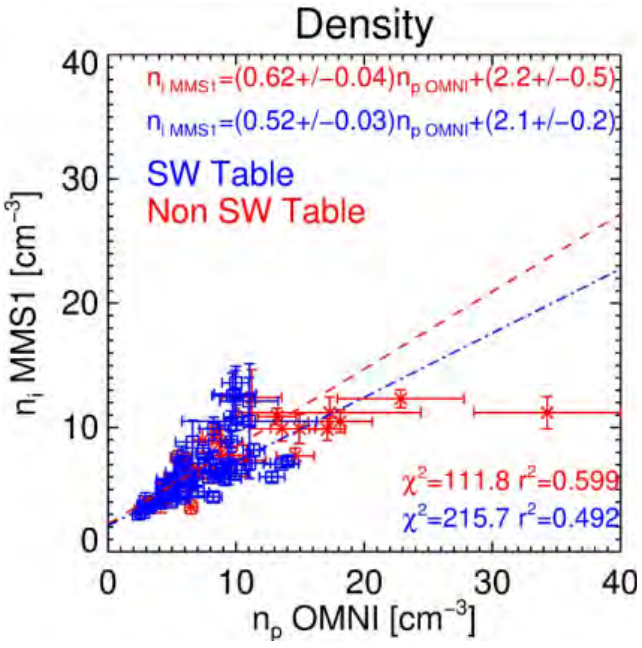

Comparison of the *MMS FPI* ion density measurement and the *OMNI* proton measurement. The blue points denote data using the *MMS* solar wind mode and red points the magnetosheath mode. χ^2 is the goodness of fit and r^2 the regression coefficient. These data show that the *FPI* density with both the solar wind and non-solar wind tables is underestimated with slopes of 0.52 and 0.62, respectively.

CSES

The *China Seismo-Electromagnetic Satellites (CSES)* are scientific missions dedicated to the investigation and monitoring of varying electromagnetic fields and waves as well as plasma parameters and particle fluxes in the near-Earth space, which are induced by natural sources on ground like seismic and volcanic events.

After the successful launch of the first satellite *CSES-1* in February 2018, the second satellite *CSES-2 i*s scheduled for launch in the beginning of 2023. It will be in the same Sun-synchronous circular low Earth orbit as *CSES-1*, with a local time of the descending node at 2 pm, but with a phase difference of 180 degrees. The combined observations of both satellites will double the detection probability of natural hazard-related events and will help to separate seismic from non-seismic events.

The *CSES* magnetometers, which are nearly identical on both spacecraft, have been developed in cooperation between the Chinese National Space Science Center (NSSC), the Institute of Experimental Physics of Graz University of Technology (TUG), and IWF. NSSC is responsible for the dual sensor fluxgate magnetometer, the instrument processor and the power supply unit, while IWF and TUG participate with the newly developed absolute scalar magnetometer, called *Coupled Dark State Magnetometer (CDSM).*

In 2021, the flight instrument for *CSES-2* was assembled and tested to make it ready for delivery to China in the beginning of 2022. Mandatory acceptance tests of the flight sensor included vibration and thermal cycling in vacuum.

Like in the years before, the magnetometer sensors of *CSES-1* operated continuously in good health. Ionospheric magnetic field variations at low Earth orbit (LEO) altitudes from the space based *CSES-1* magnetometer together with data from ESA's three spacecraft *Swarm* fleet were used to investigate natural hazards. In particular large earthquakes and volcanic eruptions are able to generate atmospheric waves which can propagate up to ionospheric heights and couple there to the ambient plasma, i.e., field- and particle-properties are modified in the satellite overflight trajectory. In terms of *CSES-1* spatio-temporal magnetic field patterns before and after the earthquakes Severo-Kurilsk (magnitude M6.5), Russia; Rio Caribe (M7.3), Venezuela; Ndoi Island (M8.2), Fiji; and Ridgecrest (M7.1), USA were analyzed. In most of the presented cases and events the statistical results, bolstered by a certain significance level, showed a change in the pattern between pre- and post-event periods.

Schirninger et al., Remote Sens., 13, 2360, 2021.

GEO-KOMPSAT-2A

GEO-KOMPSAT-2A (GEOstationary KOrea Multi-Purpose SATellite-2A) is a South Korean meteorological and environmental satellite in geostationary orbit at 128.2° East, which also hosts a space weather environment monitoring system. The Korean Meteorological Administration managed the implementation of the satellite, launched in 2018, and the necessary ground segment. The space weather observations aboard *GEO-KOMPSAT-2A* are performed by the Korean Space Environment Monitor (KSEM), which was developed under the lead of the Kyung Hee University. It consists of a set of particle detectors, a charging monitor and a four-sensor *Service Oriented Spacecraft MAGnetometer (SOSMAG).*

The *SOSMAG* development was initiated and conducted by ESA as part of the Space Situational Awareness program and built by the *SOSMAG* consortium: IWF, Magson GmbH, Technische Universität Braunschweig, and Imperial College London. The *SOSMAG* instrument is a "ready-to-use" magnetometer avoiding the need of imposing magnetic cleanliness requirements onto the hosting spacecraft. This is achieved through the use of two high quality fluxgate sensors on an approximately one meter long boom and two additional magneto-resistive sensors mounted within the spacecraft body. The measurements of the two inner-spacecraft sensors together with the inner boom sensor enable an automated correction of the outer boom sensor measurement for the dynamic stray fields from the spacecraft.

During the third year of operation, flight data verification, in-flight calibration and operation support were continued. In parallel, the *SOSMAG* team worked on the accuracy verification of the offset calibration parameters with a period of more than one day. Via the comparison with the Tsyganenko Earth's field model it could be demonstrated that the required accuracy of 10 nT has been achieved.

SOSMAG data are publicly available via the Space Weather Service Network of ESA's Space Safety program at swe.ssa.esa.int.

The South Korean satellite *GK-2A* in orbit around the Earth (© KARI).

FORESAIL-2

FORESAIL is a CubeSat program conducted by Aalto University in the frame of the Finnish Centre of Excellence in Research of Sustainable Space. *FORESAIL-2*, as the second mission in this program, is planned for launch into a geostationary transfer orbit (GTO) in 2023. The technology demonstration goal of this mission is to survive the harsh radiation of the Van Allen belt using low cost components and a fault-tolerant software approach. In addition, a Coulomb-drag experiment shall demonstrate safe de-orbiting from orbits with high apogee.

The characterization of the variability of ultra-low frequency (ULF) waves and their role in energizing particles in the inner magnetosphere are the core scientific objectives of *FORESAIL-2*. This shall be achieved by in-situ measurements of the magnetic field as well as relativistic electrons and protons.

In cooperation with the Institute of Electronics of Graz University of Technology, IWF contributes a miniaturized magnetometer, which will be based on a newly developed microchip for the readout of the triaxial magnetic field sensor. In 2021, the preliminary design of the magnetometer was finalized, the layout of the prototype microchip was finished and delivered to XFAB Silicon Foundries for fabrication. The development of an Engineering as well as an Interface-Verification Model was started.

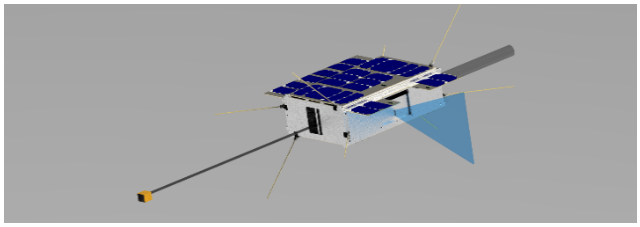

Rendering of *FORESAIL-2* with the magnetometer boom in the lower left corner (© Aalto University and Foresail consortium).

MACAO SCIENCE SATELLITE

Macao Science Satellite 1 was initiated by the State Key Laboratory of Lunar and Planetary Science at the Macau University of Science and Technology and is being implemented with support from the China National Space Administration and the local government. It is the world's first and only scientific satellite to be placed in a near-equatorial orbit to study the geomagnetic field, and specifically the South Atlantic Anomaly, from space. The launch is scheduled for the end of 2022.

The South Atlantic Anomaly is an area with a significantly weakened geomagnetic field and associated increased radiation activity. Its center lies over Brazil and its eastern coast. The inner of the two Van Allen radiation belts extends to about 700 kilometers from the Earth at the equator. In the region of the South Atlantic Anomaly, it comes much closer to Earth. Together with ESA's *SWARM* mission, launched in 2013, the South Atlantic Anomaly, which is widening and deepening, will be explored and measured in greater detail than ever before.

The scientific payload consists of a high-energy particle detector, a star tracker, a fluxgate magnetometer, and a scalar magnetometer. The sensor and sensor-related electronics of the scalar magnetometer are contributed by IWF in cooperation with the Institute of Experimental Physics of Graz University of Technology. The flight instrument is a replica of the instrument for the *CSES-2* satellite. The development of the processor and power supply electronics for the scalar magnetometer as well as its overall integration and testing are carried out by the Harbin Institute of Technology, Shenzhen. In 2021, the flight model of the scalar magnetometer (see figure below) was assembled, tested and delivered to China.

Flight model of the scalar magnetometer before delivery to China (© *CDSM* Team / A. Pollinger, https://w.wiki/4kq5, CC BY 4.0).

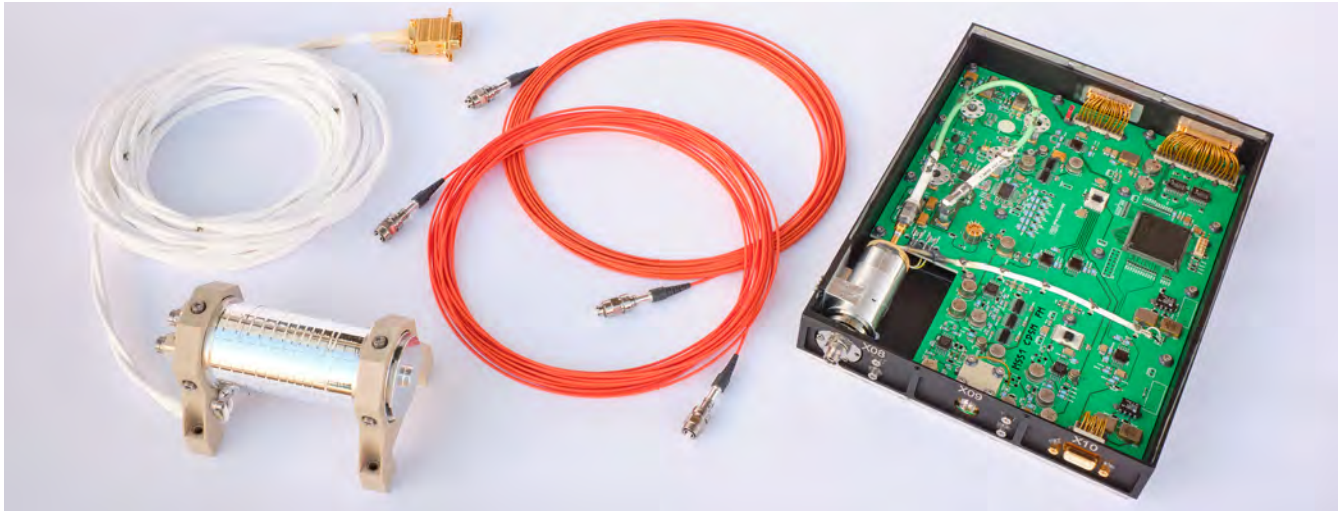

SMILE

The *Solar wind Magnetosphere Ionosphere Link Explorer (SMILE)* is a joint mission of ESA and the Chinese Academy of Sciences (CAS), scheduled for launch in 2024. It aims to complete our understanding of the Sun-Earth connection by measuring the solar wind and its dynamic interaction with the magnetosphere. IWF participates in two instruments: the *Soft X-ray Imager (SXI)*, led by the University of Leicester, and the magnetometer *(MAG)*, led by CAS.

The institute, in close cooperation with international partners, contributes the instrument's control and power unit *EBOX* for *SXI*. IWF is coordinating the development and design of the Digital Processing Unit (DPU) and is responsible for the mechanical design and the tests at box level.

In addition to hardware activities, IWF is participating in the preparation of the science working group activities such as modeling and in-situ measurements.

SPACE WEATHER FOLLOW-ON

The *Space Weather Follow-On (SWFO)* mission is a joint undertaking by NASA and the National Oceanic and Atmospheric Administration (NOAA). The satellite will collect solar wind data and coronal imagery to support NOAA's mission to monitor and forecast space weather events.

The *SWFO* satellite will orbit the Sun at approximately 1.5 million kilometers from Earth in Lagrange point 1. At this point the gravitational and centrifugal forces of Sun and Earth balance each other, which makes it an ideal place for observing the Sun.

The Southwest Research Institute together with two sub-contractors at the University of New Hampshire, Durham, and IWF design, develop, integrate, and calibrate the magnetometer instrument *SWFO-MAG*. It includes two three-axis magnetometers and associated electronics to measure the vector of the interplanetary magnetic field. IWF has the lead for the Sensor Controller Board, which hosts the front-end electronics for the two fluxgate sensors. A microchip, which has originally been developed for the *Magnetospheric Multi-Scale* mission, is the central component of the front-end electronics.

The main activities at IWF in 2021 covered the testing of a breadboard model, the design and test of the Engineering and Development Unit and the support of the Critical Design Review, which was successfully passed in December.

SMILE DPU Board (© OeAW/IWF/Steller).

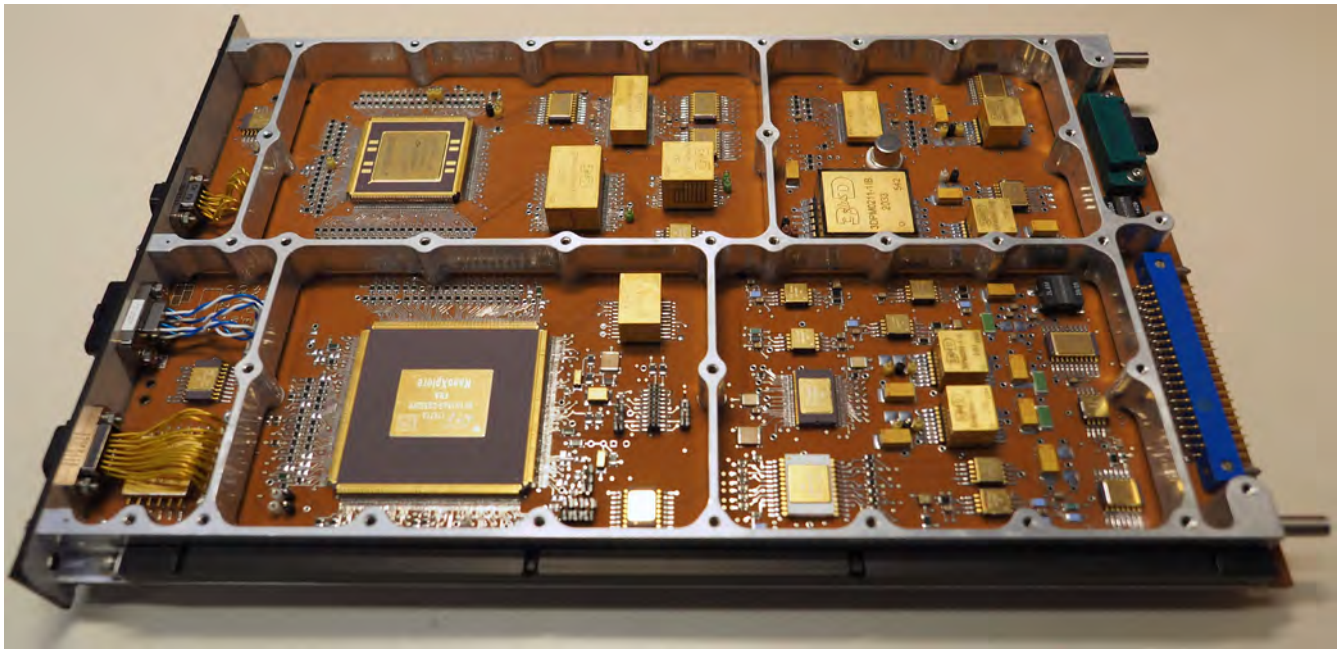

STATISTICAL STUDY OF LINEAR MAGNETIC HOLE STRUCTURES NEAR EARTH

The *Magnetospheric Multi-Scale (MMS)* mission data for eight months in the winter periods of 2017-2019, when *MMS* had its apogee in the upstream solar wind of the Earth's bow shock, are used to study linear magnetic holes (LMHs). They are characterized by a magnetic depression of more than 50% and a rotation of the background magnetic field of less than 10°. A total of 406 LMHs are found and, based on their magnetoplasma characteristics, are split into three categories: 1) cold, where there is an increase in density, and little change in ion temperature; 2) hot, where there is an increase in ion temperature, and a decrease in density, and 3) sign change, where at least one magnetic field component changes sign over the structure. The occurrence rate of LMHs is 2.3 per day. This is the first statistical study that shows that all LMHs are basically in pressure balance with the ambient plasma. Most of the linear magnetic holes are found in ambient plasmas that are stable against the generation of mirror-modes, but only half of the holes are mirror-mode-stable inside.

Volwerk et al., Ann. Geophys., 39, 239-253, 2021.

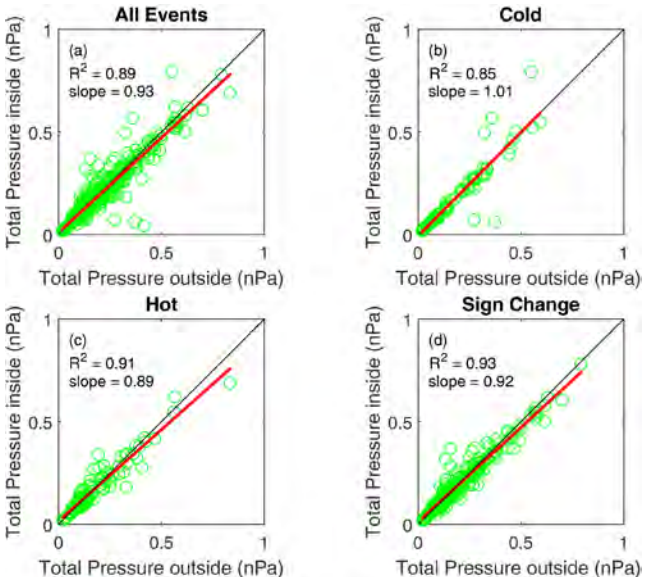

Pressure balance test across the structure of the linear magnetic holes. The total pressure is calculated at the center and outside of the structure. (a) Relation for all structures; the black line is the identity, and the red line is a fit to the points. Pressure balances follow for (b) the cold category, (c) the hot category and (d) the sign change category. The regression coefficients and the slopes are listed in the panels.

FAST CROSS-SCALE ENERGY TRANSFER DURING TURBULENT MAGNETIC RECONNECTION

Magnetic reconnection is a key fundamental process in collisionless plasmas that explosively converts magnetic energy to plasma kinetic and thermal energy through a rapid change of magnetic field topology in a central electron-scale region called the electron diffusion region (EDR). Past simulations and observations demonstrated that this process causes efficient energy conversion through the formation of multiple macro-scale (scales larger than ion-scales) and micro-scale (sub-ion or smaller scales) magnetic islands/flux ropes. However, the coupling of these phenomena on different spatiotemporal scales is still poorly understood. Here, based on a new large-scale fully kinetic particle-in-cell simulation with a realistic, initially fluctuating magnetic field, it was demonstrated that the macro-scale evolution of turbulent reconnection involving merging of macro-scale islands reduces the rate of reconnection and accordingly extends the EDR in the reconnection outflow direction. This EDR extension leads to a repeated, quick formation of new electron-scale islands within the EDR which soon grow to larger scales and eventually merge with the macro-islands (see figure). This turbulent, electron- to larger-scale island evolution causes an efficient cross-scale energy transfer from micro- to macro-scales, and leads to a strong electron energization within the growing islands.

Nakamura T.K.M. et al., Geophys. Res. Lett., 48, e2021GL093524, 2021.

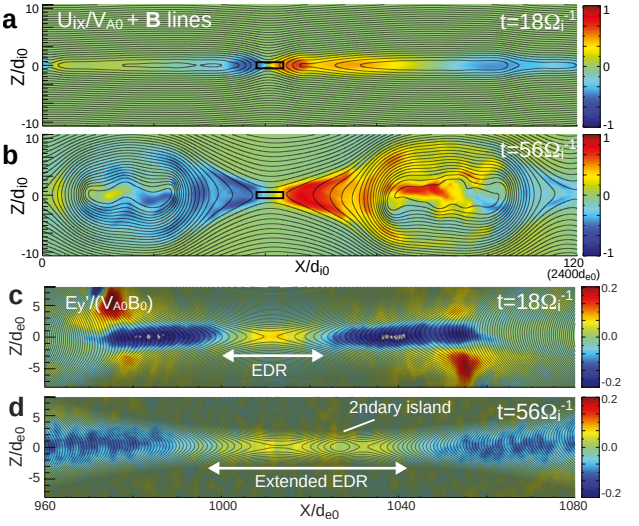

a + b: Color contours of outflow component of ion bulk velocity U_{ix}; c + d: Zoomed-in views near the EDR surrounding the most developed X-line before and after the macro-scale island merging (black boxes in a + b) of reconnection electric field E_y'. The positive E_y' in panels c + d indicates the EDR.

RECONSTRUCTION OF THE RECONNECTION KERNEL ZONE

In order to study the plasma process responsible for the magnetic field reconfiguration and transforming magnetic energy to kinetic and thermal energy of plasma in the magnetic reconnection region, using spacecraft data such as *MMS*, it is essential to infer the location of the spacecraft relative to the reconnection region by reconstructing the current sheet based on proper assumption and modeling of the overall reconnection site.

A new analytical model for Grad–Shafranov reconstruction of two-dimensional steady-state magnetic reconnection is developed for the kernel zone (electron diffusion region, EDR). For the first time, the effects of the electron inertia are regarded explicitly in the reconstruction model of such type by implementing multi-probe data analysis. The method is applied to the *MMS* data for previously studied events. The figure plots the results of reconstruction of the EDR encounter event of 11/07/2017 in the time span of 22:34:01.70-22:34:04.92 UT. It is found that the proper accounting of these effects is of major importance for the accurate reconstruction of the out-of-plane magnetic field component and the in-plane electron velocity. The model provides a self-consistent solution of the problem, depending neither on the out-of-plane component of the electron pressure tensor divergence nor on the reconnection electric field.

Korovinskiy et al., J. Geophys. Res., 126, e2020JA029045, 2021.

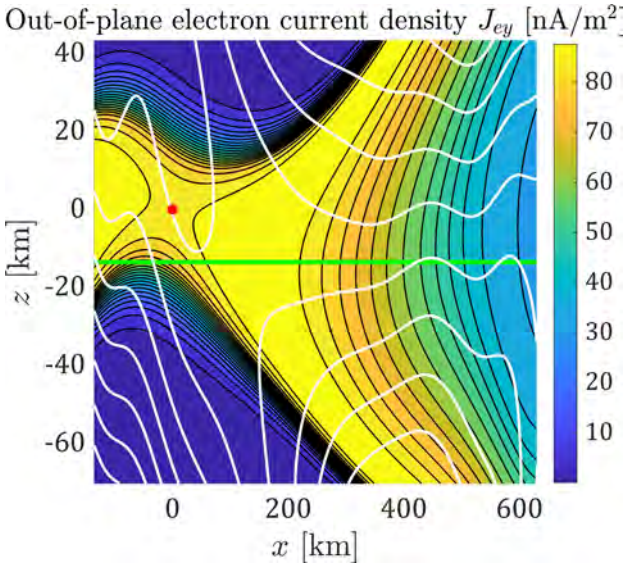

Visualization of the spatial structure of EDR obtained from the reconstruction method, for which its high accuracy is confirmed by comparing *MMS 1, 2,* and *4* data. The reconnection plane xz: the out-of-plane electron current density (color), the in-plane magnetic field lines (black contour curves), the electron in-plane streamlines (white curves), the *MMS 3* trajectory (green line), and the reconnection X-point (red dot).

REMOTE SENSING OF MAGNETIC RECONNECTION

Although magnetic reconnection is a process in which magnetic field energy is converted to particle energy in a small region, smaller than the plasma particles can complete its gyration, its signatures can be remotely detected due to the particles that are accelerated at the reconnection site and then injected along the field lines. These particle traveling along the field lines from the reconnection region can be remotely detected by spacecraft passing the separatrix region, which is the boundary between the reconnected and background field lines. The observed timing and location of these particles are expected to show differences depending on its energy and species.

Based on an observation by the four *MMS* spacecraft on 12 July 2018, the energy dispersion of the ions and electrons (see figure) is analyzed to deduce the characteristics of the remote reconnection. The remote sensing method further enabled an estimation of the reconnection electric field, which was initially 1.6-2.5 mV/m, and decreased to ~0.8 mV/m within ~20s.

Wellenzohn et al., J. Geophys. Res., 126, e2020JA028917, 2021.

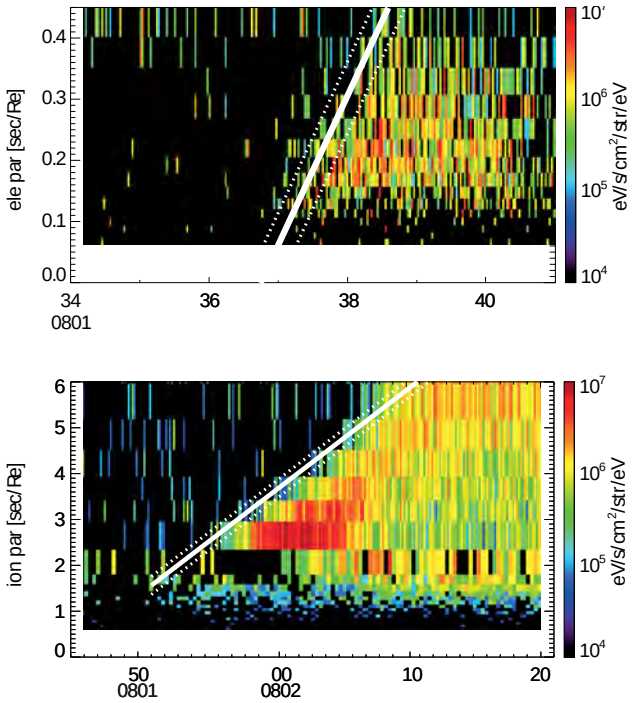

Energy dispersion of electrons (upper panel) and ions (lower panel). The linear fit of the dispersion is shown as solid white line. From the energy dispersion the location and time of the electrons or ions injection can be obtained, which was estimated to be 24 R_E downtail and at 08:01:36-08:01:42 UT for this particular event.

MAGNETIC RECONNECTION WITHIN THE BOUNDARY LAYER OF A MAGNETIC CLOUD IN THE SOLAR WIND

In a multi-point study both the large-scale helical magnetic geometry of a magnetic cloud (MC) and the structure of a magnetic reconnection (MR) outflow occurring within the boundary layer of an MC are analyzed in detail. The reconnected open field lines are expected to slip over the MC resulting in extended plasma mixing. The MR outflow channel is embedded into a large-scale vertical flow shear. The geometry and the motion of the structure provided a unique possibility to study the fluid- and kinetic-scale processes associated with MR in the solar wind. The main findings on MR include (a) first-time observation of non-Petschek-type slow-shock-like discontinuities in the inflow regions; (b) observation of turbulent Hall magnetic field associated with a Lorentz-force-deflected electron jet in the presence of a guide field (Bg); (c) acceleration of protons by reconnection electric field and their back-scatter from the slow-shock-like discontinuity in the sheath inflow region; (d) observation of relativistic electron population near the MC inflow boundary/separatrix; these electron populations can presumably appear as a result of nonadiabatic acceleration, gradient B drift, and via acceleration in the electrostatic potential well associated with the Hall current system; and (e) observation of Doppler-shifted ion-acoustic and Langmuir waves in the MC inflow region.

Vörös et al., J. Geophys. Res., 126, e2021JA029415, 2021.

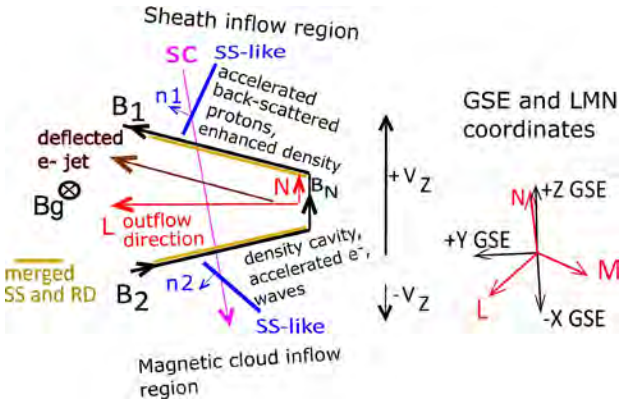

Left: Crossing of MR outflow in the LN plane. The structure is embedded into a vertical flow shear. The outflow boundaries are merged slow shocks (SS) and rotational discontinuities (RD). In the inflow regions SS-like discontinuities are developed as a consequence of interactions between the outflow and environment. Right: The reconnection LMN coordinates relative to the GSE coordinates. Here, L is the direction along the MR outflow, N is the normal direction to the current sheet and M is the "out-of-plane" direction along the MR X-line. GSE corresponds to the standard Geocentric Solar Ecliptic coordinate system.

MULTI-POINT MULTI-SCALE OBSERVATION OF A DIPOLARIZATION FRONT

In the near-Earth magnetotail localized fast flows, called bursty bulk flows (BBFs), are known to play an important role in transporting energy from the magnetotail reconnection site. These localized BBFs contain sharp enhancements in Bz (south-to-north component of the magnetic field) called dipolarization fronts (DF), which are considered an important site of energy conversion. Yet, due to its limited size in the dawn-dusk direction in a dynamic magnetotail, the study of the evolution of DFs requires multi-point multi-scale observations, where both the front and background magnetic disturbances should be monitored simultaneously.

Based on 2-point *Cluster* and 4-point *MMS* measurements, the evolution of localized fast flows and DFs was obtained by also modeling the changes in the background magnetotail current sheet from the dawn and dusk side of a localized plasma flow as illustrated in panel a. The profiles of the electron energy spectra up to about 10 keV, observed by both spacecraft (panel b), showed difference in the acceleration rate (panel c), which is consistent due to adiabatic electron acceleration from a dawn-dusk localized source region in agreement with the localization of BBF.

Nakamura R. et al., J. Geophys. Res., 126, e2021JA029518, 2021.

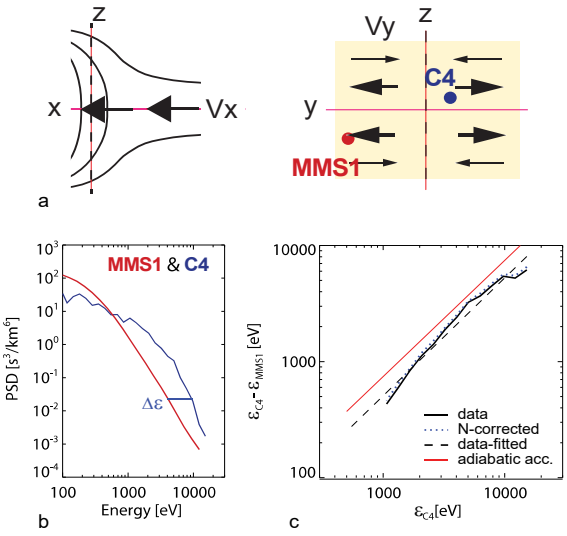

Electron observations at dipolarization front by *MMS* and *Cluster*. a: Schematics of localized fast flow and spacecraft location relative to the flow; arrows show flow vectors in X-Z (left) and Y-Z plane (right) in Geocentric Solar Magnetospheric coordinates. *MMS* and *Cluster* are located on almost the same Y-Z plane of the localized flow at duskside and dawnside of the flow center (dashed line).
b: Phase space density profile of the electrons at *MMS1* and *Cluster 4* observed just after the dipolarization front.
c: Comparison of differences in acceleration rate at *MMS1* and *C4* with those expected from adiabatic acceleration. The acceleration rate obtained from *MMS1* and *C4* data (black line) tends to become more deviated from adiabatic acceleration (red) for higher energy as expected from localized source region confined in the flow.

VLF SPECTRAL ANALYSIS ONBOARD THE CSES SATELLITE

China's Seismo-Electromagnetic Satellite (CSES) was launched in February 2018. It has an altitude of about 507 km in a polar and circular sun-synchronous orbit with local time nodes of 02 LT and 14 LT. The *Electric Field Detector (EFD)* was used to investigate the variations of VLF ground-based transmitter signals. This instrument has four spherical sensors deployed by booms at a distance of four meters from the satellite's body. A large frequency range is covered by the *EDF* experiment, separated into four bands: HF (18 kHz - 3.5 MHz), VLF (1.8 - 25 kHz), ELF (6 Hz - 2.2 kHz), and ULF (DC - 16 Hz).

The signal emitted by the North West Cape (NWC) transmitter located in Australia at 21.5° S and 114° E was studied. The figure displays NWC flux density variation as recorded by the *CSES* satellite during four weeks in September 2019. One can see that the NWC signal is continuously detected by the *EFD/CSES* experiment. Maxima of VLF radio signals occurring each five-days have been found, when the satellite is above the NWC ground-based station. In addition, one finds VLF signal enhancements at the NWC conjugate point and amplitude signal minima when the satellite is crossing the Earth's equatorial plane. In this study, the solar radio flux at 10.7 cm, adjusted to 1 au was also considered. The degree of correlation has been calculated and found to be in the order of 5% for the three key regions but increases to 20% when all satellite latitudes are considered. The correlation between the F10.7 flux and the NWC signals was on the order of 5% for the three key regions and increases to 20% for the full dataset.

Boudjada et al., Proc. Kleinheubach Conf., 3 pp, 2021.

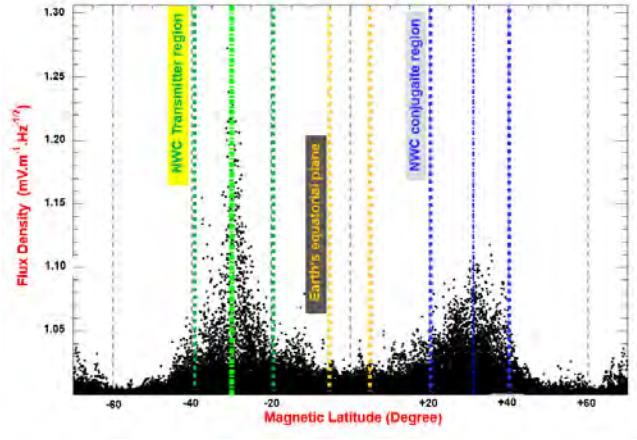

VLF flux density ($mV.m^{-1}.Hz^{-1/2}$) variation versus Earth's magnetic latitude. Three main regions have been considered: (a) above the NWC transmitter station (green-dashed box), at the NWC conjugate point (blue-dashed box), and (c) in the equatorial plane (orange-dashed box). From the figure the power radio wave heating of the ionospheric D-layers above NWC transmitter and at its conjugate point can be obtained.

TRANSIENT PARTICLE ACCELERATION BY A DAWN–DUSK ELECTRIC FIELD IN A CURRENT SHEET

The influence of a dawn-dusk electric field, E_y, on transient particles in a 1D current sheet (CS), characterized by the normal (B_z) and tangential (B_x) components of the magnetic field, was studied. The motion and energization of particles injected at the edges of the CS were investigated within the framework of a trajectory method. The analytical treatment reveals that in the case of uniform B_z and E_y, the dynamics of transient particles is described by magnetic flux conservation on specific segments of the trajectory, which allows prediction of some specific properties of the velocity space inside the CS.

Verification of the analytical treatment by means of test-particle numerical modelling demonstrates good agreement. In particular, it was shown that the CS can play the role of a converging lens that focuses particles around pitch-angle values $\theta \sim \pi$. The analysis reveals that the particle energy gain stays within the range of $\Delta W \in 2\ m[(E_y/B_z)^2, (E_y/B_z)(v_0 + E_y/B_z)]$, where m is the particle mass and v_0 is the module of the initial particle velocity. The limits of the energy gain range depend only weakly on the CS half-thickness. According to performed estimations, for the typical parameters of E_y and B_z in the stationary terrestrial magnetotail, protons with $v_0 \simeq 450$ km/s (before CS crossing) can be accelerated along the CS up to $V_x \simeq 1800$ km/s.

Sasunov et al., Phys. Plasmas 28, 042902, 2021.

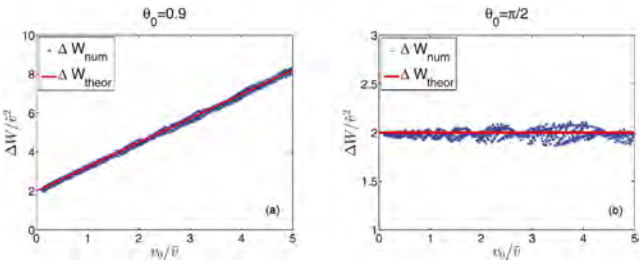

Analytical ΔW_{theor} (red) and numerically simulated ΔW_{num} (blue dots) estimates of the particle energy gain in the current sheet with a half-thickness $L = v/\omega_{gyr}$, as function of the particle initial speed v_0 for different values of pitch angle θ_0. The numerical values are distributed along the analytical curve, the energy gain is a linear function of v_0 in case the pitch angel $\theta_0 < \pi/2$ (a), whereas for particles with $\theta_0 = \pi/2$ the energy gain does not depend on the initial particle energy (b).

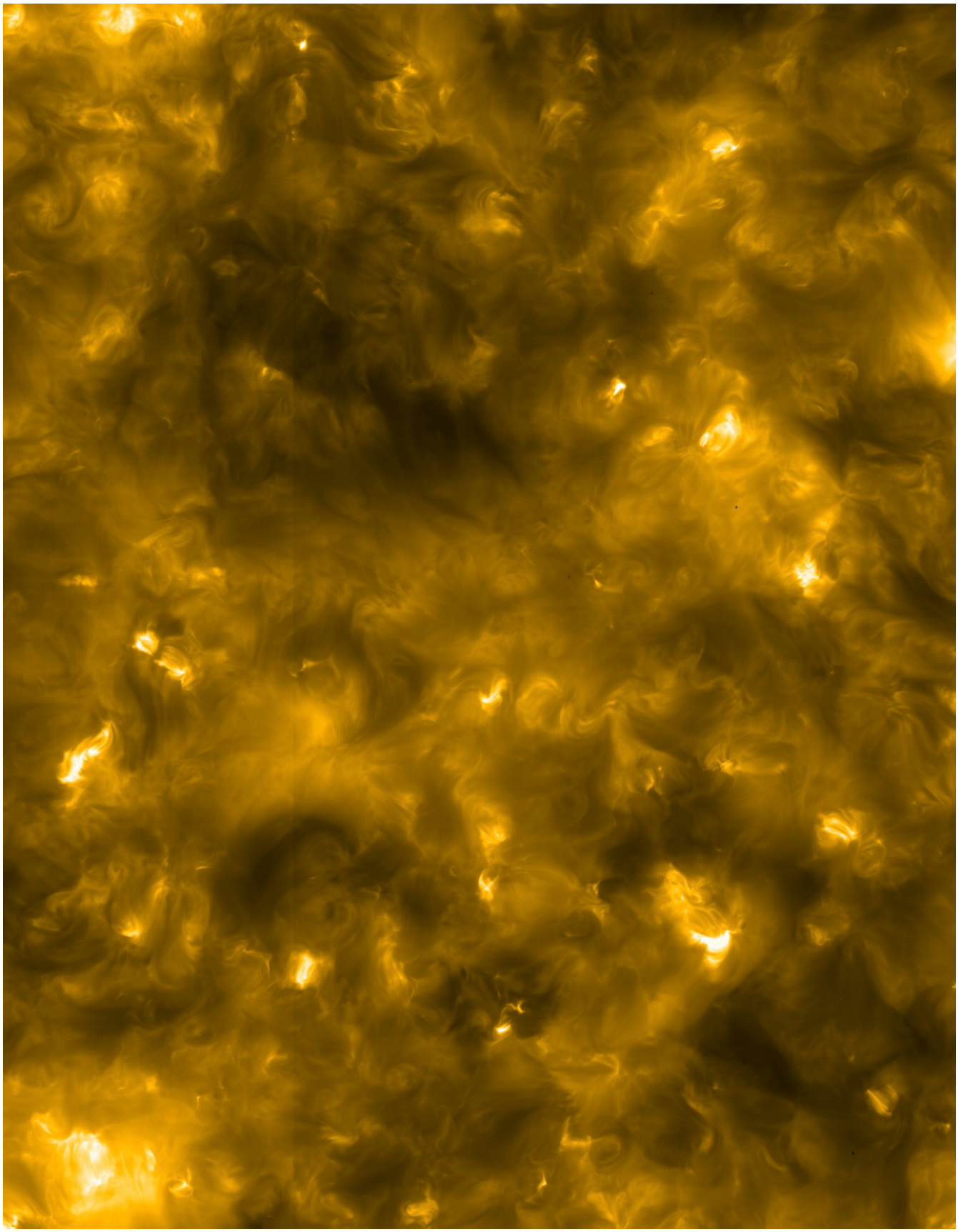

Image of the Sun's outer atmosphere, the corona, taken with the *Extreme Ultraviolet Imager* instrument onboard *Solar Orbiter* (© *Solar Orbiter/EUI* Team/ESA & NASA).

SOLAR SYSTEM

IWF is involved in many international space missions, experiments and corresponding data analysis addressing solar system phenomena. The physics of the Sun and the solar wind, its interaction with the magnetospheres, upper atmospheres or surfaces of solar system planets and bodies are under investigation. Furthermore, theoretical studies related to comparative planetology and space plasma physics between solar system planets and discovered exoplanets are also carried out for understanding the early and later evolution of Venus, Earth and Mars.

SUN & SOLAR WIND

The Sun's electromagnetic radiation, magnetic activity, and the solar wind are strong drivers for various processes in the solar system.

SOLAR ORBITER

Solar Orbiter is an ESA-led space mission with NASA participation to investigate the Sun. Flying a novel trajectory, with partial Sun-spacecraft corotation, the mission studys in-situ plasma properties of the inner solar heliosphere and to observe the Sun's magnetized atmosphere and polar regions. Its operational orbit will be a high elliptical orbit with perihelion at 0.28 au.

In February 2021 *Solar Orbiter* had its frist close approach to the Sun within 0.5 au. It performed two planetary flyby maneuvers, to get onto the right course for the rendezvous with the Sun. On 9 August, it passed Venus at a distance of 7995 km. Not much later, on 27 November, the spacecraft turned the last time around the Earth with a closest approach of just 460 km.

IWF built the Digital Processing Unit (DPU) for the *Radio and Plasma Waves (RPW)* instrument and calibrated the *RPW* antennas, using numerical analysis and anechoic chamber measurements. Furthermore, the institute contributed to the fluxgate magnetometer *(MAG)*.

RPW will measure the magnetic and electric fields at high time resolution and determine the characteristics of magnetic and electrostatic waves in the solar wind from almost DC to 20 MHz. Besides the 5 m long antennas and the AC magnetic field sensors, the instrument consists of four analyzers: the thermal noise and high frequency receiver, the time domain sampler, the low frequency receiver, and the bias unit for the antennas. The control of all analyzers and the communication will be performed by the DPU.

During the two flybys at Venus and Earth, *RPW* and *MAG* were switched on to make measurements of both magnetospheres. During the Earth flyby there was a unique configuration of more than a dozen spacecraft from five missions. *Solar Orbiter*, *Cluster*, *MMS*, *THEMIS* and *SWARM* performed simultaneous measurements. The data processing for both flybys is still going on.

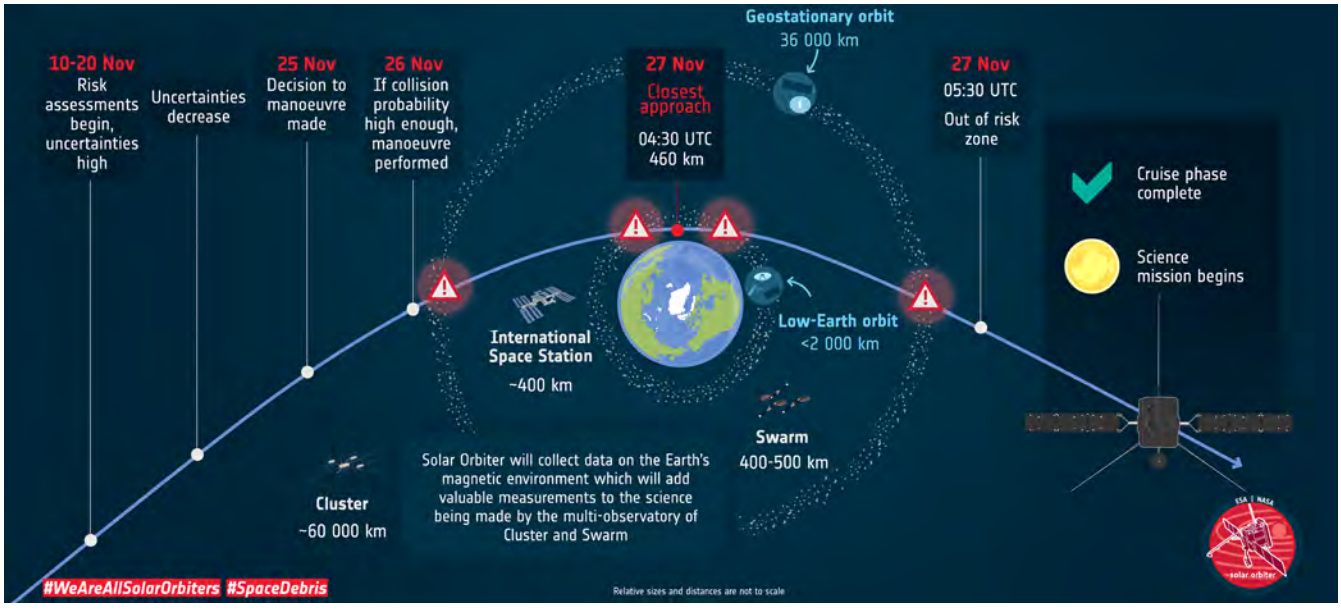

Solar Orbiter's crucial Earth flyby on 27 November 2021 placed the spacecraft onto the correct orbit for its science phase to begin (© ESA).

MERCURY

Mercury is at the center of attention because of the ESA/JAXA *BepiColombo* mission. The planet has a weak intrinsic magnetic field and develops a mini-magnetosphere, which strongly interacts with the solar wind.

In 2021, *BepiColombo* performed two planetary flybys. It visited Venus in August and had its first encounter with its final target Mercury in October.

BEPICOLOMBO

The European-Japanese spacecraft, launched 2019, is on its way to Mercury. *BepiColombo's* trajectory is bent towards the Sun and its velocity is decreased during nine gravity-assist maneuvers (GAM) such, that the spacecraft finally can reach its Mercury orbit insertion point at the end of 2025. GAMs - also known as flybys, swingbys or gravitational slingshots - use the gravitation of a planet or other astronomical objects to alter the path and speed of a spacecraft without using thrusters and propellant.

Two of such flybys took place in 2021. On 10 August, *BepiColombo* visited Venus for its second (and last) time. The spacecraft approached the surface of the planet as close as ~552 km, while hovering just above its ionosphere. And about six weeks later, on 1 October, the spacecraft flew by its targeted destination, planet Mercury, with a distance of ~200 km, for the first time.

The spacecraft traveled through the dynamic magnetosphere of Mercury, looking into the properties of its various plasma regions. Many sensors, including the three payloads with an IWF hardware contribution on both the European *Mercury Planetary Orbiter (MPO)* and the Japanese *Mercury Magnetospheric Orbiter (MMO/ Mio)* took the chance for early in situ measurements. *PICAM* was operated for about 40 hours during the second Venus flyby, and for about 24 hours during the first Mercury flyby. Beside the scientific output, the operations are also always a very good occasion to fine-tune the procedures for instrument commanding and data retrieval.

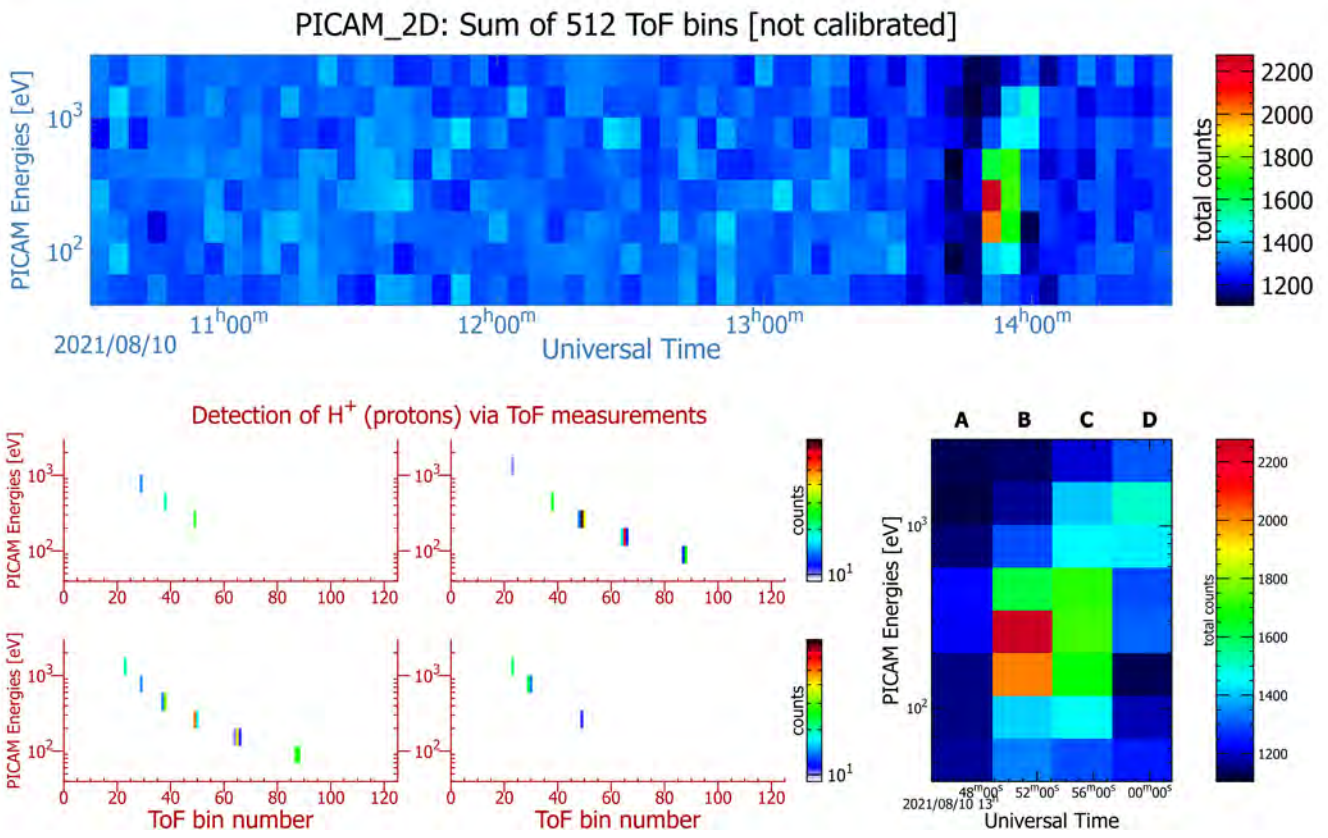

An example of *BepiColombo* observations during its second Venus flyby. The top panel shows the ion spectrogram from *PICAM* at the closest approach and the bottom panels show the corresponding time-of-flight (ToF) of the ions. *PICAM* successfully detected ions species, predominantly hydrogen.

Between the two flybys, *BepiColombo* was cruising in the solar wind, and *PICAM* did a number of performance test, as well as collecting valuable scientific solar wind data. The observations by *PICAM* during both flybys, and also the cruise phase have gained high attention from the planetary scientific community, and as a result, a number of potential publications are currently in preparation.

The *MMO-MGF* (IWF PI-ship) magnetometer with its two sensors on the still stowed boom was switched on during the flybys and other campaigns for cruise observations and instrument check-outs. The *MPO-MAG* (IWF technical management) magnetometer with both sensors on the already deployed boom has been monitoring the magnetic field almost continuously.

MPO-MAG data have again been widely used for scientific evaluation of magnetospheric features especially during the second Venus flyby and interesting structures of the solar wind.

During the Mercury flyby, data from both magnetometers are affected by magnetic disturbances coming from the spacecraft constellation. A dedicated cleaning of the data based on combining data from both magnetometers has been initiated to make good quality data available for scientific work in 2022.

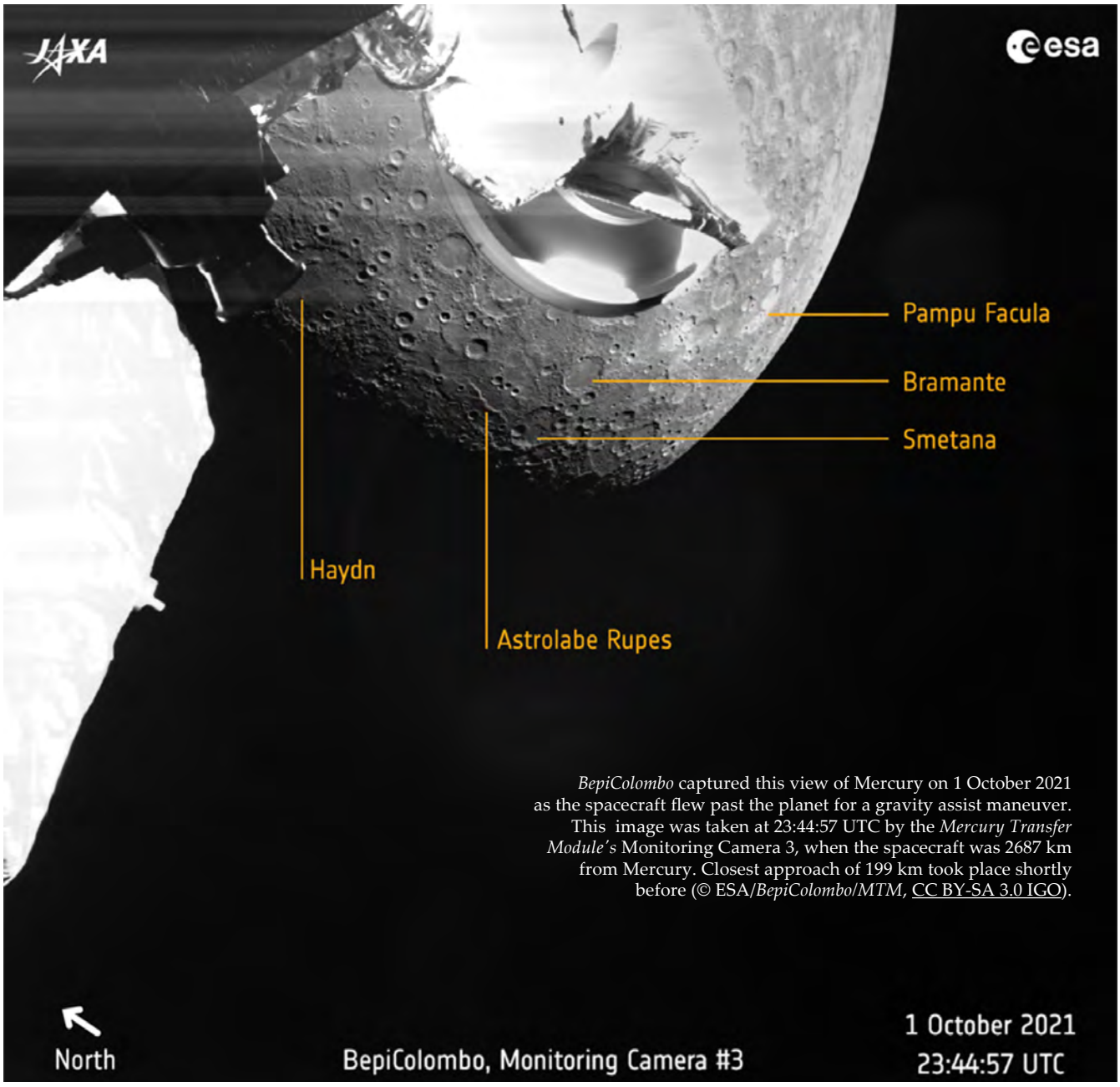

BepiColombo captured this view of Mercury on 1 October 2021 as the spacecraft flew past the planet for a gravity assist maneuver. This image was taken at 23:44:57 UTC by the *Mercury Transfer Module's* Monitoring Camera 3, when the spacecraft was 2687 km from Mercury. Closest approach of 199 km took place shortly before (© ESA/*BepiColombo/MTM*, CC BY-SA 3.0 IGO).

PICK-UP IONS AT MERCURY

Mercury possesses a magnetic field, which constitutes an obstacle to the supersonic solar wind. Upstream of the planet a bow shock emerges where the supersonic solar wind is slowed down and then flows into the magnetosheath. Mercury has an exosphere, which contains species that originate from the surface and impacting micrometeoroids. These neutral particles are ionized by the UV flux of the Sun, and will then be picked-up by the solar wind. Because the freshly picked-up particles have a different velocity than the solar wind, the solar wind plasma becomes unstable for the generation of plasma waves, particularly for ion cyclotron waves (ICWs). For the first time ICWs generated by the pick-up of H^+ at Mercury are reported. The spatial occurrence rate of the 5455 identified ICWs is shown in the figure below in Mercury Solar Magnetospheric (MSM) coordinates. They are detected over a wide spatial range, where 73% of the observed ICWs are located in the solar wind and 27% in the magnetosheath, indicating that Mercury possesses an extended hydrogen exosphere.

From the findings it can be deduced that in the solar wind the ICWs are excited by the ion resonant beam instability and in the magnetosheath from the ring-beam. To understand the difference of their excitation, these waves should be studied on basis of plasma observations from the *BepiColombo* mission.

Schmid et al., Geophys. Res. Lett., 48, e2021GL092606, 2021a.

Schmid et al., Ann. Geophys., 39, 563–570, 2021b.

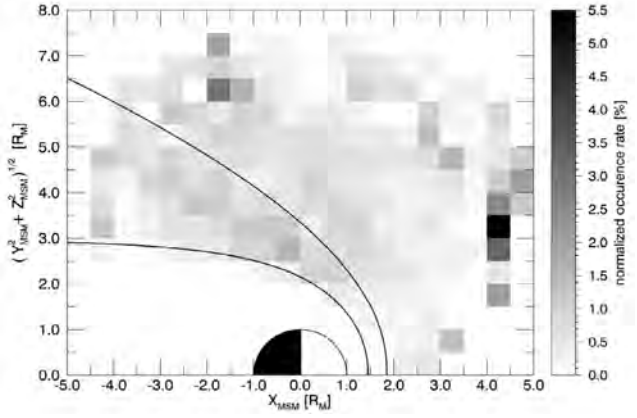

Occurrence rate of the 5455 identified ion cyclotron waves (ICWs), normalized by the *MESSENGER* dwell time. The black lines illustrate the bow shock and magnetopause obtained from the models by Slavin et al. (2009) and Korth et al. (2015). The gray lines depict the flowlines obtained from the Schmid et al. (2021b) magnetosheath plasma flow model. From the ubiquitous occurrence of ICWs around Mercury, it is therefore concluded that (1) Mercury possess an extended hydrogen exosphere and that (2) photoionization is afforded an important role in the hydrogen loss process.

ERROR ESTIMATE FOR CALIBRATED FLUXGATE MAGNETOMETER DATA IN SPACE PLASMA

The fluxgate magnetometers operate with a set of coils, often mounted on a boom extending (over several meters) from the spacecraft body to minimize the interference from spacecraft-generated fields. Like most of the other scientific instruments, the fluxgate magnetometers need to be calibrated against the standard. There are uncertainties in the magnetometer (in-flight) calibration associated with the coil properties (offset levels) and the angular deviation of sensor directions from the ideal (e.g., orthogonal) set-up. It is beneficial in space plasma observational studies to know the systematic error behavior in the (in-flight) calibrated magnetometer data.

The error estimate study was performed, finding that the magnitude of the magnetic field with respect to the offset error and the angle of the magnetic field to the spacecraft spin axis play an important role. The offset uncertainties are the major factor in a low-field environment, while the angle uncertainties (rotation angle in the spin plane, sensor non-orthogonality, and sensor misalignment to the spacecraft reference directions) become more important in a high-field environment in a proportional way to the magnetic field. The error estimate study serves as a useful tool in designing higher-precision magnetometers for future spacecraft missions as well as in developing novel data analysis methods in geophysical and solar system science.

Narita et al., Geosci. Instrum. Method. Data Syst., 10, 13-24, 2021.

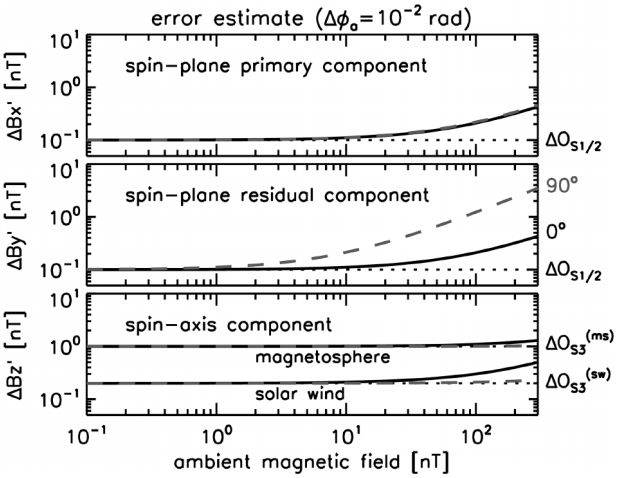

In-flight calibration error of the *BepiColombo* magnetometer *MMO-MGF*. Solid curves are for the axial ambient field. Dashed curves are for the spin-plane ambient field.

VENUS & MARS

Venus and Mars are the Earth's nearest inner and outer planetary neighbors, respectively. Venus orbits the Sun at 0.7 au in 224 days, has a radius slightly smaller than the Earth, and has a very dense atmosphere. Mars orbits the Sun at 1.5 au in 687 days, has about half the radius of the Earth, and has a very tenuous atmosphere.

Both planets do not have an internal magnetic field, although Mars does show remnant surface magnetization, which might indicate that the planet used to have a functioning dynamo. Through the interaction of Venus and Mars with the solar wind, however, a so-called induced magnetosphere is created.

Two spacecraft made historic flybys of Venus on 9 and 10 August 2021. *Solar Orbiter* and *BepiColombo* both used the planet for gravity assists within 33 hours of each other, capturing unique imagery and data during their encounters. The *Solar Orbiter* plasma package showed clear evidence of magnetic reconnection in the far tail.

TIANWEN-1

Tianwen-1 ("questions to heaven") is China's first Mars mission, consisting of an orbiter and a rover named *Zhurong*. Before *Zhurong* only NASA has successfully landed and operated spacecraft on Mars. The mission is designed to conduct a comprehensive remote sensing of the Red Planet, as well as surface investigations. IWF contributed to a magnetometer aboard the orbiter.

Several milestone events occurred in 2021 for this mission: the successful orbital insertion on 10 February, the landing of *Zhurong* on 14 May, the magnetometer boom deployment on 25 May, and the switch-on for continuous operation and observations on 13 November.

Two operational modes were selected for the *Mars Orbiter MAGnetometer (MOMAG)*: 32 Hz for 120 min around periapsis and for 60 min around apoapsis, and 1 Hz for the rest of the 8-hour orbit. *MOMAG* demonstrated good performance, nevertheless preliminary measurements indicated various spacecraft magnetic effects due to the lack of a magnetic cleanliness program and the rather short 3.2 m boom. The two-sensor gradiometer formation, where the outboard sensor is located at the end of the boom and the inboard sensor at 0.9 m from the outboard, is used to remove the spacecraft magnetic effects in order to obtain cleaned scientific data.

China's first Mars rover, *Zhurong*, is pictured next to its landing platform on the surface of the red planet. The rover traveled approximately 10 meters to drop off a wireless camera, then backed up into frame in order to capture this spectacular image (© CNSA).

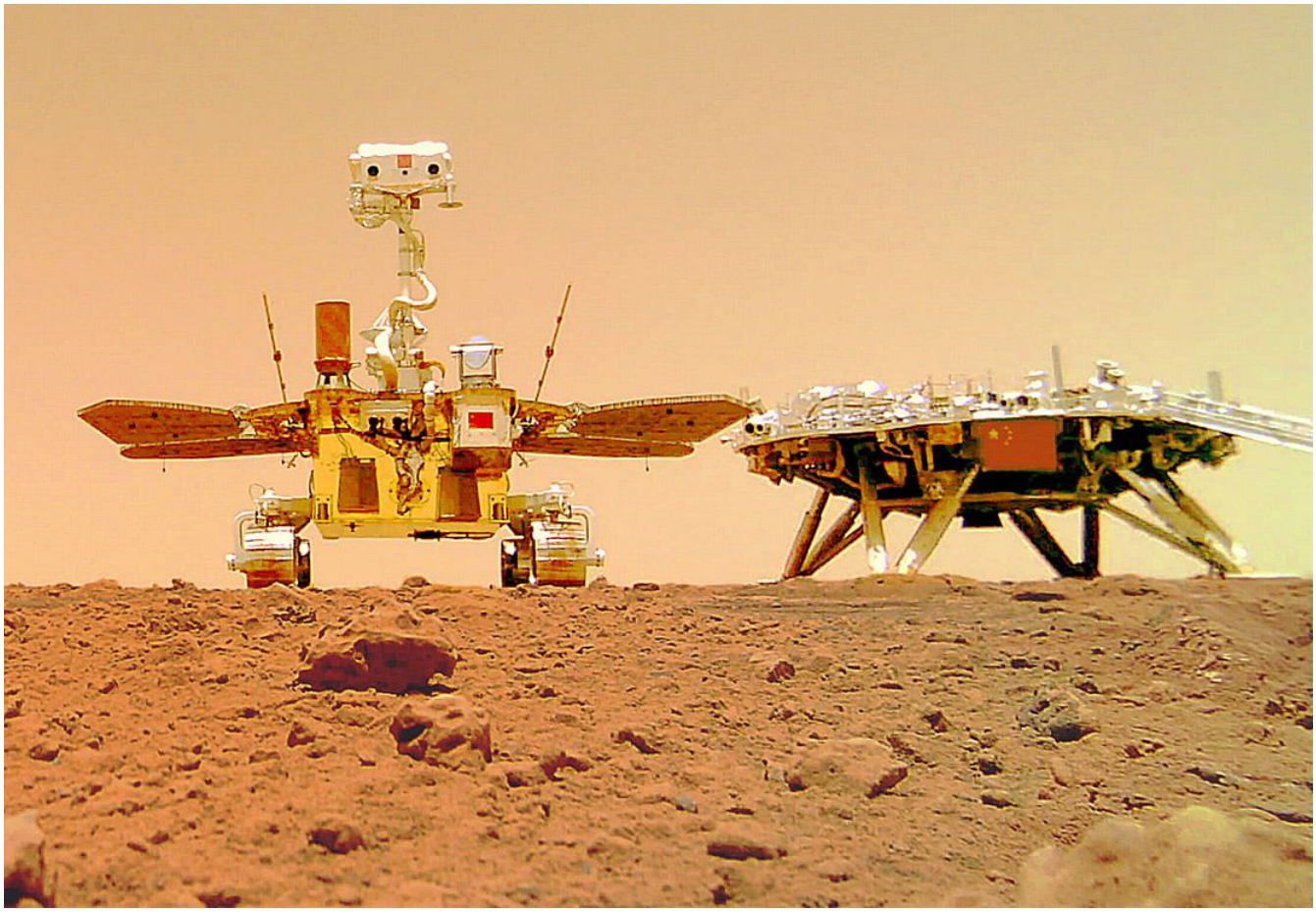

BEPI'S AND SOLO'S FIRST VENUS FLYBYS

The first of two Venus flybys that *BepiColombo* used as a gravity assist maneuver to finally arrive at Mercury, took place on 15 October 2020. After passing the bow shock, the spacecraft traveled along the induced magnetotail. The *Mercury Planetary Orbiter Magnetometer (MPO-MAG)* data were studied to investigate the structure of the induced magnetosphere. Behind the bow shock crossing, the magnetic field showed a draping pattern consistent with field lines connected to the interplanetary magnetic field wrapping around the planet: instead of pointing in a direction along the tail, the field was directed perpendicular to it. This different direction is caused by the field lines rotating away from the tail direction to remain connected with the interplanetary magnetic field direction. This flyby showed a highly active magnetotail, with e.g. strong flapping motions at a period of ~7 min. This activity was driven by solar wind conditions: Venus's magnetosphere was impacted by a stealth coronal mass ejection.

Later in the year, on 27 December, *Solar Orbiter* had its first flyby at Venus. This one took place in the opposite direction, flying along the tail towards the planet and exiting the bow shock across the north pole. Although the solar wind conditions were rather quiet, a lot of activity was observed in the tail. Using both the magnetometer data, the electron density from *RPW* and the *SpaceCraft Potential (SCP)*, and the energetic ion spectra from the *Energetic Particle Detector -Supra Thermal Electrons and Protons instrument (EPD-STEP)*, clear evidence was found for magnetic reconnection. This occurred far down the tail at ~21 RV. Closer to Venus, evidence was found for the presence of the tearing instability, which can cause reconnection.

Behind the quasi-perpendicular bow shock the expected mirror modes were not found, but instead ion cyclotron waves were measured at the proton cyclotron frequency. This happened because of the relatively low plasma-beta behind the bow shock. Interestingly, these waves changed frequency further down the tail. This is interpreted as a Doppler shift of the waves, caused by the acceleration of the plasma in the magnetosheath behind the bow shock. Using the observed frequencies, it was estimated that the magnetosheath plasma was accelerated to ~180 km/s at a down-tail location of ~55 RV.

Volwerk et al., Ann. Geophys., 39, 811-831, 2021.
Volwerk et al., Astron. Astrophys., 656, A11, 2021.

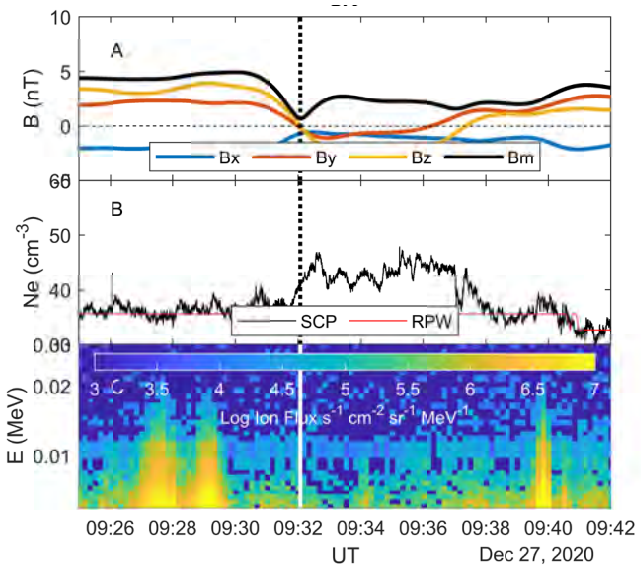

Reconnection event measured by *Solar Orbiter* in Venus's magnetotail. (A) The magnetic field measurements showing a very small total magnetic field at the dotted line. (B) The electron density from two instruments *SCP* and *RPW*. *SCP* shows a clear jump in density at the dotted line. (C) The ion flux measured by *EPD-STEP* showing accelerated ions on the left of the white line.

DID MARS POSSES A DENSE ATMOSPHERE DURING FIRST ~400 MYR?

The X-ray and EUV flux (together XUV) from the early Sun was significantly higher during the first 0.4 billion years (Gyr) than at present, ranging from ~20 times at ~4.2 Gyr ago to about 300 times the present value ~4.5 Gyr ago. It was already known that a CO_2-dominated atmosphere would expand significantly up to several Martian radii for such high values, thereby resulting in significant thermal escape that could erode 1 bar of CO_2 within just 10 million years for XUV fluxes ≥20 times the present value. Non-thermal escape processes would additionally put significant stress onto any existing atmosphere, even though these processes are very poorly understood for early Mars. Through reviewing the existing literature and by bringing together different sources (magma ocean and subsequent volcanic outgassing, impact delivery, etc.) and sinks (thermal and non-thermal escape) for the early Martian atmosphere, it was reconstructed whether a dense atmosphere could have existed early-on. Even the highest estimates for CO_2 sources on early Mars could not have counterbalanced atmospheric escape until ~4.1-4.0 Gyr ago. Mars, therefore, might just have always been a cold and dry planet that just episodically experienced liquid water afterwards, 4.0-3.6 Gyr ago, due to volcanic degassing and/or impact heating, when atmospheric escape diminished to much lower values.

Scherf & Lammer, Space Sci. Rev., 217, 2, 2021.

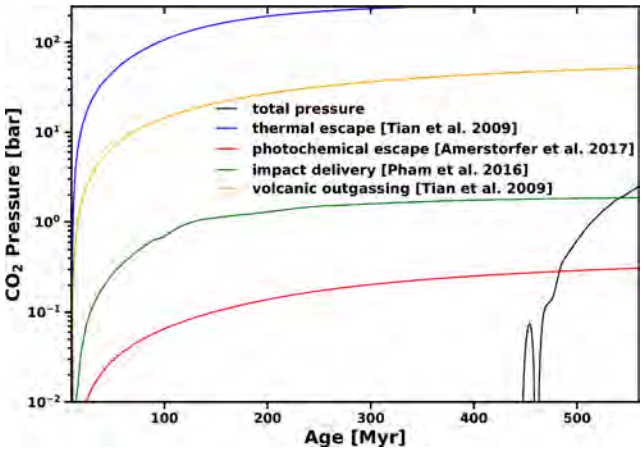

Atmospheric sources and sinks at early Mars (color lines). Black line shows a pressure scenario for which the whole Martian CO_2 inventory is outgassed continually over ~1 Gyr through volcanic degassing, contrary to most of the CO_2 being catastrophically outgassed during magma ocean solidification.

EARLY EVOLUTION OF VENUS, EARTH AND MARS

The current state of knowledge of the formation and early evolution time scales of Venus, Earth and Mars was studied, by using the latest isotopic data of various elements. Different planet formation models and isotopic data from ^{182}Hf-^{182}W, U-Pb, lithophile-siderophile elements, ^{48}Ca/^{44}Ca isotope samples from planetary building blocks, as well as reproduction attempts of atmospheric ^{36}Ar/^{38}Ar, ^{20}Ne/^{22}Ne, ^{36}Ar/^{22}Ne isotope ratios, are combined to obtain the expected solar ^{3}He abundance in Earth's interior.

By considering also, Earth's D/H seawater ratios additional light was shed on early Earth's accretion time, including a Moon-forming event at ~50 Myr after the formation of the solar system. As shown in the figure below, proto-Earth masses larger than 0.6 Earth-masses at the time when the gas disk dissipated a large amount of Earth's H_2O could have been formed from the interaction between a primordial atmosphere and the underlying magma ocean so that left behind D/H ratios would differ largely from the measured carbonaceous chondritic value.

The results of the study support the hypothesis that the bulk of Earth's mass (≥ 80 %) most likely accreted within 10-30 Myr after the Sun's origin. From the analysis of the before mentioned isotopes, one finds that proto-Earth accreted most likely 0.5-0.6 Earth-masses during the lifetime of the protoplanetary gas disk. For Venus, the present atmospheric noble gas data are too uncertain for the reconstruction of the planet's accretion. On the other hand, it was found that proto-Venus could have grown to its total mass before the disk dissipated.

Classic formation models for Venus, Earth and Mars have struggled to grow large planetary embryos, or protoplanets with masses as shown in the figure below, quickly from the tiniest materials within the typical lifetime of a protoplanetary disk. However, it is expected that so-called pebble accretion most likely solve this long-standing time scale controversy.

Lammer et al., Space Sci. Rev., 217, 7, 2021.

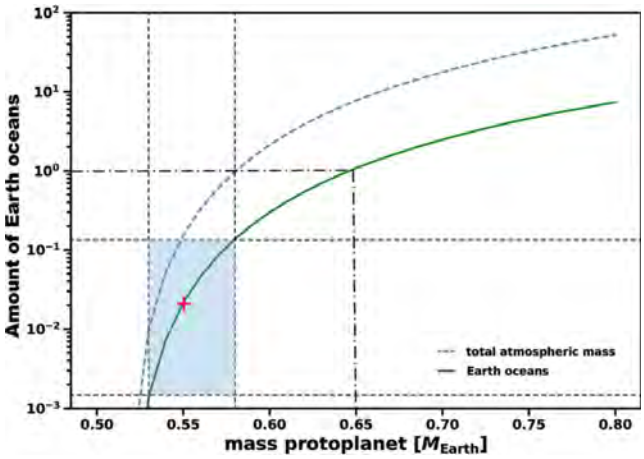

Right: The green line shows the maximum amount of Earth oceans that could be produced from an accumulated primordial atmosphere (blue dashed line) by gas-rock interactions between the atmosphere and an underlying magma ocean. The red "+" corresponds to an accretion scenario that can reproduce Earth's present atmospheric Ar and Ne noble gas isotope ratios. In such a case, a negligible water amount of only ~2 % of an Earth ocean could have been produced with solar nebula origin.

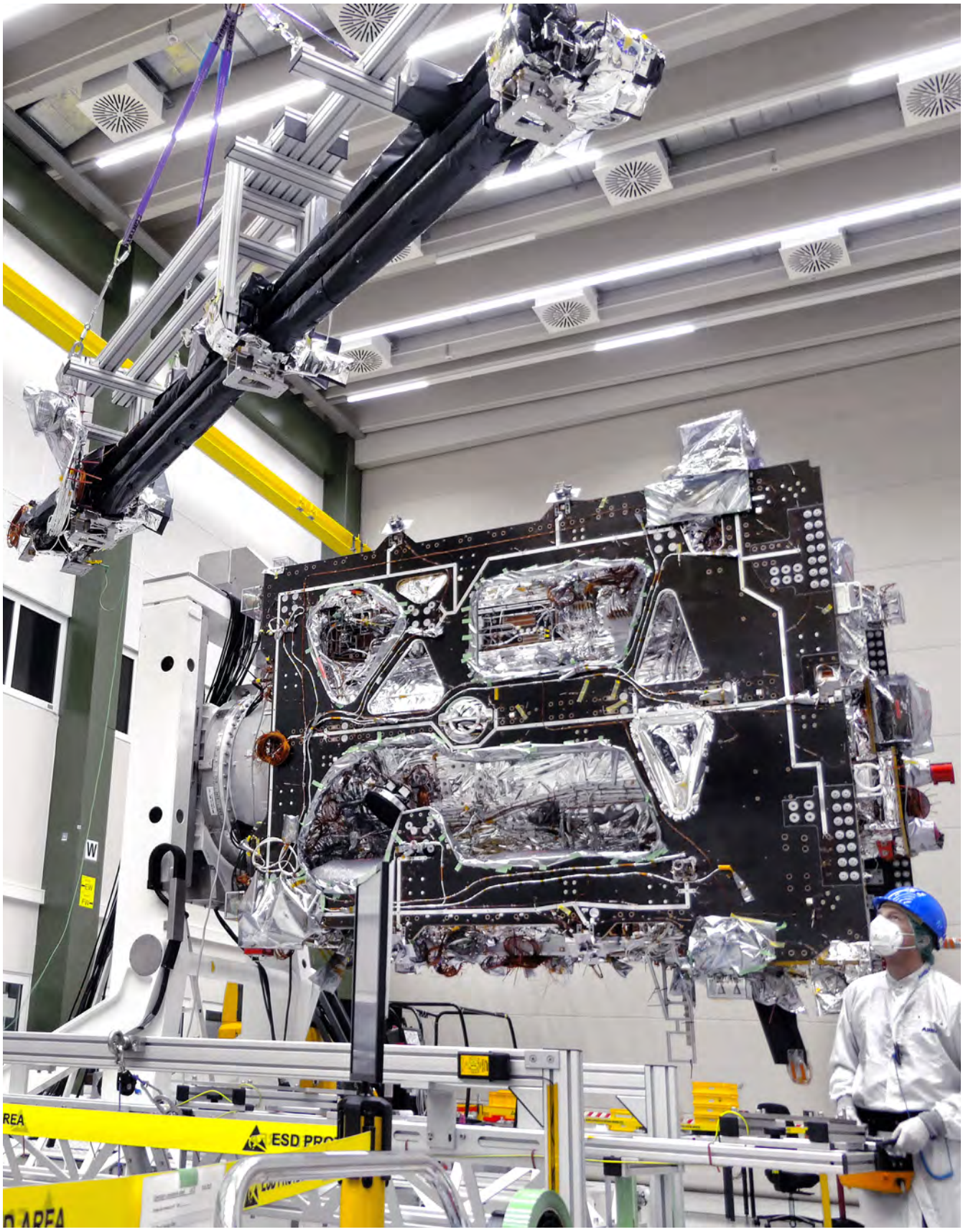

The 10.6-meter-long boom built for *JUICE's* magnetometer and *Radio and Plasma Wave Investigation (RPWI)* instruments, suspended aloft in folded configuration, being integrated to the spacecraft body in the clean room of Airbus (© Airbus, Sener).

JUPITER & SATURN

Jupiter and Saturn, the two largest planets in our solar system, both have several dozens of moons. For Jupiter, the most prominent moons are the four Galilean satellites. Callisto, Ganymede, and Europa will be visited frequently by the future *JUICE* spacecraft and the evolving trajectory of the current *JUNO* mission will allow several visits of Ganymede, Europa, and Io in the next few years. For Saturn, Titan is clearly the most prominent satellite with its dense atmosphere consisting of nitrogen and methane. However, Enceladus, with its suspected subsurface ocean is counted as a main candidate for extraterrestrial life.

In late February, *JUICE* hit a milestone when the boom for its *J-MAG* magnetometer and *Radio and Plasma Wave Investigation (RPWI)* instrument were successfully moved into place and installed at the Airbus satellite integration center facilities in Friedrichshafen, Germany. By the end of 2021 almost all scientific instruments of *JUICE* have been integrated on the spacecraft, which is undergoing extensive testing until launch in 2023.

JUICE

The launch of ESA's large mission *Jupiter ICy moons Explorer (JUICE)* had to be shifted from 2022 to 2023 due to technical reasons and delays caused by the COVID-19 pandemic. *JUICE* might arrive at Jupiter in the early 2030ies to make detailed observations of the gas giant and three of its largest moons, which are thought to have water oceans below their icy surfaces. Towards the end of the mission *JUICE* will orbit Jupiter's largest moon Ganymede.

The *Jupiter MAGnetometer (J-MAG)* is led by Imperial College London (ICL) and will measure the magnetic field vector and magnitude in the spacecraft vicinity in the bandwidth DC to 64 Hz. It is a conventional dual sensor fluxgate configuration combined with an absolute scalar sensor based on more recently developed technology. Science outcome from *J-MAG* will contribute to a much better understanding of the formation of the Galilean satellites, an improved characterization of their oceans and interiors, and will provide deep insight into the behavior of rapidly rotating magnetic bodies. IWF supplied the atomic scalar sensor *(MAGSCA)* for *J-MAG*, which was developed in collaboration with TU Graz.

In 2021, the *J-MAG* flight model was mounted on the spacecraft with the *MAGSCA* sensor at the tip of the *MAG* boom. Its proper function could be demonstrated during nominal testing in the integration hall as well as during an extensive thermal vacuum and balance test of the entire *JUICE* spacecraft. Furthermore, the spare model of *MAGSCA* was assembled and tested.

The *Particle Environment Package (PEP)* is a plasma package with sensors to characterize the plasma environment of the Jovian system and the composition of the exospheres of Callisto, Ganymede, and Europa. As part of the *PEP* consortium, IWF participates in the scientific studies related to the plasma interaction and exosphere formation of the Jovian satellites.

IWF was also responsible for the calibration of the radio antennas of *RPWI*. These antennas are three perpendicular dipoles mounted on the long magnetometer boom. Their reception properties have been determined using numerical methods applied to a mesh-grid model of the spacecraft, which is displayed in the figure below.

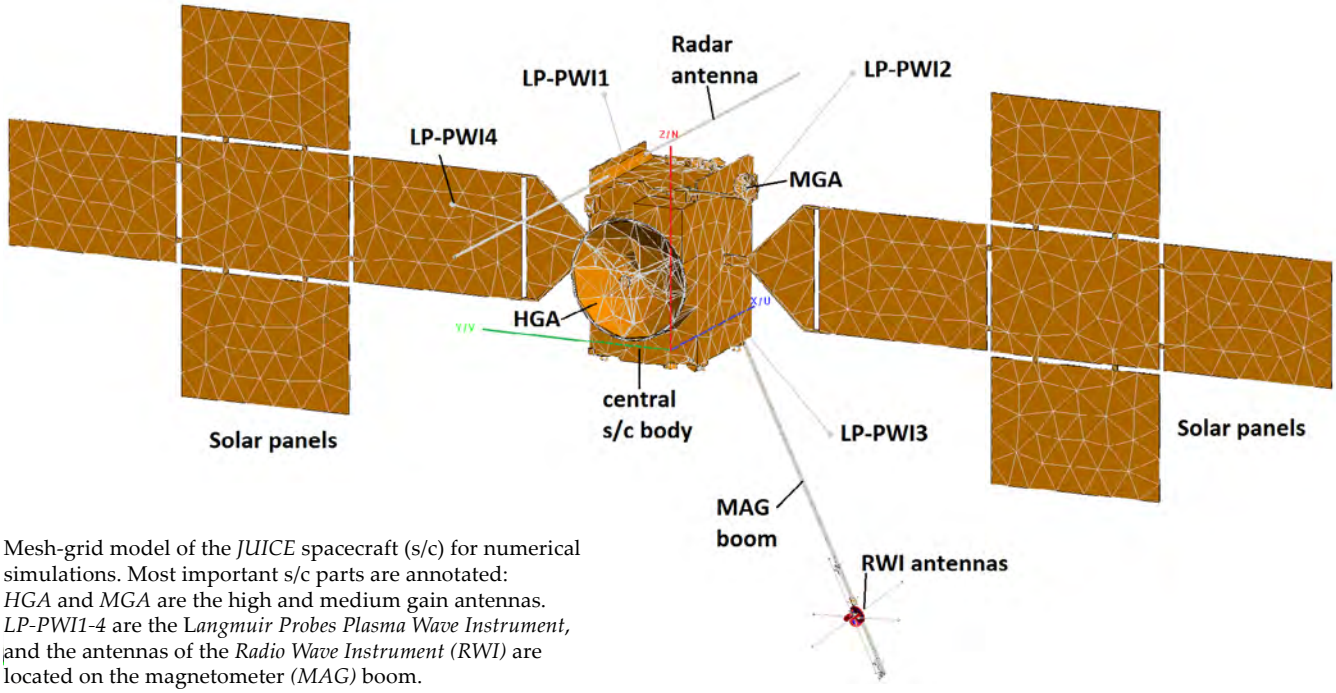

Mesh-grid model of the *JUICE* spacecraft (s/c) for numerical simulations. Most important s/c parts are annotated: *HGA* and *MGA* are the high and medium gain antennas. *LP-PWI1-4* are the L*angmuir Probes Plasma Wave Instrument*, and the antennas of the *Radio Wave Instrument (RWI)* are located on the magnetometer *(MAG)* boom.

With this antenna system it will be possible to determine intensity, polarization, and incoming wave direction of Jovian radio emissions. This can only be correctly done when the antenna reception properties are well known. Therefore, the so-called effective length vectors of the radio antennas were determined for the quasi-static frequency range. In this range the antenna reception properties are constant with a toroidal antenna pattern looking similar to a donut. The changes of the effective antenna vectors as a function of the solar panel rotation were also investigated revealing angular deviations of the vectors of up to 1°. The antenna patterns at higher frequencies up to 45 MHz show multiple lobes, and direction finding with an accuracy of 2° can only be done up to a frequency of 1.5 MHz. An estimation of the influence of pulses from the *JUICE* active radar on the *RPWI* sensors revealed that these strong pulses should not do any harm to them.

JUNO

NASA's Juno mission is dedicated to the investigation of Jupiter's gravitational and magnetic field, its polar magnetosphere, deep atmosphere and winds, as well as core composition and mass distribution. The spacecraft entered a polar orbit around Jupiter in July 2016 and its controlled de-orbit is scheduled for 2025. One of the instruments on board is the *Radio and Plasma Wave Sensor (Waves)*, which uses a dipole antenna to measure electromagnetic field components of incident waves (Jovian radio emissions or plasma waves).

The reception properties of the antenna change drastically over the instrument's frequency range from near DC to 40 MHz, so the quasi-static effective length vector cannot be used to describe the antenna system above some megahertz. Since in this frequency range the effective length vector is extremely direction-dependent, antenna gain patterns and insertion loss have been chosen as suitable properties to characterize the directional variation of the antenna sensitivity and the influence of base capacitances. These quantities were obtained by numerical computations on the basis of a suitable simulation model of the antenna system and spacecraft with all relevant features. The results can be used to evaluate observed radio wave spectra, the gain giving clues about the directions where the instrument does not see incident waves, and the insertion loss enabling a quantitative correction of wave spectra as a function of frequency.

Sampl et al., Radio Sci., 56, e2020RS007184, 2021.

SATURN STUDIES

The completed *Cassini* mission has provided an enormous wealth of data, which will keep scientists busy for the upcoming years. A new study used the complete *Cassini RPWS* (*Radio and Plasma Wave Science*) observations of Saturn Kilometric Radiation (SKR) to find about 600 events of SKR experiencing Faraday rotation. This effect is characterized by a rotation of the semi-major axis of the SKR polarization ellipse as a function of frequency during wave propagation through a birefringent plasma medium. A statistical visibility analysis showed that elliptically polarized SKR most likely experiences Faraday rotation when it is beamed from the dawn source towards high latitudes into the noon and afternoon local time sectors.

Another study used the complete *Cassini RPWS* data to statistically analyze the polarization properties and visibility of Saturn narrowband (NB) emissions at 5 and 20 kHz. The 5 kHz NB emissions show high circular polarization only when beamed to high latitudes and are almost unpolarized in the equatorial plane. 20 kHz NB emissions are usually highly circularly polarized as they are only beamed to higher latitudes and usually do not occur at the equator.

Taubenschuss et al., Icarus, 370, 114661, 2021.

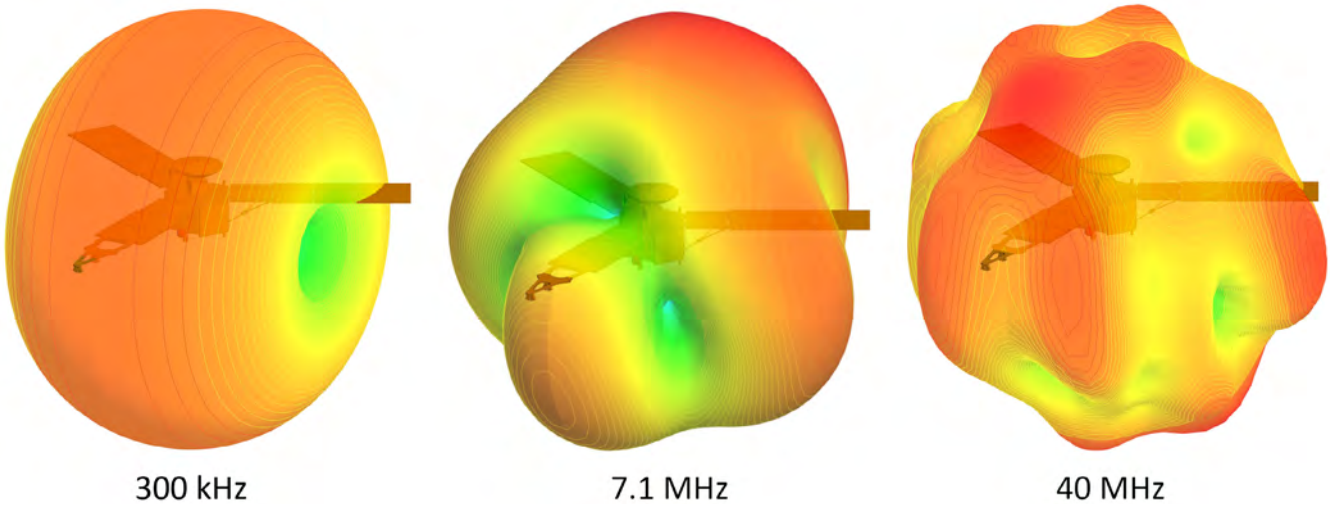

Juno dipole gain as function of direction of incidence of radio waves for three frequencies.

COMETS

Comets are assumed to be the left-overs of the solar system creation that have not been moulded into planetary bodies. Most of these objects reside in the Kuiper Belt (between 30 and 50 astronomical units from the Sun) and in the Oort Cloud (greater than 2000 au from the Sun). Now and then a body in these regions is nudged towards the inner regions of the solar system and as soon as it passes Jupiter's orbit, the solar irradiation is strong enough to let (sub)surface ices sublimate. This gas escapes, together with dust, and thereby creates the characteristic tails of comets. Around Christmas comet Leonard was well visible in the sky and captured by *Solar Orbiter's Heliospheric Imager*.

Image of comet Leonard captured by the *Solar Orbiter* spacecraft in December 2021 (© ESA/NASA/NRL/SoloHI).

COMET INTERCEPTOR

ESA's first F(ast)-class mission *Comet Interceptor* will, for the first time, study a so-called dynamically-new comet, i.e. a comet, which will have its first passage by the Sun after being nudged out of the Kuiper Belt or Oort Cloud. The surface composition and shape of the nucleus as well as the structure and composition of the coma will be investigated. This mission is unique, as - for the first time - there will be multiple-spacecraft simultaneously measuring in the cometary environment.

Comet Interceptor consists of three components. A large mother spacecraft (A), which remains furthest from the nucleus, built by ESA, also serving as a relay station for the data. And two smaller spacecraft, which will have flybys much closer to the comet: B1 built by JAXA and B2 built by ESA. The launch is scheduled for 2029 and the mission will be parked at the L2 Lagrange point (up to three years) until an appropriate target has been identified.

Discussions with ESA and two contractors to build the spacecraft have been ongoing in the last year and mission adoption is expected in June 2022.

IWF is involved in two instrument packages. On spacecraft A, the institute builds the DPU for the *MANiaC (Mass Analyzer for Neutrals and ions at Comets)* instrument, which is a mass spectrometer to sample the gases released from the comet. In 2021, the prototype design of the *MANiaC* DPU was started. All electronical key components have been selected and the design is in progress. Due to the limitation in space, the elements of the DPU will be located onto two boards. The main board will contain processor, memories and FPGA and an interface board will host the driver circuitries for all external interfaces. The first prototype hardware will become available in spring 2022. In addition, the concept for the two software packets, for boot and science mode, was developed. In particular for the boot software, a detailed requirement document has been defined. Furthermore, test routines have been generated, to confirm the compliance of the quad core LEON4 processor with the high data rate during the science mode.

IWF also develops the front-end electronics for the fluxgate magnetometer, which is part of the *Dust-Field-Plasma (DFP)* package on spacecraft B2 *(BFG)*. The *BFG* front-end electronics is based on the *SOSMAG* magnetometer and therefore on a previously developed microchip. It comprises most of the active electronics, which is required to amplify and digitize the magnetic field measured by a fluxgate sensor. For the *BFG* design, the electronics components outside of the microchip were adapted and matched to the miniaturized fluxgate sensor from Magson GmbH. Measurements with the bread board model showed excellent instrument performance, which allowed to finish the preliminary instrument design for the Engineering Model in the second half of 2021. Its production will start in early 2022.

GAS FLOW IN COMETARY ANALOG MATERIALS

Gas flow from its surface, originating in subsurface layers, belongs to the processes of utmost importance for the evolution of a comet. Outgassing affects the coma and the dust redistribution around the comet and influences the thermal evolution as well as mass loss of the comet. Many past studies focused on the effect of water sublimation. However, there are open questions about details of the gas flow through the porous medium, which builds the cometary surface layers.

Two parameters combine the properties of the porous cometary material in a way that enables a mathematical description of the gas flux: the Knudsen diffusion coefficient D and the permeability B, which describe the molecular and the viscous flow, respectively. Both kinds of flow were investigated in laboratory measurements, using dry cometary analog materials. By simultaneous evaluation of the flow rates for a wide range of pressures, D and B could be determined for the analog materials. In addition, glass bead samples were investigated to study the relations between pore sizes, porosity and the determined coefficients B and D in a systematic manner. The determined parameters cover a wide range of values, dependent on the pore structure of the materials (see figure). The results for the glass beads verified relations available for packed beads of spherical grains. However, also deviations from the models were found, where the beads become non-spherical. In addition, computer simulations were applied, which indicated potential for improvements in the setup of future measurements. These were the first simultaneous determinations of B and D for analog materials of comets and asteroids, giving clues about further paths to better understand the gas flow through the surfaces of these space objects.

Schweighart et al., MNRAS, 504 (4), 5513–5527, 2021.

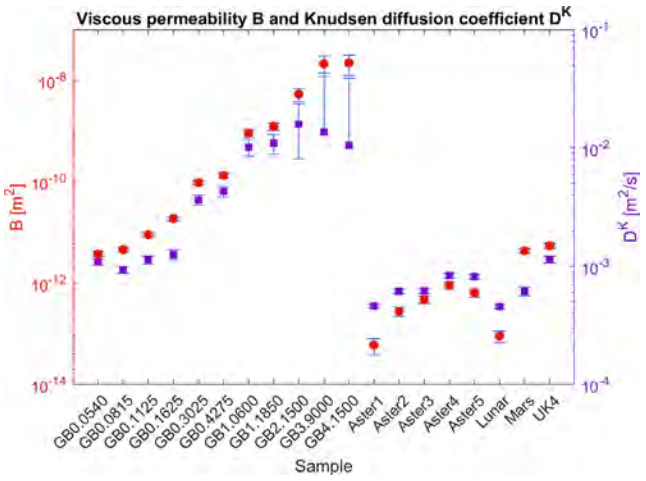

Permeability of cometary analog materials for continuous flow (B) and molecular diffusion (D) as obtained by laboratory measurements. Since the average pore size increases for larger glass beads (GB), the resistance to the gas flow decreases, resulting in higher values of B and D.

COPHYLAB

CoPhyLab started as a joint German, Swiss, and Austrian, research project between TU Braunschweig, the University of Bern, and IWF to investigate cometary processes in space simulation laboratories. Later on, the following external partners joined: MPS Göttingen, DLR Berlin, University of Stirling, Luleå University of Technology, Qian Xuesen Laboratory of Space Technology in China, and Open University.

The project aims to increase the understanding of the *Rosetta* mission results by conducting selected experiments in a controlled environment. In 2021 the general laboratory setup has been finished with all the main components installed. IWF was involved in the general chamber design, the cooling system and the light chopper for controlled illumination conditions particularly for day-night cycles. Besides the small-class gas flow experiments in Graz, IWF is also contributing to the hardware and instrument setup at the common CoPhyLab laboratory in Braunschweig. Amongst several instruments, the solar simulator mounted on the Large Chamber was contributed by IWF.

The most recent addition is the sample manipulation device, which is a mobile robotic platform designed for operations inside the large thermal-vacuum chamber. The working environment is high vacuum and temperatures as low as -200 °C. It can bring sensors close or even inside the sample, mechanically interact with the sample surface and bring close-up stereo cameras to selected positions.

Planned experiments are a Brazilian Disk test on icy samples and penetrometer measurements to determine the tensile and compressive strength of a processed sample.

Kreuzig et al., Rev. Sci. Instrum., 92, 115102, 2021.

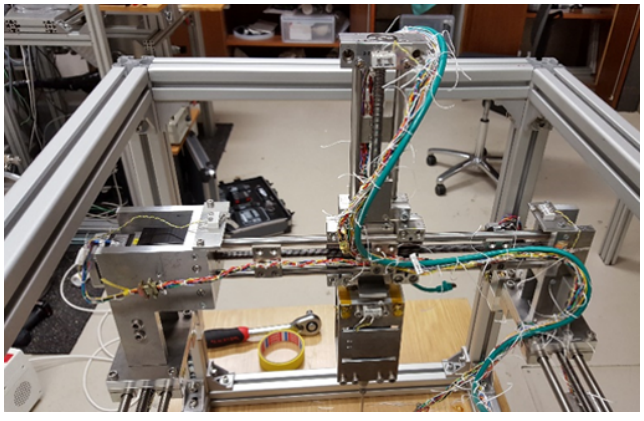

Sample manipulation device before installation in the Large Chamber.

EXOPLANETARY SYSTEMS

The field of exoplanet research (i.e. investigation of planets orbiting stars other than the Sun) has developed strongly in the past decades. The first exoplanet orbiting a Sun-like star, 51 Peg b, was detected in 1995. About 4500 exoplanets, most in planetary systems, are now known. Improved instrumentation and analysis techniques have led to the detection of smaller and lighter planets, particularly orbiting bright, nearby stars, which therefore enable in-depth structure and atmospheric characterization. Although hot Neptunes and (ultra-) hot Jupiters are still prime targets for atmospheric characterization, smaller planets are entering the realm of the planets for which the atmosphere can be directly probed.

The main exoplanet missions in which IWF is involved with hardware and/or science are *CHEOPS*, *CUTE*, *PLATO*, *ARIEL*, and *ATHENA*. IWF concentrates on the study and characterization of planetary atmospheres and of the star-planet interaction phenomenon using both theory and observations, focusing particularly on the analysis of planet formation, exoplanet clouds, and atmospheric mass-loss processes. The research is based on the collection and analysis of ground- and space-based observations to constrain the models, as well as on the modelling of planet and cloud formation from first principles.

An in-house developed exoplanetary atmosphere modelling tool enabling one to account for non-local thermodynamic equilibrium effects has been uniquely capable of reproducing the transmission spectroscopy observations of the hottest exoplanet known to date. In this way, it has been shown that non-local thermodynamic equilibrium effects impacting the metals in the planetary atmosphere control the temperature structure of the middle and upper atmosphere.

A one-dimensional, general, and open-source framework for exoplanet atmospheric modelling, spectral synthesis, and Bayesian retrieval has been developed. The framework has been successfully tested against the results of other similar tools and applied to interpret the observations collected for a wide range of close-in giant exoplanets. This framework has also been further upgraded to retrieve results considering the impact of a 3-dimensional geometry.

CHEOPS data collected during the first few months of science operations have been used to characterize the HD108236 planetary system. This is one of the very few multi-planet systems known to date containing at least five transiting planets and as such it provides critical information on the physics regulating the planetary mass-radius relation.

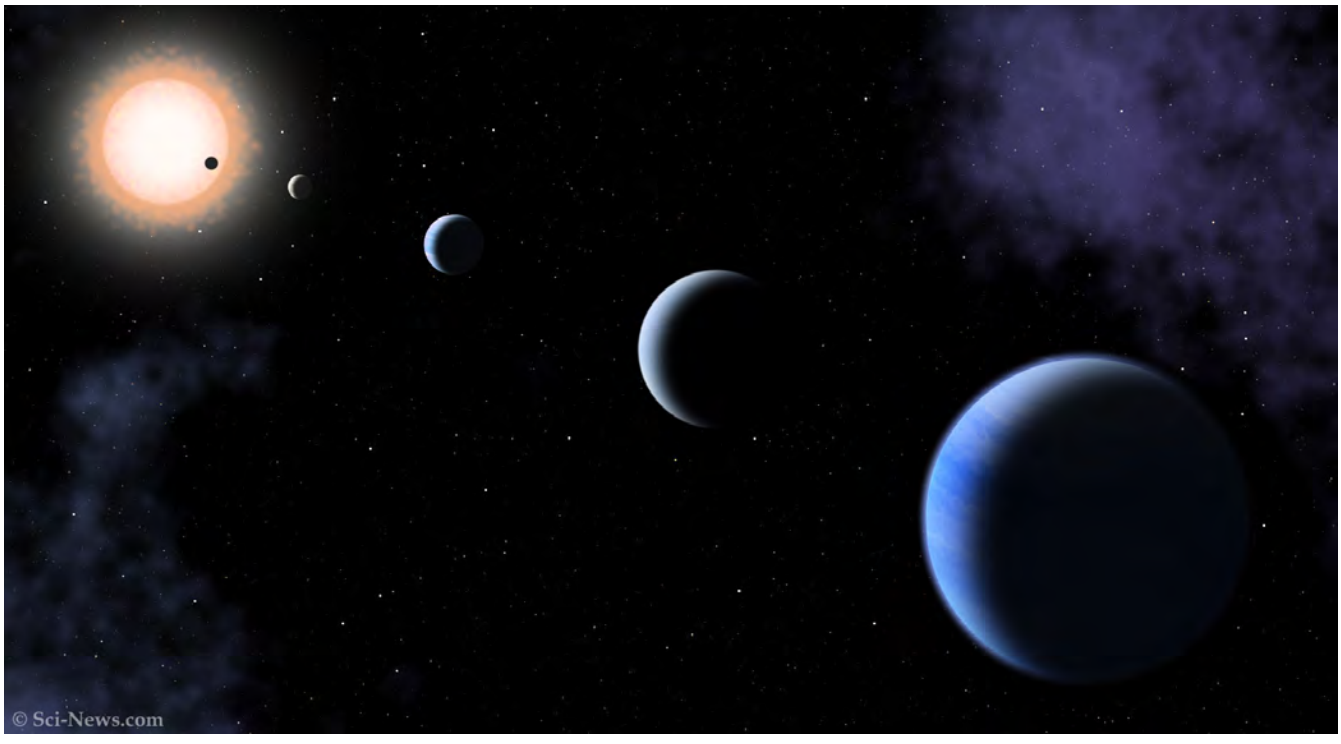

Artist's impression of the five-planet system HD108236 (© Sci-News.com).

CHEOPS

CHEOPS (CHaracterising ExOPlanet Satellite), successfully launched in December 2019, has started regular science operations in April 2020. The mission aims at studying extrasolar planets by means of ultra-high precision photometry. The main science goals are to detect transits of small planets, known to exist from radial-velocity surveys, precisely measure the radii of a large sample of planets to constrain the internal composition and atmospheric evolution of Neptune- to Earth-sized planets, study the atmospheric properties of transiting giant planets, and look for new planets particularly in already known systems.

IWF is responsible for the *Back-End-Electronics (BEE)*, one of the two on-board computers, and for controlling the data flow and the thermal stability of the telescope structure. The institute also developed and maintains the mission's signal-to-noise calculator. Within the Guaranteed Time Observations (GTO) of the *CHEOPS* consortium, IWF co-chairs the working group aiming at improving our understanding of the mass-radius relation of planets, of processes affecting planetary atmospheric evolution, and of system architecture.

In 2021, *CHEOPS* continued nominal science operations, demonstrating that the satellite performs and ages as expected. The European consortium in charge of the majority of *CHEOPS* observing time made use of *CHEOPS* observations collected in 2020 and part of 2021 to publish nine refereed articles, among which the detection of the transit of the very long period planet ν^2 Lupi d that appeared in Nature Astronomy.

One of these works has been led by IWF and presented *CHEOPS* observations characterizing the HD108236 planetary system, which hosts five transiting planets with periods ranging between 3 and 30 days and radii between 1.5 and 3 Earth radii. This is the third brightest system hosting more than three transiting planets. The stellar characterization analysis led to the determination of a stellar radius of 0.877 ± 0.008 solar radii, and stellar mass of 0.869 ± 0.049 solar masses and of an age of 6.7 ± 4.5 Gyr.

The *CHEOPS* observations led to the serendipitous detection of a fifth transiting planet, HD108236f, with an orbital period of about 29.5 days. The *CHEOPS* transit light curves (one for each planet) led also to locking the ephemerides for each planet, which is critical for enabling future further characterization observations, and to improving the planetary radii measurements by a factor of two compared to what the *TESS* satellite provided, which first discovered this system. These data were also the first direct data quality comparison between *TESS* and *CHEOPS*, which has shown the power of *CHEOPS* at significantly improving planetary radii measurements over those provided by *TESS* in a fraction of the observing time.

Bonfanti et al., Astron. Astrophys., 646, A157, 2021.

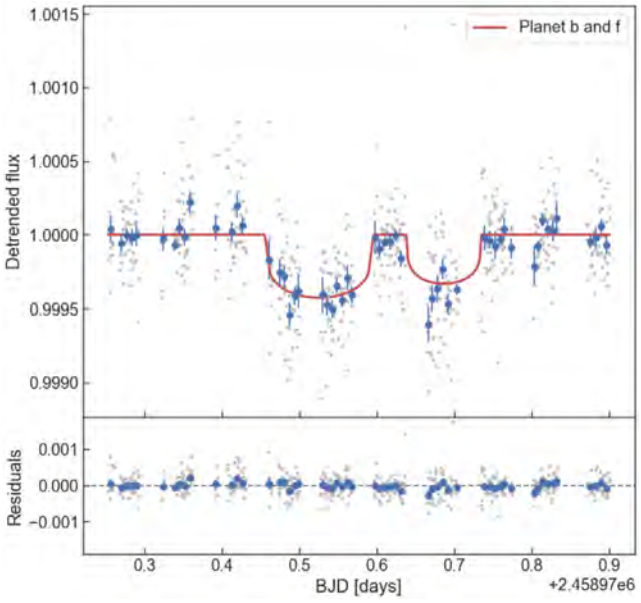

Detrended *CHEOPS* light curve showing the transits of planets b (right) and f (left). The red line shows the best fitting transit model.

CUTE

CUTE (Colorado Ultraviolet Transit Experiment) is a NASA-funded 6U-form CubeSat led by the University of Colorado that was launched on 27 September 2021 from the Vandenberg Space Force Base, in California. *CUTE* will perform low-resolution transmission spectroscopy of transiting extrasolar planets at near-ultraviolet wavelengths. It will study the upper atmosphere of short-period extrasolar planets with the aim of observationally constraining atmospheric escape processes, which are key to understand planetary evolution, and detect heavy metals, which constrain the presence and composition of aerosols in the lower atmosphere. Furthermore, *CUTE*'s continuous temporal coverage of planetary transits will allow to detect transit asymmetries, which are possibly connected with the presence of planetary magnetic fields.

IWF is the only technological contributor to the mission outside of the University of Colorado (Boulder), where *CUTE* was developed. IWF is responsible for the development of the data simulator, of the data signal-to-noise calculator, of the ground data reduction software, and of the algorithms defining the on-board data reduction software.

In 2021, IWF has defined the data reduction algorithms used on-board and finalized the development of the *CUTE* ground-based data reduction software. Commissioning of the satellite is still on-going and the first science data are awaited in early 2022.

PLATO

PLATO (PLAnetary Transits and Oscillations of stars) is ESA's third medium (M-class) mission, led by DLR. Its objective is to find and study a large number of exoplanetary systems, with emphasis on the properties of terrestrial planets in the habitable zone around solar-like stars. *PLATO* has also been designed to investigate seismic activity of stars, enabling the precise characterization of the host star, including its age.

IWF co-leads the work package aiming at studying planetary habitability and takes part in two further work packages (one on stellar characterization and one on planetary evolution) aiming at gaining the knowledge and preparing the tools necessary to best exploit the data. The institute contributes to the development of the I*nstrument Controller Unit (ICU)* with the development of the *Router and Data Compression Unit (RDCU)*. Launch is expected in 2026.

PLATO consists of 24 telescopes for nominal and two telescopes for fast observations. Each telescope has its dedicated front-end-electronics, reading and digitizing the CCD content. Twelve nominal and two fast DPUs collect the data from the front-end-electronics and extract the areas of interest. The *RDCU* is a key element in the data processing chain, providing the communication between the DPUs and the *ICU*. The second task of the *RDCU* is the lossless compression of the science data. For performance reasons, the compression algorithm is implemented in an FPGA.

In 2021 all design activities have been completed and the production of the qualification model has started. The IP core for compressor and SpaceWire link has been adopted for the FPGA technology used for flight (RTAX2000). A detailed "post place and route" simulation has been performed to check for compliance with all requirements in terms of performance and timing constraints. Furthermore, long term tests with high data rate demonstrated the failure free function of the router part. The critical design review for the *RDCU* has been successfully completed.

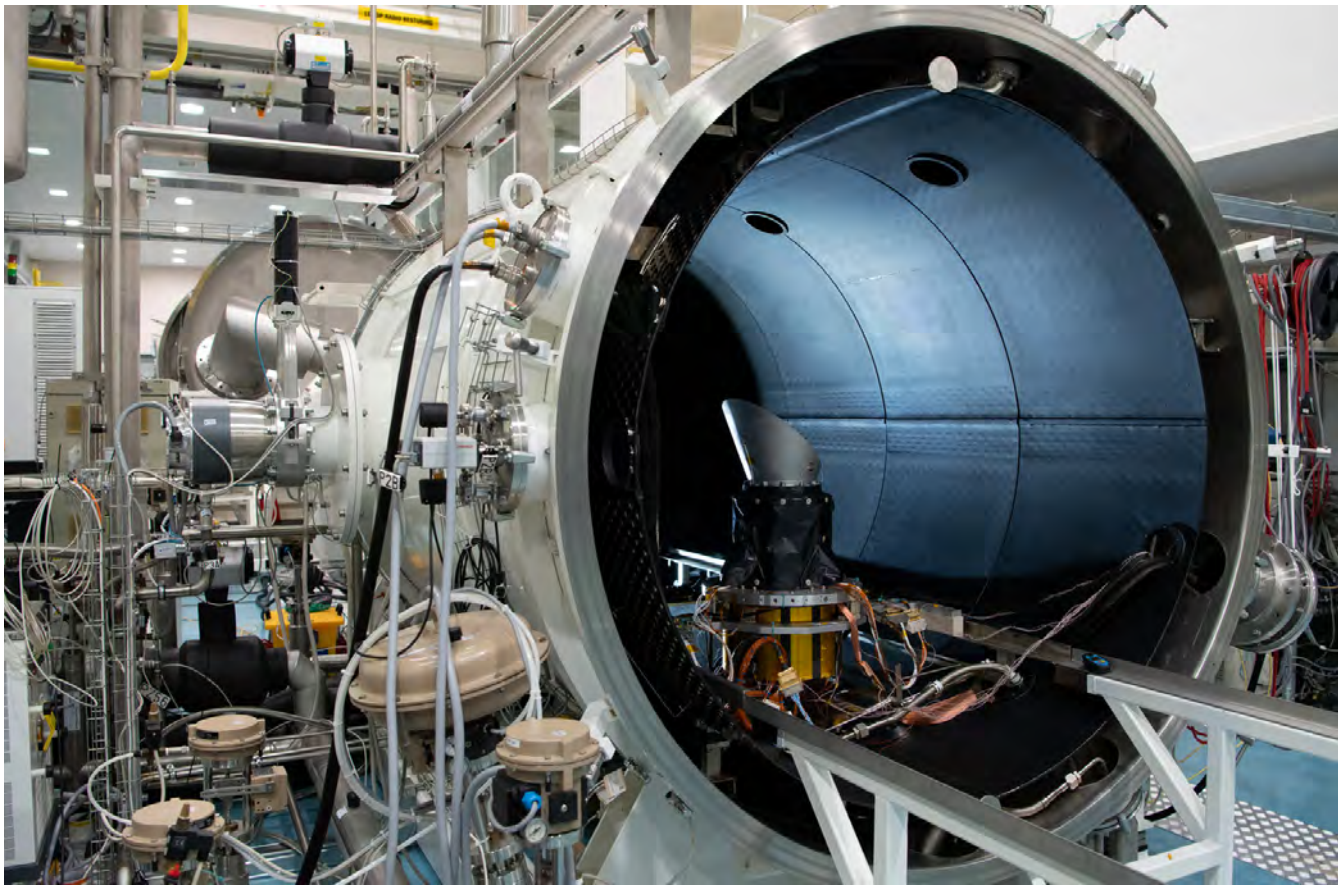

Key technology for the *PLATO* spacecraft has passed a trial by vacuum to prove the mission will work as planned. This test replica of an 80-cm high, 12-cm aperture camera spent 17 days inside a thermal vacuum chamber at the ESTEC test center in the Netherlands (© ESA-Matteo Apolloni).

ARIEL

ARIEL (Atmospheric Remote-sensing Infrared Exoplanet Large-survey) is ESA's fourth medium (M-class) mission, led by University College London, to be launched in 2029. It will investigate the atmospheres of several hundred exoplanets to address fundamental questions on how planetary systems form and evolve. During its four-year mission, *ARIEL* will observe 1000 exoplanets ranging from Jupiter- and Neptune- down to super-Earth-size in the visible and infrared with its meter-class telescope. The analysis of *ARIEL* spectra and photometric data will enable extracting the chemical fingerprints of gases and condensates in planetary atmospheres, including the elemental composition for the most favorable targets, with a particular focus on carbon and oxygen. Thermal and scattering properties of the atmosphere will also be studied.

ARIEL consists of a one-meter telescope feeding two infrared low-resolution spectrographs and the fine guiding sensor (FGS), working in the optical. To improve the satellite's pointing stability, the FGS provides optical photometry of the target in three broad bands that are used to control instrumental systematics, measure intrinsic stellar variability, and constrain the presence of high-altitude aerosols in planetary atmospheres. Within the *ARIEL* mission, IWF co-leads the upper atmosphere working group and is heavily involved in testing the mission's performances and advancing the atmospheric retrieval tools.

ATHENA

ATHENA (Advanced Telescope for High-ENergy Astrophysics), is ESA's second large (L-class) mission in the Cosmic Vision 2015-2025 plan. Its objective is to study hot gas in clusters and groups of galaxies and the intergalactic medium, to determine how ordinary matter assembles into large-scale structures. The second topic is the growth of black holes and their impact on the universe. The observations in the X-ray range of the electromagnetic spectrum will help to understand the high energetic processes close to the event horizon of black holes and provide more details for the baryonic component, locked in ultra-hot gas.

The institute will contribute to the *Wide Field Imager (WFI)* with the development of the *Central Processing Module (CPM)*. In 2021, the study concerning the processor performance has been continued. The search for efficient configuration of the level 2 cache and the efficient use of the four cores is ongoing. The technical concept for the *CPM* and the SpaceWire router has been further elaborated. All electronic components are selected and the design is ready for building the prototypes.

A CRITICAL ASSESSMENT OF THE ENERGY-LIMITED APPROXIMATION

The energy-limited atmospheric escape approach is widely used to estimate mass-loss rates for a broad range of planets that host hydrogen-dominated atmospheres as well as for performing atmospheric evolution calculations. However, its applicability has been questioned, which has called for a thorough revision of the approximation and for a comparison with sophisticated hydrodynamic models that better reproduce the physics of planetary upper atmospheres. The comparison indicated that the energy-limited approximation gives a correct order of magnitude estimate for mass-loss rates for about 76% of the planets, but there can be departures from the results of hydrodynamic simulations by up to two to three orders of magnitude in individual cases. In particular, planets for which the mass-loss rates are correctly estimated by the energy-limited approximation to within one order of magnitude have intermediate gravitational potentials (~2.5–5.5 $\times 10^8$ J kg^{-1}) as well as low-to-intermediate equilibrium temperatures and irradiation fluxes of extreme ultraviolet and X-ray radiation. However, for planets with low or high gravitational potentials, or high equilibrium temperatures and irradiation fluxes, the approximation fails in most cases. Therefore, the energy-limited approximation should not be used for planetary evolution calculations that require computing mass-loss rates for planets that cover a broad parameter space.

Krenn et al., Astron. Astrophys., 650, A94, 2021.

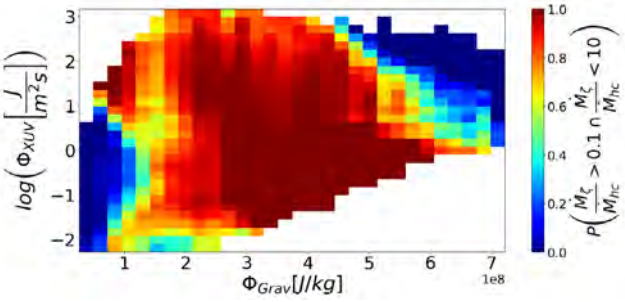

Probability of the mass-loss rate being within a factor of ten of the results given by hydrodynamic simulations as a function of planetary gravitational potential and high-energy stellar irradiation.

CONSTRAINING STELLAR ROTATION AND SUB-NEPTUNES PLANETARY ATMOSPHERIC EVOLUTION

Planetary atmospheric evolution modelling is a prime tool for understanding the observed exoplanet population and constraining formation and migration mechanisms, but it can also be used to study the evolution of the activity level of planet hosts. The PASTA (Planetary Atmospheres and Stellar roTation rAtes) code, which runs within a Bayesian framework, has been developed to model the atmospheric evolution of sub-Neptunes and super-Earths lying within a dozen systems. The Markov chain Monte Carlo scheme built inside PASTA has been used to retrieve the posterior probability density functions of the initial atmospheric mass fraction ($f_{atm,start}$) of all considered planets and the exponents of the power-law describing the rotation evolution of the host stars. Correlations have been looked for between $f_{atm,start}$ and the system parameters, but without success as a result of the large uncertainties and too small sample of exoplanets. PASTA has the potential to provide constraints to planetary atmospheric accretion models, particularly when considering warm sub-Neptunes that are less susceptible to mass loss compared to hotter and/or lower-mass planets. The *TESS*, *CHEOPS*, and *PLATO* missions are going to be instrumental in identifying and precisely measuring systems amenable to PASTA's analysis and can thus potentially constrain planet formation and stellar evolution.

Bonfanti et al., Astron. Astrophys., 656, A157, 2021.

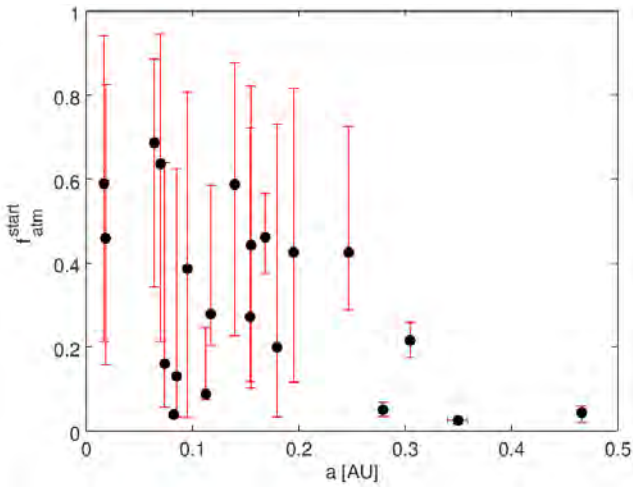

Initial atmospheric mass fractions as a function of planetary semi-major axis for the considered sample of planets.

A NEW MODELLING FRAMEWORK FOR EXOPLANETARY ATMOSPHERES

Pyrat Bay is an open-source framework developed at IWF for exoplanet atmospheric modeling, spectral synthesis, and Bayesian retrieval. The modular design of the code allows users to generate atmospheric 1D parametric models of the temperature, abundances, and altitude profiles; sample molecular cross sections from various databases; compute emission or transmission spectra considering a range of different opacities; and perform Markov chain Monte Carlo atmospheric retrievals for a given transit or eclipse dataset. The Pyrat Bay framework has been benchmarked by reproducing line-by-line sampling of molecular databases, by reproducing transmission and emission spectra produced by other comparable tools, and by accurately retrieving the atmospheric properties of simulated transmission and emission observations generated by other codes. Pyrat Bay has finally been used to perform a retrieval analysis of a population of transiting exoplanets observed by the *Hubble Space Telescope*. Consistently with previous analyses, the results indicate that the data do not enable one to distinguish whether a muted water feature is caused by clouds, high atmospheric metallicity, or low water abundance. In contrast to other comparable tools, Pyrat Bay is self-installing and it is very well documented and tested to provide maximum accessibility to the community and long-term development stability.

Cubillos & Blecic, MNRAS, 505, 2657, 2021.

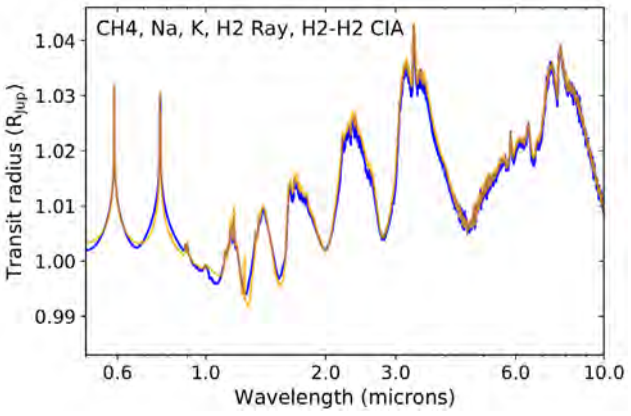

Comparison between transmission spectra computed with Pyrat Bay (blue) and petitRADTRANS (orange) considering cross section for CH_4, Na, K, H_2 Rayleigh scattering, and H_2–H_2 continuum induced absorption.

LONGITUDINALLY RESOLVED SPECTRAL RETRIEVAL OF WASP-43B

Thermal phase variations of short-period planets indicate that they are not spherically symmetric: day-to-night temperature contrasts range from hundreds to thousands of degrees, rivaling their vertical temperature contrasts. Nonetheless, the emergent spectra of short-period planets have typically been fit using one-dimensional (1D) spectral retrieval codes that only account for vertical temperature gradients. Exoplanet researchers have recently introduced multi-dimensional retrieval schemes for interpreting the spectra of short-period planets, but these codes are necessarily more complex and computationally expensive than their 1D counterparts. An alternative has been developed, namely phase-dependent spectral observations are inverted to produce longitudinally resolved spectra that can then be fitted using standard 1D spectral retrieval codes. This scheme has been successfully tested on the iconic phase-resolved spectra of WASP-43b and on simulated observations using the open-source Pyrat Bay 1D spectral retrieval framework. Furthermore, for this study the model complexity of the simulations has been taken one step further over previous studies by allowing for longitudinal variations in composition, in addition to temperature. The key result is that performing 1D spectral retrieval on longitudinally resolved spectra is more accurate than applying 1D spectral retrieval codes to disk-integrated emission spectra, despite being identical in terms of computational load.

Cubillos et al., Astrophys. J., 915, 45, 2021.

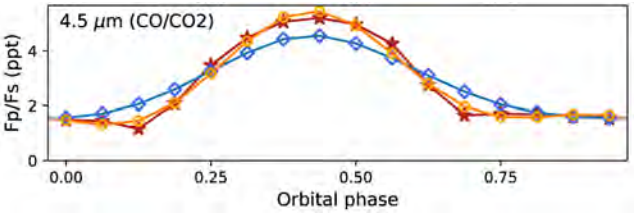

Comparison between the model flux ratios computed locally (red), disk-integrated (blue), and spatially resolved (orange) at 4.5 μm, where the spectrum is dominated by CO and CO_2 absorption. The longitudinally resolved dataset matches much better the phase curve assuming local properties at each phase than the disk-integrated dataset.

NON-LOCAL THERMODYNAMIC EQUILIBRIUM EFFECTS IN THE ATMOSPHERE OF KELT-9B

KELT-9b is the hottest exoplanet known to date. Both observational and theoretical results indicate that its atmospheric temperature in the main line formation region is a few thousand degrees higher than predicted by self-consistent models. With this in mind, the impact of non-local thermodynamic equilibrium (NLTE) effects on the atmospheric temperature profile has been tested. The Cloudy NLTE radiative transfer code has been employed to self-consistently compute the atmospheric temperature structure obtaining a profile about 2000 K hotter than obtained assuming local thermodynamic equilibrium (LTE). In particular, the higher temperature is driven principally by NLTE effects modifying the Fe and Mg level populations, affecting the thermal balance. Cloudy has been also used to generate synthetic transmission spectra finding that the NLTE model generally produces stronger absorption lines than the LTE model (up to 30%), which is largest in the ultraviolet. Furthermore, the NLTE synthetic transmission spectrum fits significantly better the observed Hα and Hβ Balmer line profiles. It can thus be used to guide future observations aiming at detecting features in the planet's transmission spectrum. Finally, these results call for checking whether NLTE effects have a similar impact also on the planetary atmospheres of cooler planets.

Fossati et al., Astron. Astrophys., 653, A52, 2021.

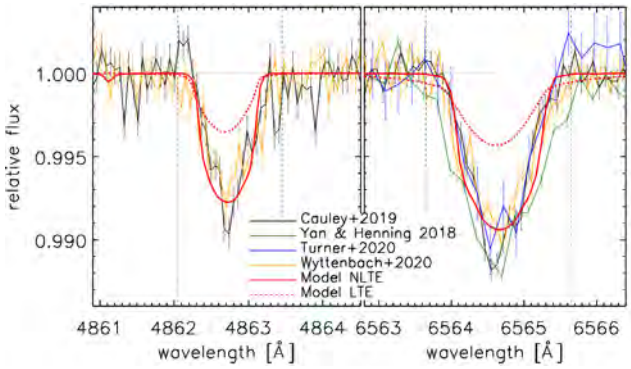

Observed transmission spectra of the Hα (right) and Hβ (left) Balmer lines presented in the literature compared to LTE and NLTE synthetic transmission spectra.

PROBING MAGNETIC FIELDS AND COMPOSITION OF ESCAPING EXOPLANETARY ATMOSPHERES

The global 3D self-consistent (M)HD modelling of the expanding upper atmospheres of WASP-107b and HD209458b interacting with stellar winds enabled simulation of their complex dynamic environments and the related observed transit absorption features of HI (Lyα), OI (1306 Å), CII (1337 Å), and HeI (10830 Å). For WASP-107b, the observed HeI (10830 Å) absorption profiles were reproduced within the uncertainties, and the stellar high-energy flux was constrained to realistic values of 6 - 10 erg cm^{-2} s^{-1} at 1 au. The simulations revealed a solar helium abundance at the level of He/H = 0.075 - 0.15. The performed modelling demonstrates the importance of radiation pressure acting on the HeI atoms, as well as electron and atom impact processes, which were shown to influence the absorption profiles. For HD209458b, particular attention has been paid to the structure and behavior of the planetary magnetosphere and possible influence of the planetary magnetic field on the dynamics of the escaping upper atmosphere and the measured transit absorption profiles. Fitting of the simulation results to observations enabled constraining the stellar high-energy flux and helium abundance to 10 erg cm^{-2} s^{-1} at 1 au and He/H ≈ 0.02, respectively, as well as setting an upper limit for the magnetic dipole moment of HD209458b. The latter appeared to be less than 6% of the Jovian value.

Khodachenko et al., MNRAS, 503, L23, 2021.
Khodachenko et al., MNRAS, 507, 3626, 2021.

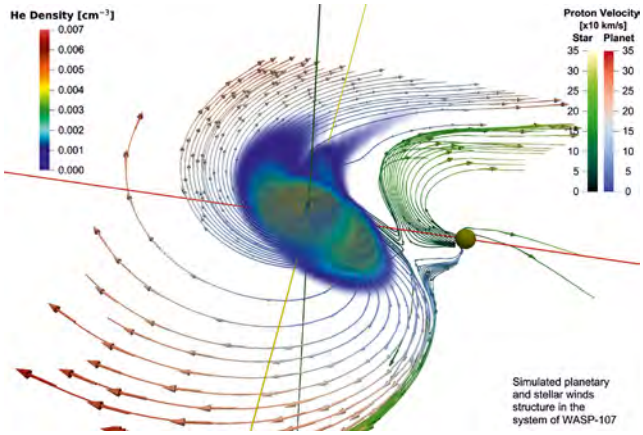

Helium 3D distribution in the atmosphere of WASP-107b. The planet is at the center of the coordinate system and moves anti-clockwise relative the star shown on the right.

PECULIAR NON-CIRCULAR SHADOWS OF SOME HOT JUPITERS FROM TRANSIT LIGHT-CURVES

The transit parameters provided by the Kepler mission enabled to look for photometric manifestations of non-spherical obscuring matter (e.g., exorings, dusts clouds, etc.) for a number of systems. Prior to this, the exoplanet parameters have been derived by fitting their transit light-curves (TLCs) assuming spherical planets and semi-major axes (calculated according to Kepler's third law), stellar radii and surface gravities. In the most typical case of a spherical transiting planet, the latter assumption does not break the consistency of the calculations. However, in the case of a non-spherical transiting planet and its non-circular shadow, the actual (i.e., obtained from the TLCs) value of the orbital semi-major axis may be inconsistent with respect to the rest of the transit parameters. The goal was to search for such inconsistencies, which manifest as differences between simulated and observed transit durations. A set of 21 hot Jupiters and 2 hot Neptunes have been investigated. The majority presented consistent transit parameters and quasi-circular shadows. However, seven objects were classified as outliers. Among them, Kepler-45b and Kepler-840b are the most intriguing because of the significant inconsistency of the parameter sets and the reconstructed elongated shadows. These finds could be interpreted in terms of dusty or aerosol contamination in the upper atmosphere or exorings.

Arkhypov et al., Astron. Astrophys., 646, A136, 2021.

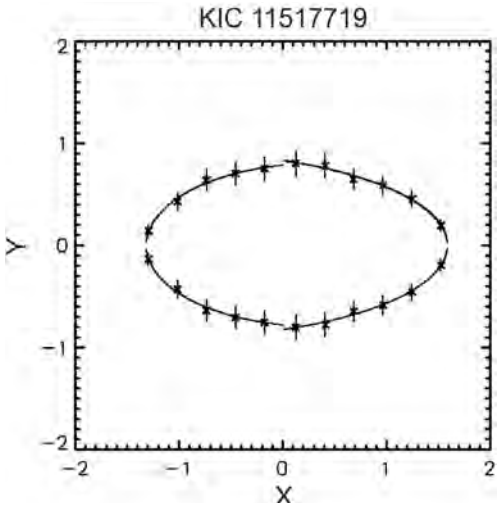

Reconstruction of elongated shadows for Kepler-840b orbiting KIC 11517719.

PROPERTIES OF RIEGER-TYPE CYCLES OF STELLAR ACTIVITY

The different driving mechanisms of Rieger cycles (a 154-day periodicity of solar flare occurrence) need verification in non-solar-like stars. Rieger-type cycles (RTCs) variability has been studied for 1726 main-sequence stars spanning a range of temperatures (T_{eff}) and rotation periods (P) employing Kepler light curves. Two kinds of the RTCs were found: 1) activity cycles with periods independent on the stellar rotation (for stars with T_{eff} < 5500 K) and 2) activity cycles with periods proportional to P (for stars with T_{eff} > 6300 K).

These two types of RTCs can be driven by Kelvin and Rossby waves, respectively. Rossby wave-driven RTCs correlate with the location of the tachocline, confirming the theoretical predictions. The Kelvin wave-driven RTCs do not show this correlation. Both types of wave drivers appear to coexist, leading to a joint modulation of the magnetic flux tubes, and the corresponding behavior of the activity period.

Arkhypov & Khodachenko, Astron. Astrophys., 651, A28, 2021.

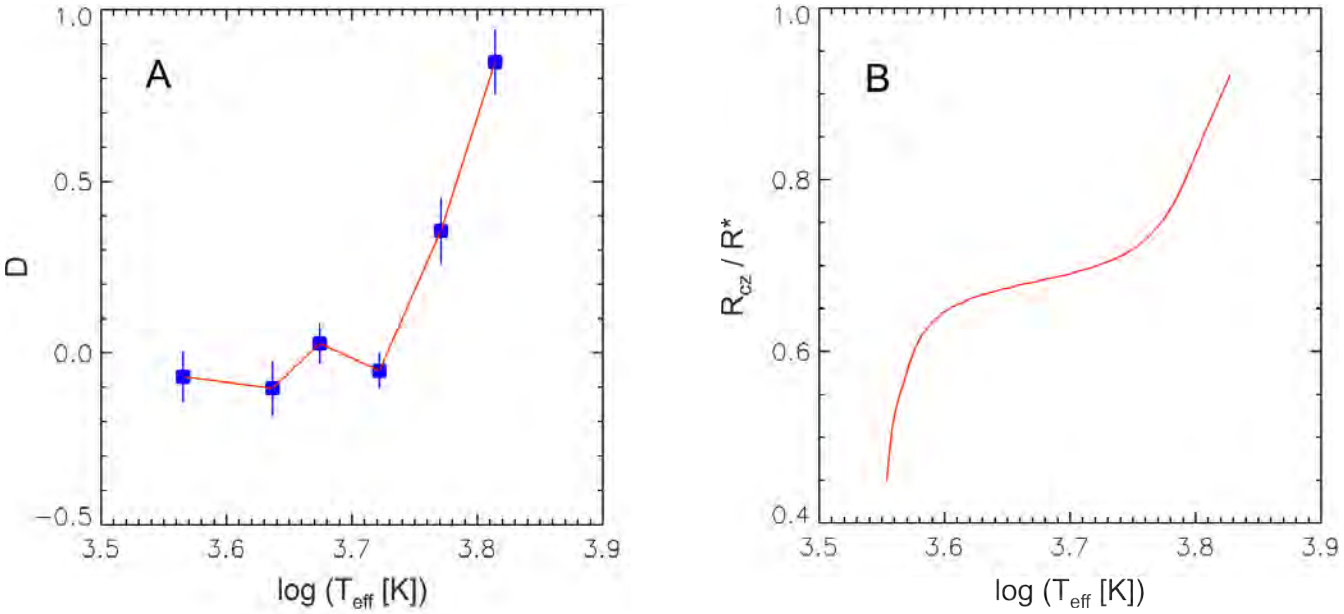

Change in power index D with varying log of stellar effective temperature T_{eff} (panel A) in comparison with the location of tachocline (panel B), revealed by the models of young (0.5 Gyr) main sequence stars with the solar abundance of metals.

SATELLITE LASER RANGING

In addition to routinely tracking more than 150 targets, which are equipped with laser retro-reflectors, the Satellite Laser Ranging (SLR) station of IWF is working on various international projects. Within the ESA tumbling motion project a large number of rotating space debris objects were characterized with respect to their tumbling behavior. Furthermore, range measurements to a spare *Galileo* panel were conducted at a remote location. Within a Stare and Chase experiment orbit predictions were improved during space debris tracking.

A new MHz laser has been installed at Graz SLR station and hardware and software is currently being upgraded to progress towards routine operation.

GALILEO ATTITUDE DETERMINATION

A *Galileo* in orbit validation (IOV) retro-reflector array identical to the panels mounted on the first four *Galileo* satellites was provided by ESA for laser ranging measurements at a remote location at 32.4 km distance with direct sight to the SLR station. A method is developed to measure the incidence angle on the panel by analyzing high repetition rate satellite laser ranging residuals. The panel was attached to an astronomical mount which allows the alignment of the geometrical axes to the *Galileo* panel with respect to the mount rotation axes (see figure below).

The *Galileo* IOV panel fixed on an astronomical mount and placed at a remote location located 32 km away from the SLR station Graz on a hill of 1200 m altitude.

By tilting the panel using the polar alignment screws of the mount, the panel was adjusted to point to the observatory (located 1.2° below the remote location). Fine adjustment of the panel reference orientation was done by optimizing the laser returns reflected by adjustment mirrors. A software tool was developed by which the mount/panel was rotated automatically into arbitrary positions corresponding to the desired incident/symmetry angle conditions. At the same time the nominal mount position with respect to the reference position was stored and time-tagged to be able to correlate the measurements to the laser ranging results which are also time-tagged.

Due to the hexagonal arrangement of the retro-reflectors, at given rotation angles, different rows of the retro-reflectors appear at constant distances relative to the observer. Symmetry conditions at 0°, 30°, 60° and 90° azimuthal rotation are most obvious but also intermediate symmetries exist. From the mm-precision range measurements to the panel and the statistical distribution of the returns range differences between rows down to 7 mm can be detected. Knowing the geometry of the panel, the incident angle of the laser beam on the panel can be calculated from the measurements. Data sheets are generated to analyze and visualize the results (see figure below). A range-histogram distribution (blue), a smoothed range dataset and the first derivative is calculated. The 12 peaks in the data result from the different rows at 30° azimuthal rotation while tilting the panel by 12°, corresponding to typical incident angle conditions on navigation satellites. By applying a Lomb analysis to the derivative, a most probable incident angle was derived. From the results it was concluded that the method allows to calculate the incident angle for 30° or 90° azimuthal rotation with an accuracy of 0.1°, independent of the distance to the target. Within an extensive tracking campaign approx. 100 symmetry passes of 24 different *Galileo* satellites were measured. The calculated incident angles of the *Galileo* panels will be compared to telemetry data of the respective *Galileo* spacecraft.

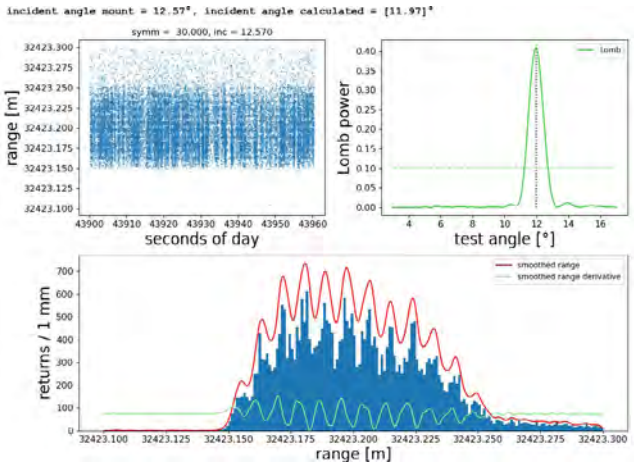

Data sheet for 30° symmetry orientation and 12° laser beam incident angle.

TUMBLING MOTION OF SPACE DEBRIS

Within the framework of the ESA project "Tumbling motion assessment for space debris objects" more than 20 different tumbling rocket bodies or defunct satellites are monitored and analyzed with respect to their tumbling behavior.

The Graz SLR station contributes by performing measurements with different measurement techniques. Besides satellite laser ranging to satellites equipped with retro-reflectors and space debris laser ranging relying on diffuse reflections of uncooperative targets, single photon light curves are recorded simultaneously. In addition to Graz' measurements, the Astronomical Institute of the University Bern gathers optical light curves, while the Fraunhofer Institute for High Frequency Physics and Radar Techniques in Wachtberg, Germany, conducts imaging radar and radar cross section measurements.

The "spin-up" of the defunct ocean topographic satellite *Jason 2* (NORAD ID: 33105) was discovered by the Graz SLR station to have occurred at the end of July 2020. Since then the tumbling behavior was monitored by IWF so far collecting 80 light curves and 60 satellite laser ranging datasets in the year 2021. Simultaneous light curve and satellite laser ranging measurements clearly show periodic signatures in both datasets (see figure). Due to the tumbling motion every 20 seconds the retro-reflector pyramid turns towards the observer and reaches its closest approach. Within one full rotation, the acceptance cone of the pyramid temporarily moves outside the observer's field of view and a gap in the SLR dataset occurs. The peaks in the light curve corresponds to sunlight reflections of the individual surfaces of the satellite and aligns well with the laser ranging measurements.

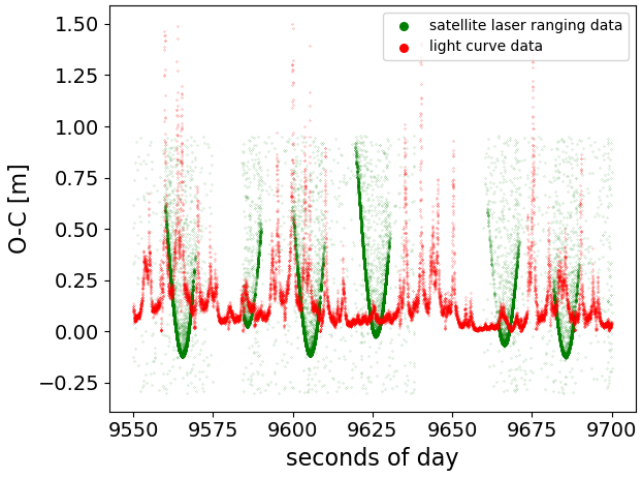

Simultaneous satellite laser ranging and light curve measurements to the defunct satellite *Jason 2*, clearly highlighting the tumbling behavior.

STARE AND CHASE TO SPACE DEBRIS

Together with the Comenius University in Bratislava a "Stare and Chase" tracking experiment was conducted within the project "Improvement of European capabilities for LEO objects tracking with optical passive sensors". The University of Bratislava tracked different space debris objects, acquiring a series of images (staring). From that the pointing direction was calculated via plate solving (analyzing the stellar background on the image). The observations were immediately used to improve two line element (TLE) predictions by optimizing the right ascension of the ascending node and the mean anomaly at the reference epoch. The improved TLE predictions were then transferred to the IWF server. Simultaneously, Graz started space debris laser ranging by using the non-optimized TLE prediction. As soon as Bratislava confirmed that improving the predictions was successful, Graz downloaded the predictions, implemented them into the internal tracking system and continued tracking with the improved TLE predictions. As typical LEO satellites pass over the observing station within only a few minutes the joint experiment had to be optimized regarding coordination. The big advantage of SLR is that due to the highly accurate laser ranging data, different sets of prediction can be evaluated regarding accuracy. Using Graz SLR measurements it was possible to prove that the time bias of the predictions - the time a space object is ahead or behind its prediction – could be reduced by a factor of 4. Furthermore, using these improved predictions it was possible to conduct "blind tracking" of an upper stage SL-8 rocket body (NORAD: 7009) - without visual feedback to center the object in the field of view of the telescope (see figure).

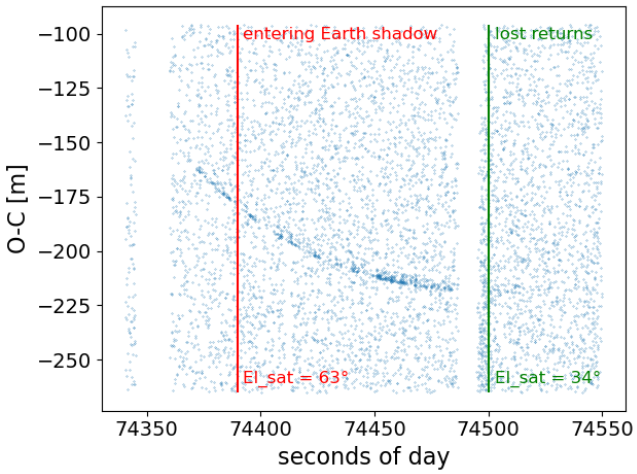

Blind tracking of an upper stage rocket body using an improved set of TLE predictions. The upper stage entered Earth shadow at an elevation of 63°. For more than 100 seconds returns could be detected afterwards.

TECHNOLOGIES

NEW DEVELOPMENTS

One possible aspect to reduce costs of space exploration and hence allowing for more frequent missions is to reduce the spacecraft size and consequently the launch masses. Scientific instruments also have to decrease their resource requirements such as volume, mass, and power, but at the same time achieve at least the same performance as heritage instruments. Therefore, the development of new instrument technologies is essential for competitive and excellent space research.

NEXT GENERATION ASPOC

For future science missions, active spacecraft potential control down to < 10 V is crucial to be able to operate sensitive scientific payloads. This does not only apply to large and medium-sized spacecraft, but also to micro- and nano-spacecraft, such as CubeSats. IWF, together with FOTEC, started a two-year technology study with the goal to develop a miniaturized version (50% power, 40% mass) of the *ASPOC* instruments built for NASA's *MMS* mission, which, seven years after launch, are still operating flawlessly.

In 2021, IWF entered the assembly and test phase of the *next generation ASPOC (ASPOC-NG)* instrument. After the integration of the processor and power supply boards into the electronics box, IWF fine-tuned a specific filter module, which is necessary to keep the electromagnetic interference at a level suitable for space missions. The box assembly was followed by a functional verification of the instrument with the ion and electron test modules provided by FOTEC. In parallel, IWF continued the setup of the facilities for the unit level tests.

Concerning the onboard software for operating the unit, IWF ported the relevant parts of the *MMS* flight S/W to *ASPOC-NG*, whereby the hardware-specific abstraction layers were adapted to support the *ASPOC-NG* setup. IWF conducted the respective S/W acceptance test by means of a dedicated emitter emulation board, which allowed for simulating various emitter conditions to achieve 100% code coverage.

After successfully passing the test board review with ESA in July, IWF performed the unit level test with the electronics box, while FOTEC tested the prototype emitter module. ESA carefully examined the test results in the following system test readiness review, which finally resulted in the go-ahead for the last project phase.

In October, IWF handed over the *ASPOC-NG* electronics box to FOTEC for the integration of the emitter module and execution of the system level test. With support from IWF, the test activities were completed successfully right before the end of the year.

ASPOC-NG electromagnetic compatibility (EMC) test with the new EMI Test Receiver (© OeAW/IWF/Jeszenszky).

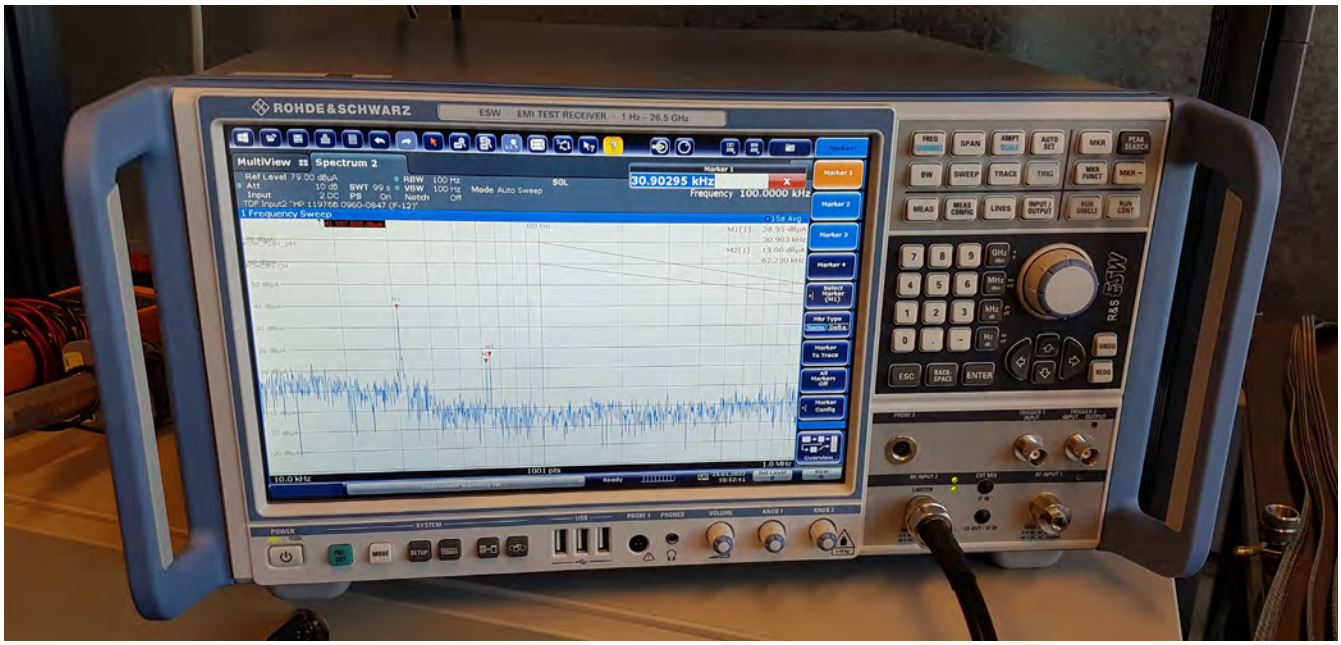

MAGNETOMETER FRONT-END ASIC

IWF and the Institute of Electronics of the Graz University of Technology (TUG) are collaborating on the next generation of the space proven Magnetometer Front-end ASIC (MFA). It features the readout electronics for magnetic field sensors which is optimized in terms of size and power consumption. The next generation Application Specific Integrated Circuit (ASIC) will overcome dynamic range limitations and be space qualified in the frame of the *FORSESAIL* mission.

Based on the evaluation results from two earlier test chips, which have contained just a single axis of the required feedback path including a high performance digital-to-analog converter (DAC), a first triple-axes feedback chip has been designed, simulated, routed and manufactured in 2021. XFAB Silicon Foundries was selected as chip manufacture because of the excellent noise performance of the transistor elements which come with a well-defined radiation characterization.

Each axis consists of a high-resolution current-steering DAC, a signal conditioning block and a fully differential current source to drive the feedback coil. The proposed current source offers an increased dynamic range and a very good low-noise performance. This results in a signal-to-noise ratio of more than 104 dB for a bandwidth of 512 Hz, requiring only a supply voltage of 3.3 V. The current source is capable of driving highly linear currents of more than 18 mA into the fluxgate sensors with an inductance of up to 9 mH while consuming 70 mW of power. An interface based on the I2S protocol was implemented for communication. Moreover, low voltage differential signaling receivers have been employed to keep the noise level low. A system monitoring block was also placed on chip to keep track of necessary environmental conditions.

The designed front-end occupies a total area of less than 11 mm^2.

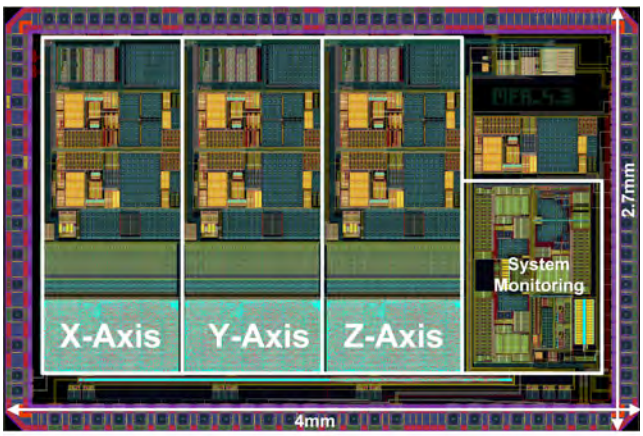

Layout of the designed chip. It contains three feedback paths including the proposed current source to compensate the ambient magnetic field within a fluxgate sensor.

MACHINE LEARNING ACTIVITIES

Funded through the European Commission's Horizon 2020 program, Europlanet 2024 Research Infrastructure (RI) provides free access to planetary simulation and analysis facilities, data services and tools, a ground-based observational network and program of community support activities. The University of Kent, UK, leads the Europlanet 2024 RI consortium, which has 57 beneficiary institutions from 25 countries in Europe and around the world, with a further 44 affiliated partners. The work package Machine Learning (ML) Solutions for Data Analysis and Exploitation in Planetary Science, led by IWF, develops ML powered data analysis and exploitation tools optimized for planetary science and integrates expert knowledge on ML into the planetary community. The goal is to build a multi-purpose toolset for ML-based data analysis that will be applicable to a range of scientific research questions in planetary science with minor or easily achievable customization efforts.

The scientific research questions range from the automatic detection of various features (e.g., bow shock and magnetopause crossings around Mercury and Earth, interplanetary mass ejections in in-situ solar wind observations - see figure - or surface features on Mars) to different classification problems (e.g., surface composition on Mercury, plasma wave emissions, or mineral identification).

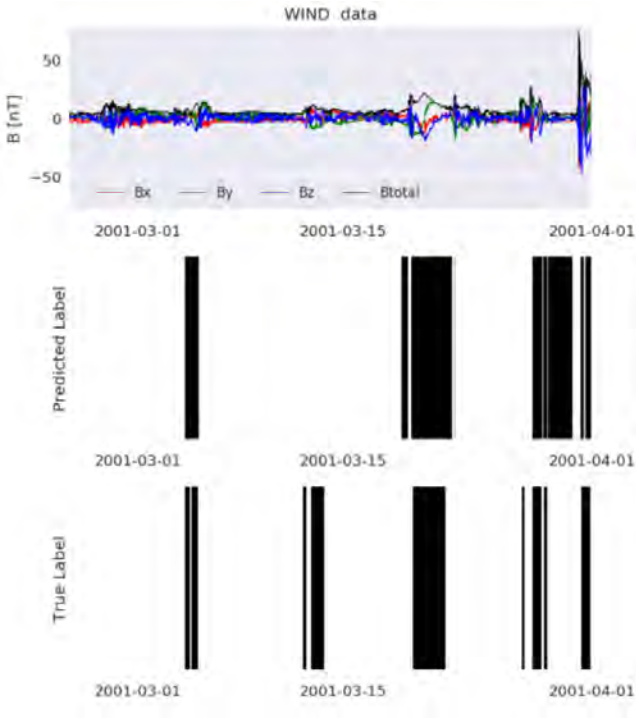

Comparison of predicted and true labels for Integrated Computational Materials Engineering (ICME) detections in *Wind* data in March 2001. Upper panel: Magnetic field measurements by *Wind*. Middle panel: Prediction of ICMEs (black areas). Lower panel: Observed ICMEs (black areas).

INFRASTRUCTURE

Space-born instruments are exposed to harsh environments, e.g., vacuum, large temperature ranges, radiation, and high mechanical loads during launch. They are expected to be highly reliable, providing full functionality over the entire mission duration, which could last for more than a decade.

IWF operates several test facilities and special infrastructure for the production of flight hardware. A high-performance computer helps the scientists to cope with the enormous data, which have to be analyzed for space missions. For further information on the IWF infrastructure refer to www.oeaw.ac.at/en/iwf/institute/infrastructure.

MEASUREMENT EQUIPMENT

In 2021, IWF updated and enhanced its measurement equipment for electromagnetic compatibility (EMC).

The official EMC tests for the flight electronics is typically done in an external test house, either ESA Test Service in Noordwijk or IABG close to Munich. Although the tests are limited to conductive measurements only, since the institute has no anechoic chamber, it is important to do a characterization of the electronics already in an early development phase.

Typically EMC tests are performed in a frequency range from 50 Hz to 100 MHz for conductive emissions and 30 MHz to 18 GHz for radiative emissions. Since the existing spectrum analyzer could not be calibrated anymore and was quite limited in the upper frequency range, IWF decided to purchase a new device. The selection process identified the EMI Test Receiver FSW26 from Rohde & Schwarz as the best solution. This device has an outstanding radio frequency band characteristics, high dynamic range and accuracy. Measurements from 10 Hz up to 26.5 GHz are supported. The device is in line with several relevant test specifications, captures and weights spectra with Fast Fourier Transformation based time domain scans and offers flexible configuration and multiple operation modes for best instrument usability.

In particular for the development of the space magnetometers the noise budget in low and ultra-low frequency ranges is of importance. This area is not supported by classical spectrum analyzers, but by high-performance audio analyzers. Thus, for the low frequency range the audio-analyzer UPV was selected, a device which supports measurements from DC to 250 kHz.

Both devices support the usage of scripts and remote operation via Ethernet, thus tests can be easily automated and standardized.

EMC test in the IWF lab (© OeAW/Klaus Pichler).

Work before pleasure. After all their questions had been answered, the kids of VS Krems-Stein had fun launching rockets in the schoolyard (© OeAW/IWF/Scherr).

LAST BUT NOT LEAST

6391 DAYS

On 1 January 2001 Wolfgang Baumjohann took over the management of the Department of Experimental Space Research and became the institute's director on 1 April 2004. He has led IWF for exactly 6391 days, which makes him the longest serving IWF director. During these 17.5 years he made the institute fit for the new millennium.

Baumjohann led the institute with very clear ideas, adapted and partly reoriented it. The highest goals were always scientific excellence and a clear connection between science and instrumentation as well as a good understanding with the central administration in Vienna. The number of publications has quadrupled to around 170 per year. The citation rate has increased almost tenfold to 7100 per year. In 2011, an independent evaluation committee rated the institute as "outstanding" and "certainly at the top of its field for an institute of this size". IWF's Scientific Advisory Board described the institute repeatedly as "unique in Austria, certainly amongst the 5% best institutions of its kind internationally" and "playing a leading role in Europe and world-wide in very exciting research fields, such as space plasma physics, (exo-)planet atmospheres and star-planet-interactions".

Baumjohann has received numerous honors, which impressively demonstrate the value of his work. He is member of OeAW, the German National Academy of Sciences Leopoldina (Executive Council), the Academia Europaea, the International Academy of Astronautics, and the European Academies Science Advisory Council, Fellow of the American Geophysical Union, recipient of the Austrian Cross of Honor for Science and Art, First Class and the Styrian Medal of Honor for Science, Research and Arts, the Cardinal Innitzer Recognition Price, and was named Austrian Scientist of the Year 2014.

Baumjohann's scientific legacy includes more than 600 papers in scientific journals and four books. He is one of the most cited space scientists. Since the beginning, he was available at and for the institute almost continuously and exclusively; his commitment was enormous. During his directorship, 27 space-born instruments were designed, built, tested, launched and successfully operated in space; ten of them led by IWF with Baumjohann as Principal Investigator of the magnetometer aboard the Japanese *MMO* spacecraft of the *BepiColombo* mission.

Baumjohann has very successfully led and further developed the institute to its current high standard. IWF owes him a great debt of gratitude and wishes him many healthy years in retirement. We look forward to future, fruitful discussions and a joint exchange of ideas.

Werner Magnes, Christiane Helling, Wolfgang Baumjohann, Julia Fröhlich (OeAW Vienna), and Hans Sünkel during the handover ceremony at IWF on 1 October 2021 (© OeAW/IWF/Scherr).

PUBLIC OUTREACH

IWF is actively engaged in science education and public outreach. Due to Covid-19, another year passed without visitors being guided through the labs. However, IWF continued its mission to find new ways to bring science to the public.

From 9 April to 31 October, the "Steiermark Schau" showed Styria's past, present, and future. IWF participated in the exhibition in the Folk Life Museum, where visitors could look through a microscope and discover the Styrian panther, "hidden" on a magnetometer microchip designed for NASA's *MMS* mission.

From 30 September to 4 October, the institute was part of SpaceTech 2021, a special exhibition at the Graz Autumn Fair. IWF presented its participation in the current ESA missions *CHEOPS, BepiColombo,* and *Solar Orbiter*.

On 2 October, IWF was invited to participate in the Austrian "Lange Nacht der Museen". Günter Kargl and Sunny Laddha presented the *CoPhyLab* project at the Vienna Museum of Science and Technology.

Throughout the year, several (online) public lectures were given. At Antares-NOe Volkssternwarte Günter Kargl reported news from NASA's *InSight* mission and Rumi Nakamura gave an overview of plasma in space. At URANIA Steiermark in Graz Luca Fossati talked about habitable worlds in the universe and Wolfgang Voller about the autumn sky. In the frame of the science program of Wiener Volkshochschulen, Günter Kargl presented the possibilities of a holiday in space and Luca Fossati explained how *ARIEL* will investigate exoplanetary atmospheres.

Luca Fossati and Günter Kargl participated in the Science Academy Niederösterreich with a workshop on satellite design. For the lecture series "Facetten der Physik" of University of Graz Günter Kargl explained the different Mars landers. As Young Science Ambassadors of OeAD, Günter Kargl and Christian Möstl held several lectures for school classes allover Austria.

Following the OeAW "Young Science Initiative", IWF participates in the project "Akademie im Klassenzimmer". Luca Fossati and Alexandra Scherr visited the Volksschule Krems-Stein, where they answered questions of the school kids ranging from aliens, along black holes to exoplanets (see left photos).

In the frame of OeAW's Science Bites series, Luca Fossati explained how to search for extraterrestrial life and Günter Kargl talked about how to develop instruments for missions to Mars and other planets.

Volume 8 of the OeAW comics series "Akademics" takes young readers on an exciting journey through time and the fascinating world of stars and planets to learn how Johannes Kepler unravelled their secrets some 400 years ago. Researchers from IWF acted as "scientific advisors" (www.oeaw.ac.at/akademics/sternenkunde).

Topics discussed in the space blog of the Austrian newspaper "Der Standard" were inhospitable exoplanets, nitrogen atmospheres as the basis for life, the Venus flybys of *Solar Orbiter* and *BepiColombo,* and auroral beads.

In the Servus TV show "P.M. Wissen" Magda Delva explained the differences between the Earth and its "twin" Venus. In the ORF youth magazine "Fanny's Friday Doku", Christian Möstl and Luca Fossati tried to answer the question of all questions: Are we alone in the universe? Finally, *Rosetta's* atomic force microscope *MIDAS* was one of the main actors in "Museum AHA", ORF's knowledge show for kids by and with Thomas Brezina.

IWF team at the pre-opening of SpaceTech 2021, organized on 29 September with and for representatives from industry, research and politics (© Fritz Höllerbauer).

There is a lot to discover in the exhibition MISSION POSSIBLE! (© Universalmuseum Joanneum/J.J. Kucek).

Last but not least, IWF started to celebrate its 50th birthday with MISSION POSSIBLE!, a hands-on special exhibition at CoSA - Center of Science Activities in Graz. In cooperation with the Children's Museum FRida&freD, a 30-meter long comic was created, on which the activities of the institute are vividly depicted. Original space instruments from IWF's 50-year history are integrated into the comic and have to be discovered. This way the visitors find out how a space mission is developed while they participate in a fictitious mission to Enceladus, one of Saturn's largest moons. The exhibition opened on 18 December and can be visited until 11 September 2022.

RECOGNITION

Martin A. Reiss was awarded the "Alexander Chizhevsky Medal for Space Weather and Space Climate".

The medal was presented by Christoph Crepaz, the Honorary Consul of Austria in Great Britain (© OeAW/IWF/Reiss).

MEETINGS

T. Amerstorfer, U. Amerstorfer, M. Boudjada, G. Kargl, H. Lammer, R. Nakamura, C. Simon-Wedlund, and M. Volwerk were members of thirteen scientific program and/or organizing committees at seven international conferences.

LECTURING

In summer 2021 and in winter term 2021/2022 IWF members gave (online) lectures at the University of Graz, Graz University of Technology, University of Vienna, TU Braunschweig, and FH Wiener Neustadt.

THESES

Besides lecturing, IWF members are supervising Bachelor, Diploma, Master and Doctoral Theses. In 2021, the following supervised theses have been completed:

Bauer, M.: Prediction of CME Arrival Time and Speed Using STEREO-HI Beacon Data, Master Thesis, Universität Graz, 58 p., 2021.

Hinterreiter J., Enhancing and Evaluating an Analytical Model to Improve the Prediction of Solar Storm Arrivals, Doctoral Thesis, Universität Graz, 126 p., 2021.

INTERNSHIPS

During summer time, three (high-school) students performed an internship at IWF. They worked on the design and layout of a printed circuit board for a power supply unit, the design, assembly and test of several new magnetic field demo experiments, as well as on the development of an automatic target selection algorithm for planetary atmospheric evolution modeling.

NEW PROJECTS

In 2021, the following third party projects with a budget greater than 100,000 EUR were acquired:

Project	Lead
EU - Marie Curie ITN CHAMELEON "Virtual Laboratories for Exoplanets and Planet-Forming Disks"	Ch. Helling, P. Woitke
FFG - Operation & Test of the *MAGSCA* Flight Model	W. Magnes
FFG - Development of the DPU Prototype for *MANiaC*	M. Steller
FFG - Modeling of Science Cases for *BepiColombo/PICAM*	G. Laky
FWF - Magnetosheath Jets throughout the Solar Cycle	F. Plaschke
HITSZ - Scalar Magnetometer for *Macao* Science Satellite	A. Pollinger
SwRI - Front-End Electronics for *SWFO* Magnetometer	D. Fischer
Yebes Observatory - Laser and Detection Package	G. Kirchner

IN MEMORIAM

SIEGFRIED JOSEF BAUER (1930-2021)

Siegfried J. Bauer (© Chris Bauer).

On 19 September 2021, Siegfried Josef Bauer passed away shortly after his 91st birthday.

Bauer studied meteorology, geophysics and physics at Graz University and earned his PhD in 1953 with a dissertation on experimental radio measurement techniques for ionospheric investigations with Prof. Otto Burkard. Shortly after graduation he joined the US Army Signal Corps Research and Development Laboratory in Fort Monmouth, New Jersey. He worked in the meteorological branch and dealt with weather radar and sferics (radio noise signals from lightning strokes). In 1957 he changed the branch and was then performing research with the Diana moon radar.

After six years at the military laboratory Bauer joined the then recently-established NASA Goddard Space Flight Center (GSFC) in 1961, where he worked on sounding rocket campaigns mainly from Wallops Island, Virgina, and on preparations for the topside sounders of the two Canadian Alouette satellites launched in 1962 and 1965. In 1965 he was promoted to head of the Planetary Ionospheres Branch (later renamed Ionospheric and Radio Physics Branch) and in 1970 to Associate Chief of the Laboratory for Planetary Atmospheres. In 1974 he gained the NASA Medal for Exceptional Scientific Achievement. From 1975 to 1981 he served as Associate Director of Sciences at GSFC.

In September 1981 Bauer succeeded his doctoral thesis adviser Burkard as Professor of Meteorology and Geophysics at University of Graz, where he taught geophysics/physics students in the field of space sciences/ geophysics/meteorology until his retirement in 1998.

Supplementary to his university enrollment Bauer was head of the Department of Physics of Near-Earth Space of the Space Research Institute of the Austrian Academy of Sciences in Graz (1982 to 1998) and its Vice Director. His research interests concentrated on the comparison of the ionospheres of Venus, Earth and Mars, as well as the upper atmospheres of planetary moons in the outer solar system. During his career he was Co-Investigator of several scientific instruments on space probes (e.g. *Ariel 3*, *Aeros 1 & 2*, *Pioneer Venus*, *Mars Global Surveyor*, and the Titan entry probe *Huygens* of the *Cassini* mission) and thereby responsible for the successful data analysis and interpretation.

Between 1983 and 1998 Bauer served in several advisory committees of ESA. From 1984 to 2011 he was the Austrian National Representative to COSPAR (Committee on Space Research) and from 1983 to 2011 he served as Austrian delegate to URSI (International Union of Radio Science).

Bauer was elected member of the Austrian Academy of Sciences (1983), the International Academy of Astronautics (1986) and the Academia Europaea (1992). His scientific work was honored by being named Fellow of the American Association for the Advancement of Sciences (1970), Fellow of the American Geophysical Union (1978), and Honorary Fellow of the Royal Astronomical Society (2011). He received the Erwin-Schrödinger Award of the Austrian Academy of Sciences (1991) and the David Bates Medal of the European Geophysical Society (2000). Since 2017 the Minor planet 73701 bears the name "Siegfriedbauer". In 1996 he was awarded the "Österreichisches Ehrenzeichen für Wissenschaft und Kunst" (Austrian Decoration for Science and Art) and became a member of the "Kurie für Wissenschaft" (Curia for Science).

Bauer was author of two textbooks on the upper atmospheres of planets, editor of several scientific books and author/co-author of more than 150 scientific publications in the scientific fields of ionospheric physics, aeronomy, and global environmental problems.

IWF not only lost a prominent scientist and mentor but also a remarkable person. Through his work, he was inspiration and model for „several generations“ of scientists, who were lucky enough to work, discuss and/ or communicate with him. The institute's members will always remember him gratefully.

PUBLICATIONS

REFEREED ARTICLES

Alho, M., R. Jarvinen, C. Simon Wedlund, H. Nilsson, E. Kallio, T.I. Pulkkinen: Remote sensing of cometary bow shocks: Modelled asymmetric outgassing and pickup ion observations, *MNRAS*, **506**, 4735-4749, doi, 2021.

Alken, P., E. Thébault, C.D. Beggan, H. Amit, J. Aubert, …, W. Magnes, et al.: International Geomagnetic Reference Field: The thirteenth generation, *Earth Planets Space*, **73**, 49, doi, 2021.

Allen, R.C., G.C. Ho, L.K. Jian, S.K. Vines, S.D. Bale, …, C. Möstl, et al.: A living catalog of stream interaction regions in the Parker Solar Probe era, *Astron. Astrophys.*, **650**, A25, doi, 2021.

Allen, R.C., I. Cernuda, D. Pacheco, L. Berger, Z.G. Xu, …, M. Volwerk, …, M. Steller, et al.: Energetic ions in the Venusian system: Insights from the first Solar Orbiter flyby, *Astron. Astrophys.*, **656**, A7, doi, 2021.

Amerstorfer, T., J. Hinterreiter, M.A. Reiss, C. Möstl, J.A. Davies, R.L. Bailey, A.J. Weiss, M. Dumbovic, M. Bauer, U.V. Amerstorfer, R.A. Harrison: Evaluation of CME arrival prediction using ensemble modeling based on heliospheric imaging Observations, *Space Weather*, **19**, e2020SW002553, doi, 2021.

Archer, M.O., M.D. Hartinger, F. Plaschke, D.J. Southwood, L. Rastaetter: Magnetopause ripples going against the flow form azimuthally stationary surface waves, *Nat. Comm.*, **12**, 5697, doi, 2021.

Arkhypov, O.V., M.L. Khodachenko: Empirically revealed properties of Rieger-type cycles of stellar activity, *Astron. Astrophys.*, **651**, A28, doi, 2021.

Arkhypov, O.V., M.L. Khodachenko, A. Hanslmeier: Revealing peculiar exoplanetary shadows from transit light curves, *Astron. Astrophys.*, **646**, A136, doi, 2021.

Attree, N., E. Kaufmann, A. Hagermann: Gas flow in Martian spider formation, *Icarus*, **359**, 114355, doi, 2021.

Bailey, R.L., M.A. Reiss, C.N. Arge, C. Möstl, C.J. Henney, M.J. Owens, U.V. Amerstorfer, T. Amerstorfer, A.J. Weiss, J. Hinterreiter: Using gradient boosting regression to improve ambient solar wind model predictions, *Space Weather*, **19**, e2020SW002673, doi, 2021.

Bauer, M., T. Amerstorfer, J. Hinterreiter, A.J. Weiss, J.A. Davies, C. Möstl, U.V. Amerstorfer, M.A. Reiss, R.A. Harrison: Predicting CMEs using ELEvoHI with STEREO-HI beacon data, *Space Weather*, **19**, e2021SW002873, doi, 2021.

Benkhoff, J., G. Murakami, W. Baumjohann, S. Besse, E. Bunce, et al.: BepiColombo - mission overview and science goals, *Space Sci. Rev.*, **217**, 90, doi, 2021.

Benni, P., A.Y. Burdanov, V.V. Krushinsky, A. Bonfanti, G. Hébrard, et al.: Discovery of a young low-mass brown dwarf transiting a fast-rotating F-type star by the Galactic Plane eXoplanet (GPX) survey, *MNRAS*, **505**, 4956-4967, doi, 2021.

Benz, W., C. Broeg, A. Fortier, N. Rando, T. Beck, …, W. Baumjohann, …, L. Fossati, …, J. Hasiba, …, H. Ottacher, …, M. Steller, et al.: The CHEOPS mission, *Exp. Astron.*, **51**, 109-151, doi, 2021.

Birn, J., M. Hesse, S.T. Bingham, D.L. Turner, R. Nakamura: Acceleration of oxygen ions in dipolarization events: 1. CPS distributions, *J. Geophys. Res.*, **126**, e2021JA029184, doi, 2021.

Birn, J., M. Hesse, S.T. Bingham, D.L. Turner, R. Nakamura: Acceleration of oxygen ions in dipolarization events: 2. PSBL distributions, *J. Geophys. Res.*, **126**, e2021JA029143, doi, 2021.

Bonfanti, A., L. Delrez, M.J. Hooton, T.G. Wilson, L. Fossati, …, W. Baumjohann, …, J. Hasiba, …, H. Ottacher, …, M. Steller, et al.: CHEOPS observations of the HD 108236 planetary system: A fifth planet, improved ephemerides, and planetary radii, *Astron. Astrophys.*, **646**, A157, doi, 2021.

Bonfanti, A., L. Fossati, D. Kubyshkina, P.E. Cubillos: Constraining stellar rotation and planetary atmospheric evolution of a dozen systems hosting sub-Neptunes and super-Earths, *Astron. Astrophys.*, **656**, A157, doi, 2021.

Borsa, F., A.F. Lanza, I. Raspantini, M. Rainer, L. Fossati, et al.: The GAPS programme at TNG XXXI. The WASP-33 system revisited with HARPS-N, *Astron. Astrophys.*, **653**, A104, doi, 2021.

Borsato, L., G. Piotto, D. Gandolfi, V. Nascimbeni, G. Lacedelli, …, W. Baumjohann, …, L. Fossati, …, J. Hasiba, …, M. Steller, et al.: Exploiting timing capabilities of the CHEOPS mission with warm-Jupiter planets, *MNRAS*, **506**, 3810-3830, doi, 2021.

Brandenburg, A., A. Johansen, P.A. Bourdin, W. Dobler, W. Lyra, et al.: The Pencil Code, a modular MPI code for partial differential equations and particles: Multipurpose and multiuser-maintained, *J. Open Source Softw.*, **6 (58)**, 2807, doi, 2021.

Broeren, T., K.G. Klein, J.M. TenBarge, I. Dors, O.W. Roberts, D. Verscharen: Magnetic field reconstruction for a realistic multi-point, multi-scale spacecraft observatory, *Front. Astron. Space Sci.*, **8**, 727076, doi, 2021.

Carbone, F., L. Sorriso-Valvo, Yu.V. Khotyaintsev, K. Steinvall, A. Vecchio, …, M. Steller, et al.: Statistical study of electron density turbulence and ion-cyclotron waves in the inner heliosphere: Solar Orbiter observations, *Astron. Astrophys.*, **656**, A16, doi, 2021.

Carleo, I., A. Youngblood, S. Redfield, N.C. Barris, T.R. Ayres, …, L. Fossati, et al.: A multiwavelength look at the GJ 9827 system: No evidence of extended atmospheres in GJ 9827b and d from HST and CARMENES data, *Astron. J.*, **161**, 136, doi, 2021.

Chen, Y.Q., M. Wu, T.L. Zhang, Y. Huang, G.Q. Wang, R. Nakamura, W. Baumjohann, et al.: Statistical characteristics of field-aligned currents in the plasma sheet boundary layer, *J. Geophys. Res.*, **126**, e2020JA028319, doi, 2021.

Cheng, Z.W., J.K. Shi, K. Torkar, G.P. Lu, M.W. Dunlop, et al.: Impact of the solar wind dynamic pressure on the field-aligned currents in the magnetotail: Cluster observation, *J. Geophys. Res.*, **126**, e2021JA029785, doi, 2021.

Chust, T., M. Kretzschmar, D.B. Graham, O. Le Contel, A. Retinò, …, M. Steller, et al.: Observations of whistler mode waves by Solar Orbiter's RPW Low Frequency Receiver (LFR): In-flight performance and first results, *Astron. Astrophys.*, **656**, A17, doi, 2021.

Comisel, H., Y. Narita, U. Motschmann: Wavevector spectral signature of decay instability in space plasmas, *Ann. Geophys.*, **39**, 165-170, doi, 2021.

Cozzani, G., Yu.V. Khotyaintsev, D.B. Graham, J. Egedal, M. André, …, R. Nakamura, et al.: Structure of a perturbed magnetic reconnection electron diffusion region in the Earth's magnetotail, *Phys. Rev. Lett.*, **127**, 215101, doi, 2021.

Cubillos, P.E., D. Keating, N.B. Cowan, J.M. Vos, B. Burningham, et al.: Longitudinally Resolved Spectral retrieval (ReSpect) of WASP-43b, *Astrophys. J.*, **915**, 45, doi, 2021.

Cubillos, P.E., J. Blecic: The PYRAT BAY framework for exoplanet atmospheric modelling: A population study of Hubble/WFC3 transmission spectra, *MNRAS*, **505**, 2675-2702, doi, 2021.

Davies, E.E., C. Möstl, M.J. Owens, A.J. Weiss, T. Amerstorfer, J. Hinterreiter, M. Bauer, R.L. Bailey, M.A. Reiss, …, W. Magnes, W. Baumjohann, D. Fischer, et al.: In situ multi-spacecraft and remote imaging observations of the first CME detected by Solar Orbiter and BepiColombo, *Astron. Astrophys.*, **656**, A2, doi, 2021.

Davies, E.E., R.J. Forsyth, R.M. Winslow, C. Möstl, N. Lugaz: A catalog of Interplanetary Coronal Mass Ejections observed by Juno between 1 and 5.4 AU, *Astrophys. J.*, **923**, 136, doi, 2021.

Deibert, E.K., E.J.W. de Mooij, R. Jayawardhana, J.D. Turner, A. Ridden-Harper, L. Fossati, et al.: Detection of ionized calcium in the atmosphere of the ultra-hot Jupiter WASP-76b, *Astrophys. J. Lett.*, **919**, L15, doi, 2021.

Delrez, L., D. Ehrenreich, Y. Alibert, A. Bonfanti, L. Borsato, L. Fossati, …, W. Baumjohann, …, M. Steller, et al.: Transit detection of the long-period volatile-rich super-Earth ν2 Lupi d with CHEOPS, *Nat. Astron.*, **5**, 775–787, doi, 2021.

Denton, R.E., R.B. Torbert, H. Hasegawa, K.J. Genestreti, R. Manuzzo, …, R. Nakamura, et al.: Two-dimensional velocity of the magnetic structure observed on July 11, 2017 by the Magnetospheric Multiscale spacecraft, *J. Geophys. Res.*, **126**, e2020JA028705, doi, 2021.

Dumbadze, G., B.M. Shergelashvili, S. Poedts, T.V. Zaqarashvili, M. Khodachenko, et al.: Eigenspectra of solar active region long-period oscillations, *Astron. Astrophys.*, **653**, A39, doi, 2021.

Erkaev, N.V., M. Scherf, S.E. Thaller, H. Lammer, A.V. Mezentsev, V.A. et al.: Escape and evolution of Titan's N-2 atmosphere constrained by N-14/N-15 isotope ratios, *MNRAS*, **500**, 2020-2035, doi, 2021.

Farrugia, C.J., A.J. Rogers, R.B. Torbert, K.J. Genestreti, T.K.M. Nakamura, et al.: An encounter with the ion and electron diffusion regions at a flapping and twisted tail current sheet, *J. Geophys. Res.*, **126**, e2020JA028903, doi, 2021.

Fischer, G., M. Panchenko, W. Macher, Y. Kasaba, H. Misawa, et al.: Calibration of the JUICE RWI antennas by numerical simulation, *Radio Sci.*, **56**, e2021RS007309, doi, 2021.

Forget, F., O. Korablev, J. Venturini, T. Imamura, H. Lammer, M. Blanc: Editorial: Topical collection on understanding the diversity of planetary atmospheres, *Space Sci. Rev.*, **217**, 51, doi, 2021.

Fossati, L., M.E. Young, D. Shulyak, T. Koskinen, C. Huang, P.E. Cubillos, …, A.G. Sreejith: Non-local thermodynamic equilibrium effects determine the upper atmospheric temperature structure of the ultra-hot Jupiter KELT-9b, *Astron. Astrophys.*, **653**, A52, doi, 2021.

Fu, G.W., D. Deming, J. Lothringer, N. Nikolov, D.K. Sing, …, M. Lendl, et al.: The Hubble PanCET program: Transit and eclipse spectroscopy of the strongly irradiated giant exoplanet WASP-76b, *Astron. J.*, **162**, 108, doi, 2021.

Garcia Muñoz, A., L. Fossati, A. Youngblood, N. Nettelmann, D. Gandolfi, et al.: A heavy molecular weight atmosphere for the super-Earth pi Men c, *Astrophys. J. Lett.*, **907**, L36, doi, 2021.

Giacobbe, P., M. Brogi, S. Gandhi, P.E. Cubillos, A.S. Bonomo, …, L. Fossati, et al.: Five carbon- and nitrogen-bearing species in a hot giant planet's atmosphere, *Nature*, **592**, 205–208, doi, 2021.

Graham, D.B., Yu.V. Khotyaintsev, A. Vaivads, N.J.T. Edberg, A.I. Eriksson, …, M. Steller, et al.: Kinetic electrostatic waves and their association with current structures in the solar wind, *Astron. Astrophys.*, **656**, A23, doi, 2021.

Hadid, L.Z., N.J.T. Edberg, T. Chust, D. Píša, A.P. Dimmock, …, M. Volwerk, …, M. Steller, et al.: Solar Orbiter's first Venus flyby: Observations from the Radio and Plasma Wave instrument, *Astron. Astrophys.*, **656**, A18, doi, 2021.

Hansel, P.J., F.D. Wilder, D.M. Malaspina, R.E. Ergun, N. Ahmadi, J.C. Holmes, et al.: Mapping MMS observations of solitary waves in Earth's magnetic field, *J. Geophys. Res.*, **126**, e2021JA029389, doi, 2021.

Hasegawa, H., T.K.M. Nakamura, R.E. Denton: Reconstruction of the electron diffusion region with inertia and compressibility effects, *J. Geophys. Res.*, **126**, e2021JA029841, doi, 2021.

Hayakawa, H., C. Kuroyanagi, V.M.S. Carrasco, S. Uneme, B.P. Besser, et al.: Sunspot observations at the Eimmart observatory and in its neighborhood during the late Maunder Minimum (1681-1718), *Astrophys. J.*, **909**, 166, doi, 2021.

Hayakawa, H., K. Schlegel, B.P. Besser, Y. Ebihara: Candidate auroral observations indicating a major solar-terrestrial storm in 1680: Implication for space weather events during the Maunder Minimum, *Astrophys. J.*, **909**, 29, doi, 2021.

Hayakawa, H., M. Lockwood, M.J. Owens, M. Sôma, B.P. Besser, et al.: Graphical evidence for the solar coronal structure during the Maunder Minimum: Comparative study of the total eclipse drawings in 1706 and 1715, *J Space Weather Space Clim*, **11**, 1, doi, 2021.

Hayakawa, H., T. Iju, C. Kuroyanagi, V.M.S. Carrasco, B.P. Besser, et al.: Johann Christoph Müller's sunspot observations in 1719 – 1720: Snapshots of the immediate aftermath of the Maunder Minimum, *Solar Phys.*, **296**, 154, doi, 2021.

Hayakawa, H., T. Iju, K. Murata, B.P. Besser: Daniel Mögling's sunspot observations in 1626-1629: A manuscript reference for the solar activity before the Maunder Minimum, *Astrophys. J.*, **909**, 194, doi, 2021.

Hayakawa, H., T. Iju, S. Uneme, B.P. Besser, S. Kosaka, et al.: Reanalyses of the sunspot observations of Fogelius and Siverus: Two 'long-term' observers during the Maunder Minimum, *MNRAS*, **506**, 650-658, doi, 2021.

Hayakawa,H., S. Uneme, B.P. Besser, T. Iju, S. Imada: Stephan Prantner's sunspot observations during the Dalton Minimum, *Astrophys. J.*, **919**, 1, doi, 2021.

He, M., J. Vogt, E. Dubinin, T.L. Zhang, Z. Rong: Spatially highly resolved solar-wind-induced magnetic field on Venus, *Astrophys. J.*, **923**, 73, doi, 2021.

Heyner, D., H.-U. Auster, K.-H. Fornaçon, C. Carr, I. Richter, …, W. Baumjohann, …, W. Magnes, G. Berghofer, D. Fischer, F. Plaschke, R. Nakamura, Y. Narita, M. Delva, M. Volwerk, et al.: The BepiColombo Planetary Magnetometer MPO-MAG: What can we learn from the Hermean magnetic field?, *Space Sci. Rev.*, **217**, 52, doi, 2021.

Hinterreiter, J., T. Amerstorfer, M. Temmer, M.A. Reiss, A.J. Weiss, C. Möstl, …, M. Bauer, U.V. Amerstorfer: Drag-based CME modeling with heliospheric images incorporating frontal deformation: ELEvoHI 2.0, *Space Weather*, **19**, e2021SW002836, doi, 2021.

Hinterreiter, J., T. Amerstorfer, M.A. Reiss, C. Möstl, M. Temmer, M. Bauer, U.V. Amerstorfer, R.L. Bailey, A.J. Weiss, et al.: Why are ELEvoHI CME arrival predictions different if based on STEREO-A or STEREO-B heliospheric imager observations?, *Space Weather*, **19**, e2020SW002674, doi, 2021.

Holmes, J.C., R. Nakamura, D. Schmid, T.K.M. Nakamura, O. Roberts, Z. Vörös: Wave activity in a dynamically evolving reconnection separatrix, *J. Geophys. Res.*, **126**, e2020JA028520, doi, 2021.

Hwang, K.-J., K. Dokgo, E. Choi, J.L. Burch, D.G. Sibeck, …, T.K.M. Nakamura, et al.: Bifurcated current sheet observed on the boundary of Kelvin-Helmholtz vortices, *Front. Astron. Space Sci.*, **8**, 782924, doi, 2021.

Iqbal, F., G. Kirchner, F. Koidl, E. Leitgeb: Laser back scatter: Limitation to higher repetition rate [kHz] Satellite Laser Ranging system, *Geod. Geodyn.*, **12**, 48-53, doi, 2021.

Johansen, A., T. Ronnet, M. Bizzarro, M. Schiller, M. Lambrechts, …, H. Lammer: A pebble accretion model for the formation of the terrestrial planets in the solar system, *Sci. Adv.*, **7**, eabc0444, doi, 2021.

Johnstone, C.P., H. Lammer, K.G. Kislyakova, M. Scherf, M. Güdel: The young Sun's XUV-activity as a constraint for lower CO2-limits in the Earth's Archean atmosphere, *Earth Planet Sci Lett*, **576**, 117197, doi, 2021.

Kajdič, P., B. Sánchez-Cano, L. Neves-Ribeiro, O. Witasse, G.C. Bernal, D. Rojas-Castillo, et al.: Interaction of space weather phenomena with Mars plasma environment during Solar Minimum 23/24, *J. Geophys. Res.*, **126**, e2020JA028442, doi, 2021.

Kajdič, P., Y. Pfau-Kempf, L. Turc, A.P. Dimmock, M. Palmroth, …, L. Preisser, et al.: ULF wave transmission across collisionless shocks: 2.5D local hybrid simulations, *J. Geophys. Res.*, **126**, e2021JA029283, doi, 2021.

Kamp, I., M. Honda, H. Nomura, M. Audard, D. Fedele, …, M. Kim, et al.: The formation of planetary systems with SPICA, *Pub. Astron. Soc. Aust.*, **38**, e055, doi, 2021.

Karlsson, T., D. Heyner, M. Volwerk, M. Morooka, F. Plaschke, et al.: Magnetic holes in the solar wind and magnetosheath near Mercury, *J. Geophys. Res.*, **126**, e2020JA028961, doi, 2021.

Khodachenko, M.L., I.F. Shaikhislamov, H. Lammer, I.B. Miroshnichenko, M.S. Rumenskikh, …, L. Fossati: The impact of intrinsic magnetic field on the absorption signatures of elements probing the upper atmosphere of HD209458b, *MNRAS*, **507**, 3226-3637, doi, 2021.

Khodachenko, M.L., I.F. Shaikhislamov, L. Fossati, H. Lammer, M.S. Rumenskikh, et al.: Simulation of 10 830 Å absorption with a 3D hydrodynamic model reveals the solar He abundance in upper atmosphere of WASP-107b, *MNRAS*, **503**, L23-L27, doi, 2021.

Khotyaintsev, Yu.V., D.B. Graham, A. Vaivads, K. Steinvall, N.J.T. Edberg, …, M. Steller, et al.: Density fluctuations associated with turbulence and waves. First observations by Solar Orbiter, *Astron. Astrophys.*, **656**, A19, doi, 2021.

Korovinskiy, D.B., S.A. Kiehas, E.V. Panov, V.S. Semenov, N.V. Erkaev, ...: The inertia-based model for reconstruction of the electron diffusion region, *J. Geophys. Res.*, **126**, e2020JA029045, doi, 2021.

Krenn, A.F., L. Fossati, D. Kubyshkina, H. Lammer: A critical assessment of the applicability of the energy-limited approximation for estimating exoplanetary mass-loss rates, *Astron. Astrophys.*, **650**, A94, doi, 2021.

Kretzschmar, M., T. Chust, V. Krasnoselskikh, D. Graham, L. Colomban, …, M. Steller, et al.: Whistler waves observed by Solar Orbiter/RPW between 0.5 AU and 1 AU, *Astron. Astrophys.*, **656**, A24, doi, 2021.

Kreuzig, C., G. Kargl, A. Pommero, J. Knollenberg, A. Lethuillier, …, E. Kaufmann, M. Schweighart, W. Macher, P. Tiefenbacher, et al.: The CoPhyLab comet simulation chamber, *Rev. Sci. Instr.*, **92**, 115102, doi, 2021.

Kucharski, D., D. Kirchner, M.K. Jah, J.C. Bennett, F. Koidl, M.A. Steindorfer, P.Y. Wang: Full attitude state reconstruction of tumbling space debris TOPEX/Poseidon via light-curve inversion with Quanta Photogrammetry, *Acta Astronaut.*, **187**, 115-122, doi, 2021.

Kvas, A., J.M. Brockmann, S. Krauss, T. Schubert, T. Gruber, et al.: GOCO06s - a satellite-only global gravity field model, *Earth Syst. Sci. Data*, **13**, 99-118, doi, 2021.

Lammer, H., B. Marty, A.L. Zerkle, M. Scherf, H. O'Neill, et al.: Editorial: Topical collection to "Reading terrestrial planet evolution in isotopes and element measurements", *Space Sci. Rev.*, **217**, 55, doi, 2021.

Lammer, H., R. Brasser, A. Johansen, M. Scherf, M. Leitzinger: Formation of Venus, Earth and Mars: Constrained by isotopes, *Space Sci. Rev.*, **217**, 7, doi, 2021.

LaMoury, A.T., H. Hietala, F. Plaschke, L. Vuorinen, J.P. Eastwood: Solar wind control of magnetosheath jet formation and propagation to the magnetopause, *J. Geophys. Res.*, **126**, e2021JA029592, doi, 2021.

Le, G., P.J. Chi, R.J. Strangeway, C.T. Russell, J.A. Slavin, …, R. Nakamura, F. Plaschke, et al.: MMS observations of field line resonances under disturbed solar wind conditions, *J. Geophys. Res.*, **126**, e2020JA028936, doi, 2021.

Leleu, A., Y. Alibert, N.C. Hara, M.J. Hooton, T.G. Wilson, …, W. Baumjohann, …, A. Bonfanti, …, L. Fossati, …, M. Steller, et al.: Six transiting planets and a chain of Laplace resonances in TOI-178, *Astron. Astrophys.*, **649**, A26, doi, 2021.

Leto, P., C. Trigilio, J. Krtička, L. Fossati, R. Ignace, et al.: A scaling relationship for non-thermal radio emission from ordered magnetospheres: From the top of the main sequence to planets, *MNRAS*, **507**, 1979-1998, doi, 2021.

Li, C., R. Zhang, D. Yu, G. Dong. J. Liu, …, T.-L. Zhang, et al.: China's Mars exploration mission and science investigation, *Space Sci. Rev.*, **217**, 57, doi, 2021.

Li, W.-Y., Yu.V. Khotyaintsev, B.-B. Tang, D.B. Graham, C. Norgren, …, F. Plaschke, et al.: Upper-hybrid waves driven by meandering electrons around magnetic reconnection X line, *Geophys. Res. Lett.*, **48**, e2021GL093164, doi, 2021.

Liu, T., J.J. Eckl, M. Steindorfer, P.Y. Wang, K.U. Schreiber: Accurate ground-to-ground laser time transfer by diffuse reflections from tumbling space debris objects, *Metrologia*, **58**, 025009, doi, 2021.

Lou, Y., X. Cao, B. Ni, M. Wu, T.-L. Zhang: Parametric dependence of polarization reversal effects on the particle pitch angle scattering by EMIC waves, *J. Geophys. Res.*, **126**, e2021JA029966, doi, 2021.

Maksimovic, M., J. Soucek, T. Chust, Y. Khotyaintsev, M. Kretzschmar, …, M. Steller, et al.: First observations and performance of the RPW instrument on board the Solar Orbiter mission, *Astron. Astrophys.*, **656**, A41, doi, 2021.

Malykhin, A.Y., E.E. Grigorenko, D.R. Shklyar, E.V. Panov, O. Le Contel, et al.: Characteristics of resonant electrons interacting with whistler waves in the nearest dipolarizing magnetotail, *J. Geophys. Res.*, **126**, e2021JA029440, doi, 2021.

Mangano, V., M. Dósa, M. Fränz, A. Milillo, J.S. Oliveira, …, M. Volwerk, …, A. Varsani, …, F. Plaschke, …, H.I.M. Lichtenegger, G. Laky, …, W. Baumjohann: BepiColombo science investigations during cruise and flybys at the Earth, Venus and Mercury, *Space Sci. Rev.*, **217**, 23, doi, 2021.

Marsch, E., Y. Narita: Connecting in the Dirac equation the Clifford algebra of Lorentz invariance with the Lie algebra of SU(N) gauge symmetry, *Symmetry*, **13**, 475, doi, 2021.

Marsch, E., Y. Narita: CPTM symmetry for the Dirac equation and its extended version based on the vector representation of the Lorentz group, *Front. Physics*, **9**, 618392, doi, 2021.

Marsch, E., Y. Narita: Threefold spin helicity as possible origin of SU(3) gauge symmetry, *Eur. Phys. J. Plus*, **136**, 652, doi, 2021.

Matteini, L., R. Laker, T. Horbury, L. Woodham, S.D. Bale, …, M. Steller, et al.: Solar Orbiter's encounter with the tail of comet C/2019 Y4 (ATLAS): Magnetic field draping and cometary pick-up ion waves, *Astron. Astrophys.*, **656**, A39, doi, 2021.

Morris, B.M., L. Delrez, A. Brandeker, A.C. Cameron, A.E. Simon, …, W. Baumjohann, …, L. Fossati, …, M. Steller, et al.: CHEOPS precision phase curve of the Super-Earth 55 Cancri e, *Astron. Astrophys.*, **653**, A173, doi, 2021.

Nakamura, R., W. Baumjohann, T.K.M. Nakamura, E.V. Panov, D. Schmid, A. Varsani, et al.: Thin current sheet behind the dipolarization front, *J. Geophys. Res.*, **126**, e2021JA029518, doi, 2021.

Nakamura, T.K.M., H. Hasegawa, K.J. Genestreti, R.E. Denton, T.D. Phan, …, R. Nakamura, et al.: Fast cross-scale energy transfer during turbulent magnetic reconnection , *Geophys. Res. Lett.*, **48**, e2021GL093524, doi, 2021.

Narita, Y.: Electromotive force in the solar wind, *Ann. Geophys.*, **39**, 759-768, doi, 2021.

Narita, Y., F. Plaschke, W. Magnes, D. Fischer, D. Schmid: Error estimate for fluxgate magnetometer in-flight calibration on a spinning spacecraft, *Geosci. Instrum. Method. Data Syst.*, **10**, 13-24, doi, 2021.

Niu, D.-D., J. Cui, H. Gu, X.-S. Wu, Y.-T. Cao, …, T.-L. Zhang, et al.: In situ heating of the nightside Martian upper atmosphere and ionosphere: The role of solar wind electron precipitation, *Astrophys. J.*, **909**, 108, doi, 2021.

Niu, D.-D., J. Cui, S.Q. Wu, H. Gu, Y.T. Cao, …, T.-L. Zhang: Species-dependent response of the Martian ionosphere to the 2018 global dust event, *J. Geophys. Res. Planets*, **126**, e2020JE006679, doi, 2021.

Niu, D.D., H. Gu, J. Cui, X.S. Wu, M.Y. Wu, T.-L. Zhang: Effects of the solar wind dynamic pressure on the Martian topside ion distribution: Implications on the variability of bulk ion outflow, *Astrophys. J.*, **922**, 231, doi, 2021.

Noack, L., K.G. Kislyakova, C.P. Johnstone, M. Güdel, L. Fossati: Interior heating and outgassing of Proxima Centauri b: Identifying critical parameters, *Astron. Astrophys.*, **651**, A103, doi, 2021.

O'Kane, J., L.M. Green, E.E. Davies, C. Möstl, J. Hinterreiter, …, A.J. Weiss, …, T. Amerstorfer: Solar origins of a strong stealth CME detected by Solar Orbiter, *Astron. Astrophys.*, **656**, L6, doi, 2021.

Orsini, S., S.A. Livi, H.I.M. Lichtenegger, S. Barabash, A. Milillo, …, G. Laky, …, K. Torkar, …, H. Lammer, …, G. Fremuth, F. Giner, …, H. Jeszenszky, …, W. Baumjohann, …, M. Delva, …, C. Kürbisch, …, M. Leichtfried, …, A. Varsani, …, R. Wallner, et al.: SERENA: Particle instrument suite for determining the Sun-Mercury interaction from BepiColombo, *Space Sci. Rev.*, **217**, 11, doi, 2021.

Palmerio, E., E.K.J. Kilpua, O. Witasse, D. Barnes, B. Sánchez-Cano, A.J. Weiss, …, C. Möstl, et al.: CME magnetic structure and IMF preconditioning affecting SEP transport, *Space Weather*, **19**, e2020SW002654, doi, 2021.

Palmerio, E., T. Nieves-Chinchilla , E.K.J. Kilpua, D. Barnes, A.N. Zhukov, …, C. Möstl, et al.: Magnetic structure and propagation of two interacting CMEs from the Sun to Saturn, *J. Geophys. Res.*, **126**, e2021JA029770, doi, 2021.

Paschmann, G., J.M. Quinn, R.B. Torbert, C.E. McIlwain, H. Vaith, …, W. Baumjohann, et al.: Results of the electron drift instrument on Cluster, *J. Geophys. Res.*, **126**, e2021JA029313, doi, 2021.

Perri, S., D. Perrone, O. Roberts, A. Settino, E. Yordanova, et al.: Nature of electrostatic fluctuations in the terrestrial magnetosheath, *Astrophys. J.*, **919**, 75, doi, 2021.

Philishvili, E., B.M. Shergelashvili, S. Buitendag, J. Raes, S. Poedts, M.L. Khodachenko: Case study on the identification and classification of small-scale flow patterns in flaring active region, *Astron. Astrophys.*, **645**, A52, doi, 2021.

Píša, D., J. Soucek, O. Santolík, M. Hanzelka, G. Nicolaou, …, M. Steller, et al.: First-year ion-acoustic wave observations in the solar wind by the RPW/TDS instrument on board Solar Orbiter, *Astron. Astrophys.*, **656**, A14, doi, 2021.

Przybilla, N., L. Fossati, C.S. Jeffery: HD 144941: The most extreme helium-strong star, *Astron. Astrophys.*, **654**, A119, doi, 2021.

Reiss, M.A., C. Möstl, R.L. Bailey, H.T. Rüdisser, U.V. Amerstorfer, T. Amerstorfer, A.J. Weiss, J. Hinterreiter, et al.: Machine learning for predicting the Bz magnetic field component from upstream in situ observations of solar coronal mass ejections, *Space Weather*, **19**, e2021SW002859, doi, 2021.

Reiss, M.A., K. Muglach, C. Möstl, C.N. Arge, R.L. Bailey, et al.: The observational uncertainty of coronal hole boundaries in automated detection schemes, *Astrophys. J.*, **913**, 28, doi, 2021.

Roberts, O.W., R. Nakamura, V.N. Coffey, D.J. Gershman, M. Volwerk, A. Varsani, et al.: A study of the solar wind ion and electron measurements from the Magnetospheric Multiscale mission's fast plasma investigation, *J. Geophys. Res.*, **126**, e2021JA029784, doi, 2021.

Sampl, M., W. Macher, T. Oswald, D. Plettemeier, H.O. Rucker, et al.: Juno Waves high frequency antenna proper7Steinvall, K., Yu.V. Khotyaintsev, G. Cozzani, A. Vaivads, E. Yordanova, …, M. Steller, et al.: Solar wind current sheets and deHoffmann-Teller analysis. First results from Solar Orbiter's DC electric field measurements, *Astron. Astrophys.*, **656**, A9, doi, 2021.

Swayne, M.I., P.F.L. Maxted, A.H.M.J Triaud, S.G. Sousa, C. Broeg, …, A. Bonfanti, …, W. Baumjohann, …, L. Fossati, …, M. Steinberger, M. Steller, et al.: The EBLM project - VIII. First results for M-dwarf mass, radius, and effective temperature measurements using CHEOPS light curves, *MNRAS*, **506**, 306-322, doi, 2021.

Szabó, Gy.M., D. Gandolfi, A. Brandeker, Sz. Csizmadia, Z. Garai, …, L. Fossati, …, W. Baumjohann, …, M. Steller, et al.: The changing face of AU Mic b: Stellar spots, spin-orbit commensurability, and transit timing variations as seen by CHEOPS and TESS, *Astron. Astrophys.*, **654**, A159, doi, 2021.

Taubenschuss, U., L. Lamy, G. Fischer, D. Píša, O. Santolík, et al.: The Faraday rotation effect in Saturn Kilometric Radiation observed by the CASSINI spacecraft, *Icarus*, **370**, 114661, doi, 2021.

Telloni, D.C., C. Scolini, C. Möstl, G.P. Zank, L.-L. Zhao, A.J. Weiss, M.A. Reiss, et al.: Study of two interacting interplanetary coronal mass ejections encountered by Solar Orbiter during its first perihelion passage. Observations and modeling, *Astron. Astrophys.*, **656**, A5, doi, 2021.

Toepfer, S., Y. Narita, D. Heyner, U. Motschmann: Error propagation of Capon's minimum variance estimator, *Front. Physics*, **9**, 684410, doi, 2021.

Toepfer, S., Y. Narita, K.-H. Glassmeier, D. Heyner, P. Kolhey, et al.: The Mie representation for Mercury's magnetic field, *Earth Planets Space*, **73**, 65, doi, 2021.

Toepfer, S., Y. Narita, W. Exner, D. Heyner, P. Kolhey, et al.: The Mie representation for Mercury's magnetospheric currents, *Earth Planets Space*, **73**, 204, doi, 2021.

Tong, Y.Q., B.J. Cheng, Y.Q. Miao, B. Zhou, X.H. Zhu, …, W. Magnes, …, A. Pollinger, et al.: Analysis and elimination of tri-band beacon interference with the fluxgate sensors onboard CSES, *Sci. China Technol. Sci.*, **64**, 1869-1900, doi, 2021.

Trautner, R., P. Reiss, G. Kargl: A drill-integrated miniaturized device for detecting ice in lunar regolith: The PROSPECT permittivity sensor, *Meas. Sci. Technol.*, **32**, 125117, doi, 2021.

Treumann, R.A., W. Baumjohann: Condensate formation in collisionless plasma, *Front. Physics*, **9**, 713551, doi, 2021.

Treumann, R.A., W. Baumjohann: Diffuse Josephson radiation in turbulence, *Front. Physics*, **9**, 711882, doi, 2021.

Treumann, R.A., W. Baumjohann: Mirror mode junctions as sources of radiation, *Front. Astron. Space Sci.*, **8**, 648744, doi, 2021.

Treumann,R.A., W. Baumjohann: Olbert's Kappa Fermi and Bose distributions, *Front. Physics*, **9**, 672836, doi, 2021.

Van Grootel, V., F.J. Pozuelos, A. Thuillier, S. Charpinet, L. Delrez, …, W. Baumjohann, …, L. Fossati, …, M. Steller, et al.: A search for transiting planets around hot subdwarfs I. Methods and performance tests on light curves from Kepler, K2, TESS, and CHEOPS, *Astron. Astrophys.*, **650**, A205, doi, 2021.

Vecchio, A., M. Maksimovic, V. Krupar, X. Bonnin, A. Zaslavsky, …, M. Steller, et al.: Solar Orbiter/RPW antenna calibration in the radio domain and its application to type III burst observations, *Astron. Astrophys.*, **656**, A33, doi, 2021.

Verscharen, D., D. Stansby, A.J. Finley, C.J. Owen, T. Horbury, …, Solar Orbiter MAG, RPW teams: The angular-momentum flux in the solar wind observed during Solar Orbiter's first orbit, *Astron. Astrophys.*, **656**, A28, doi, 2021.

Volwerk, M., B. Sánchez-Cano, D. Heyner, S. Aizawa, N. André, A. Varsani, …, W. Baumjohann, D. Fischer, …, H. Jeszenszky, …, G. Laky, H.I.M. Lichtenegger, …, R. Nakamura, F. Plaschke, …, D. Schmid, …, C. Simon Wedlund: Venus's induced magnetosphere during active solar wind conditions at BepiColombo's Venus 1 flyby, *Ann. Geophys.*, **39**, 811-839, doi, 2021.

Volwerk, M., D. Mautner, C. Simon Wedlund, C. Goetz, F. Plaschke, …, D. Schmid, D. Rojas-Castillo, O.W. Roberts, A. Varsani: Statistical study of linear magnetic hole structures near Earth, *Ann. Geophys.*, **39**, 239-253, doi, 2021.

Volwerk, M., T.S. Horbury, L.D. Woodham, S.D. Bale, C. Simon Wedlund, D. Schmid, …, W. Baumjohann, …, W. Magnes, …. M.B. Steller, et al.: Solar Orbiter's first Venus flyby: MAG observations of structures and waves associated with the induced Venusian magnetosphere, *Astron. Astrophys.*, **656**, A11, doi, 2021.

von Forstner, J.L.F., M. Dumbović, C. Möstl, J. Guo, A. Papaioannou, …, A.J. Weiss, J. Hinterreiter, T. Amerstorfer, M. Bauer, et al.: Radial evolution of the April 2020 stealth coronal mass ejection between 0.8 and 1 AU. Comparison of Forbush decreases at Solar Orbiter and near the Earth, *Astron. Astrophys.*, **656**, A1, doi, 2021.

Vörös, Z., A. Varsani, E. Yordanova, Y.L. Sasunov, O.W. Roberts, …, R. Nakamura, Y. Narita: Magnetic reconnection within the boundary layer of a magnetic cloud in the solar wind, *J. Geophys. Res.*, **126**, e2021JA029415, doi, 2021.

Vuorinen, L., H. Hietala, F. Plaschke, A.T. LaMoury: Magnetic field in magnetosheath jets: A statistical study of Bz near the magnetopause, *J. Geophys. Res.*, **126**, e2021JA029188, doi, 2021.

Wang, G. Q., M. Volwerk, S.D. Xiao, M.Y. Wu, Y.Q. Chen, T.-L. Zhang: Foreshock as a source region of electron-scale magnetic holes in the solar wind at 1 AU , *Astrophys. J.*, **915**, 3, doi, 2021.

Wang, G., M.Wu, G.Wang, S. Xiao, I. Zhelavskaya, …, T.-L. Zhang: Reflection of low-frequency fast magnetosonic waves at the local two-ion cutoff frequency: Observation in the plasmasphere, *Ann. Geophys.*, **39**, 613-625, doi, 2021.

Wang, G., Z.L. Gao, M.Y. Wu, G.Q. Wang, S.D. Xiao, …, T.-L. Zhang: Trapping and amplification of unguided mode EMIC waves in the radiation belt, *J. Geophys. Res.*, **126**, e2021JA029322, doi, 2021.

Wang, G.Q., M. Volwerk, A.M. Du, S.D. Xiao, M.Y. Wu, …, T.L. Zhang: Statistical study of small-scale magnetic holes in the upstream regime of the Martian bow shock, *Astrophys. J.*, **921**, 153, doi, 2021.

Wang, G.Q., M. Volwerk, M.Y. Wu, Y.F. Hao, S.D. Xiao, …, T.L. Zhang: First observations of an ion vortex in a magnetic hole in the solar wind by MMS, *Astron. J.*, **161**, 110, doi, 2021.

Wang, G.Q., M. Volwerk, S.D. Xiao, M.Y. Wu, Y.Q. Chen, T.L. Zhang: Electron-scale magnetic peaks upstream of the terrestrial bow shock observed by the Magnetospheric Multiscale mission, *Astrophys. J.*, **914**, 101, doi, 2021.

Wang, G.Q., M. Volwerk, S.D. Xiao, M.Y. Wu, Y.Q. Chen, T.L. Zhang: Statistical properties of electron-scale magnetic peaks in the solar wind at 1 AU, *Astrophys. J.*, **921**, 152, doi, 2021.

Wang, G.Q., T.-L. Zhang, M.Y. Wu, S.D. Xiao, G. Wang, …, M. Volwerk: Field-aligned currents originating from the chaotic motion of electrons in the tilted current sheet: MMS observations, *Geophys. Res. Lett.*, **48**, e2020GL088841, doi, 2021.

Wang, J., X.H. Shen, Y.Y. Yang, Z.M. Zeren, G. Hulot, …, W. Magnes, et al.: Initial scalar lithospheric magnetic anomaly map of China and surrounding regions derived from CSES satellite data, *Sci. China Technol. Sci.*, **64**, 1118-1126, doi, 2021.

Wang, P.Y., M.A. Steindorfer, F. Koidl, G. Kirchner, E. Leitgeb: Megahertz repetition rate satellite laser ranging demonstration at Graz observatory, *Opt. Lett.*, **46**, 937-940, doi, 2021.

Weiss, A.J., C. Möstl, E.E. Davies, T. Amerstorfer, M. Bauer, J. Hinterreiter, M.A. Reiss, R.L. Bailey, …, W. Magnes, D. Fischer, W. Baumjohann: Multi-point analysis of coronal mass ejection flux ropes using combined data from Solar Orbiter, BepiColombo, and Wind, *Astron. Astrophys.*, **656**, A13, doi, 2021.

Weiss, A.J., C. Möstl, T. Amerstorfer, R.L. Bailey, M.A. Reiss, J. Hinterreiter, U.V. Amerstorfer, M. Bauer: Analysis of coronal mass ejection flux rope signatures using 3DCORE and approximate Bayesian computation, *Astrophys. J. Suppl. Ser.*, **252**, 9, doi, 2021.

Wellenzohn, S., R. Nakamura, T.K.M. Nakamura, A. Varsani, V.A. Sergeev, et al.: Remote sensing of magnetic reconnection in the magnetotail using in situ multipoint observations at the plasma sheet boundary layer, *J. Geophys. Res.*, **126**, e2020JA028917, doi, 2021.

Wu, M., Y. Chen, A. Du, G. Wang, S. Xiao, …, T.-L. Zhang: Statistical properties of small-scale linear magnetic holes in the Martian magnetosheath, *Astrophys. J.*, **916**, 104, doi, 2021.

Wu, S., S. Ye, G. Fischer, J. Wang, M. Long, et al.: Statistical study on spatial distribution and polarization of Saturn narrowband emissions, *Astrophys. J.*, **918**, 64, doi, 2021.

Xiao, S.D., M.Y. Wu, G.Q. Wang, Y.Q. Chen, T.L. Zhang: The spectral scalings of magnetic fluctuations upstream and downstream of the Venusian bow shock, *Earth Planets Space*, **73**, 13, doi, 2021.

Xu, Q., X. Xu, T.-L. Zhang, Z.J. Rong, M. Wang, et al.: The Venus Express observation of Venus' induced magnetosphere boundary at solar maximum, *Astron. Astrophys.*, **652**, A113, doi, 2021.

Yang, Y., B. Zhou, G. Hulot, N. Olsen, Y. Wu, …, A. Pollinger, …, W. Magnes, et al.: CSES high precision magnetometer data products and example study of an intense geomagnetic storm, *J. Geophys. Res.*, **126**, e2020JA028026, doi, 2021.

Yang, Y., G. Hulot, P. Vigneron, X. Shen, Z. Zhima, …, W. Magnes, …, A. Pollinger, et al.: The CSES global geomagnetic field model (CGGM): An IGRF-type global geomagnetic field model based on data from the China Seismo-Electromagnetic Satellite, *Earth Planets Space*, **73**, 45, doi, 2021.

Yordanova, E., Z. Vörös, L. Sorriso-Valvo, A.P. Dimmock, E. Kilpua: A possible link between turbulence and plasma heating, *Astrophys. J.*, **921**, 65, doi, 2021; Erratum, *Astrophys. J.*, **923**, 282, doi, 2021.

Yushkov, E.V., A.A. Petrukovich, A.V. Artemyev, R. Nakamura: Thermodynamics of the magnetotail current sheet thinning, *J. Geophys. Res.*, **126**, e2020JA028969, doi, 2021.

Zaitsev, I., A. Divin, V.S. Semenov, I. Kubyshkin, D. Korovinskiy, et al.: Cold ion energization at separatrices during magnetic reconnection, *Phys. Plasmas*, **28**, 032104, doi, 2021.

Zaslavsky, A., I. Mann, J. Soucek, A. Czechowski, D. Píša, …, M. Steller, et al.: First dust measurements with the Solar Orbiter Radio and Plasma Wave instrument, *Astron. Astrophys.*, **656**, A30, doi, 2021.

Zhang, L., J. He, Y. Narita, X. Feng: Reconstruction test of turbulence power spectra in 3D wavenumber space with at most 9 virtual spacecraft Measurements, *J. Geophys. Res.*, **126**, e2019JA027413, doi, 2021.

Zhang, L.Q., C. Wang, L. Dai, H.S. Fu, A.T.Y. Lui, W. Baumjohann, et al.: MMS observation on the cross-tail current sheet rollup at the dipolarization front, *J. Geophys. Res.*, **126**, e2020JA028796, doi, 2021.

Zhou, L., C. Lhotka, C. Gales, Y. Narita, L.-Y. Zhou: Dynamics of charged dust in the orbit of Venus, *Astron. Astrophys.*, **645**, A63, doi, 2021.

Zou, Y., Y. Zhu, Y. Bai, L. Wang, Y. Jia, …, T.-L. Zhang, et al.: Scientific objectives and payloads of Tianwen-1, China's first Mars exploration mission, *Adv. Space Res.*, **67**, 812-823, doi, 2021.

BOOKS

Lammer, H., B. Marty, A. Zerkle, M. Blanc, H. O'Neill, T. Klein (Eds.): Reading Terrestrial Planet Evolution in Isotopes and Element Measurements, Springer, The Netherlands, 445 pages, 2021.

PROCEEDINGS & BOOK CHAPTERS

Barbero, J., I. Jernej, C. Hagen, W. Magnes, R. Lammegger, et al.: Monitoring of JUICE optical fibers during thermal cycles keeping the optical connectors at different stable temperatures in 3-chambers setup. In: *Proceedings SPIE, Vol. 11852, International Conference on Space Optics - ICSO 2020*, Eds. Cugny, B., Z. Sodnik, N. Karafolas, SPIE, Bellingham WA, USA, 118522S, doi, 2021.

Boudjada, M.Y., H.U. Eichelberger, X. Zhang, W. Magnes, V. Denisenko, A. Pollinger, …, K. Schwingenschuh, B.P. Besser: Analysis of ground-based very low frequency signal recorded onboard CSES satellite. In: *Proceedings of the 2021 Kleinheubach Conference*, Ed. Chandra, M., IEEE, Bellingham WA, USA, 3 p., doi, 2021.

Cosentino, R., M. Focardi, S. Pezzuto, G. Giusi, E. Galli, …, J. Hasiba, K. Hofmann, H. Jeszenszky, G. Laky, H. Ottacher, M. Steinberger, M. Steller, J. Tonfat, R. Wallner, S. Neukirchner, M. Leichtfried, et al.: The instrument control unit of the PLATO payload: Design consolidation following the preliminary design review by ESA. In: *Proceedings of SPIE, Vol. 11443, Conference on Space Telescopes and Instrumentation 2020: Optical, Infrared, and Millimeter Wave*, Eds. Lystrup, M., M.D. Perrin, N. Batalha, N. Siegler, E.C. Tong, SPIE, Bellingham WA, USA, 114434V, doi, 2021.

Echim, M., T. Chang, P. Kovacs, A. Wawrzaszek, E. Yordanova, Y. Narita, Z. Vörös, et al.: Turbulence and Complexity of magnetospheric plasmas. In: *Magnetospheres in the Solar System*, Eds. Maggiolo, R., N. André, H. Hasegawa, D.T. Welling, Y. Zhang, L.J. Paxton, Wiley-American Geophysical Union, Hoboken, NJ, 67-91, doi, 2021.

Fichtner, H., K. Scherer, M. Lazar, H.-J. Fahr, Z. Vörös: Kappa distributions and entropy. In: *Kappa Distributions. Astrophysics and Space Science Library, vol 464*, Eds. Lazar, M., H. Fichtner, Springer, Cham, 299-306, doi, 2021.

Fossati, L., P.R. McCullough, I.R. Parry: Small satellites for exoplanet science. In: *ExoFrontiers. Big Questions in Exoplanetary Science*, Ed. Madhusudhan, N., IOP, Bristol, 7 pp., doi, 2021.

France, K., B. Fleming, A. Youngblood, J. Mason, T. Patton, …, L. Fossati, …, U.V. Amerstorfer, et al.: EUV spectroscopy with the ESCAPE mission: Exploring the stellar drivers of exoplanet habitability. In: *Proceedings of SPIE, Vol. 11444: Conference on Space Telescopes and Instrumentation 2020: Ultraviolet to Gamma Ray*, Eds. den Herder, J.-W.A., S. Nikzad, K. Nakazawa, SPIE, Bellingham, Washington, USA, 1144405, doi, 2021.

Helling, Ch.: Clouds in exoplanetary atmospheres. In: *ExoFrontiers. Big Questions in Exoplanetary Science*, Ed. Madhusudhan, N., IOP, Bristol, 7 pp., doi, 2021.

Jernej, I., M. Faust, R. Lammegger, I. McKenzie, J. Kuhnhenn, …, M. Agú, …, C. Hagen, …, M. Leichtfried, W. Magnes, …, A. Pollinger, et al.: Design and test of the optical fiber assemblies for the scalar magnetic field sensor aboard the JUICE mission. In: *Proceedings of SPIE, Vol. 11852, International Conference on Space Optics - ICSO 2020*, Eds. Cugny, B., Z. Sodnik, N. Karafolas, SPIE, Bellingham WA, USA, 1185264, doi, 2021.

Liu, Y.J., Z. Hatab, E. Leitgeb, P.Y. Wang, P. Pezzei: Preliminary results of an optical wireless communications prototype developed at TU Graz. In: *Proceedings of the 16th International Conference on Telecommunications (CONTEL 2021)*, Eds. Antonic, M., J. Babic, IEEE, New York, 29-32, doi, 2021.

Loidolt, D., R. Ottensamer, A. Luntzer, F. Kerschbaum, H. Ottacher, J. Tonfat, M. Steller, et al.: A combined software and hardware data compression approach in PLATO. In: *Proceedings of SPIE, Vol. 11443, Conference on Space Telescopes and Instrumentation 2020: Optical, Infrared, and Millimeter Wave*, Eds. Lystrup, M., M.D. Perrin, N. Batalha, N. Siegler, E.C. Tong, SPIE, Bellingham WA, USA, 114434S, doi, 2021.

Nakamura, T.K.M.: The Earth's low-latitude boundary layer. In: *Magnetospheres in the Solar System*, Eds. Maggiolo, R., N. André, H. Hasegawa, D.T. Welling, Y. Zhang, L.J. Paxton, Wiley-American Geophysical Union, Hoboken, NJ, 177-191, doi, 2021.

Narita, Y., F. Plaschke, Z. Vörös: The magnetosheath. In: *Magnetospheres in the Solar System*, Eds. Maggiolo, R., N. André, H. Hasegawa, D.T. Welling, Y. Zhang, L.J. Paxton, Wiley-American Geophysical Union, Hoboken, NJ, 137-151, doi, 2021.

Ripka, P., M.H. Acuna, W. Magnes: Application of magnetic field sensors and magnetometers. In: *Magnetic Sensors and Magnetometers*, Ed. Ripka, P., Artech House, Boston, 279-312, 2021.

Ripka, P., W. Magnes: Fluxgate sensors. In: *Magnetic Sensors and Magnetometers*, Ed. Ripka, P., Artech House, Boston, 51-98, 2021.

PERSONNEL

Acaro Narvaez, Andrea Stefania, BSc
Agú, Martín A., Dipl.-Ing.
Amerstorfer, Tanja, Dr.
Amerstorfer, Ute, Dr.
Bach-Moeller, Nanna, MSc
Balduin, Thorsten, MSc
Berghofer, Gerhard, Ing.
Besser, Bruno P., Dr.
Blasl, Kevin, BSc
Bonfanti, Andrea, Dr.
Boudjada, Mohammed Y., Dr.
Delva, Magda, Dr.
Eichelberger, Hans U., Dr.
Fabian, Peter
Fischer, David, Dipl.-Ing.
Fischer, Georg, Dr.
Flock, Barbara, Mag.
Fossati, Luca, Doz.
Fremuth, Gerhard, Dipl.-Ing.
Giner, Franz, Dipl.-Ing.
Graf, Christian, Ing.
Gratzer, Alexander J.
Grill, Claudia
Hagen, Christian, Dipl.-Ing.
Hasiba, Johann, Dipl.-Ing.
Helling, Christiane, Prof. Dr.
Herbort, Oliver, MSc
Höck, Eduard, Dipl.-Ing.
Hofmann, Karl, Dipl.-Ing.
Hosner, Martin, MSc
Hradecky, Doris
Jernej, Irmgard, Ing.
Jeszenszky, Harald, Dipl.-Ing.
Kargl, Günter, Dr.
Käufer, Till, MSc
Khodachenko, Maxim L., Dr.
Kim, Minjae, Dr.
Kirchner, Georg, Dr.
Koidl, Franz, Ing.
Korovinskiy, Daniil, Dr.
Krenn, Andreas F., MSc
Kubyshkina, Daria, Dr.
Kürbisch, Christoph, Ing.
Laddha, Sunny, MSc
Laky, Gunter, Dipl.-Ing.
Lammer, Helmut, Doz.
Lecoq Molinos, Helena, MSc
Leichtfried, Mario, Ing.
Macher, Wolfgang, Dr.
Magnes, Werner, Dr.
Mannel, Thurid, Dr.
Möstl, Christian, Dr.
Muck, Cosima
Nakamura, Rumi, Doz.
Narita, Yasuhito, Doz.
Neukirchner, Sonja, Ing.
Nischelwitzer-Fennes, Ute, Ing.
Ottacher, Harald, Dipl.-Ing.
Panov, Evgeny, Dr.
Pitterle, Martin
Pollinger, Andreas, Dr.
Posch, Oliver F.
Preisser Renteria, Luis F., Dr.
Reiss, Martin A., Dr.
Roberts, Owen W., Dr.
Samra, Dominic, MSc
Scherr, Alexandra, Mag.
Scherzer, Maximilian, MSc
Schirninger, Christoph, BSc
Schmid, Daniel, Dr.
Schneider, Sebastian
Simon Wedlund, Cyril Laurent, Dr.
Stachel, Manfred, Dipl.-Ing.
Steinberger, Michael, Dipl.-Ing.
Steindorfer, Michael, Dr.
Steller, Manfred B., Dr.
Stieninger, Reinhard, Ing.
Teubenbacher, Daniel, BSc
Tonfat Seclen, Jorge L., Dr.
Tschachler, Elvira, Mag.
Valavanoglou, Aris, Dipl.-Ing.
Varsani, Ali, Dr.
Voller, Wolfgang G., Mag.
Volwerk, Martin, Dr.
Vörös, Zoltan, Dr.
Wallner, Robert, Ing.
Wang, Peiyuan, MSc
Weiss, Andreas J., MSc
Wilfinger, Josef, BSc
Woitke, Peter, Dr.
Zhang, Tie-Long, Prof.
Zivithal Stephan, BSc

As of 31 December 2021

IMPRESSUM

PUBLISHER

Prof. Dr. Christiane Helling, Director
Institut für Weltraumforschung (IWF)
Österreichische Akademie der Wissenschaften (OeAW)
Schmiedlstraße 6, 8042 Graz, Austria
www.oeaw.ac.at/iwf
Twitter: @IWF_oeaw

EDITORS

Bruno Besser, Alexandra Scherr, Martin Volwerk

DESIGN

Alexandra Scherr
pr.iwf@oeaw.ac.at

PRINT

Servicebetrieb ÖH-Uni Graz GmbH


ÖAW IWF